

**FILTER COMPONENT ASSESSMENT  
— CERAMIC CANDLES —**

**Final Report**

DOE/NETL Contract No. DE-AC21-94MC31147

April 23, 2004

by

M. A. Alvin

Siemens Westinghouse Power Corporation  
Science and Technology Center  
1310 Beulah Road  
Pittsburgh, PA 15235-5098

Prepared for

U.S. Department of Energy  
National Energy Technology Laboratory  
626 Cochran's Mill Road  
P.O. Box 10940  
Pittsburgh, PA 15236-0940

R. Dunst and T. J. McMahon — DOE/NETL Project Manager

## **DISCLAIMER**

This report was prepared as an account of work sponsored by the United States Government. Neither the United States nor the United States Department of Energy, nor any of their employees, makes any warranty, expressed or implied, or assumes any legal liability or responsibility for the accuracy, completeness, or usefulness of any information, apparatus, product, or process disclosed, or represents that its use would not infringe privately owned rights. Reference herein to any specific commercial product, process, or service by trade name, mark, manufacturer, or otherwise, does not necessarily constitute or imply its endorsement, recommendation, or favoring by the United States Government or any agency thereof. The views and opinions of authors expressed herein do not necessarily state or reflect those of the United States Government or any agency thereof.

## **ABSTRACT**

Efforts at Siemens Westinghouse Power Corporation (SWPC) have been focused on development of hot gas filter systems as an enabling technology for advanced coal and biomass-based gas turbine power generation applications. SWPC has been actively involved in the development of advanced filter materials and component configuration, has participated in numerous surveillance programs characterizing the material properties and microstructure of field tested filter elements, and has undertaken extended, accelerated filter life testing programs. This report summarizes the results of SWPC's filter component assessment efforts, identifying the performance and stability of porous monolithic, fiber reinforced, and filament wound ceramic hot gas candle filters, potentially for  $\geq 3$  years of viable pressurized fluidized-bed combustion (PFBC) service operating life.

## LIST OF ACRONYMS

AEP	American Electric Power
APF	Advanced Particulate Filtration
CFCC	Continuous fiber ceramic composite
CVD	Chemical vapor deposition
CVI	Chemical vapor infiltration
DOE	Department of Energy
EDX	Energy dispersive x-ray analysis
IF&P	Industrial Filter and Pump
IGCC	Integrated Gasification Combined Cycle
PCD	Particle Collection Device
PCFBC	Pressurized circulating fluidized-bed combustion
PFBC	Pressurized fluidized-bed combustion
NETL	National Energy Technology Laboratory
SCS	Southern Company Services
SEM	Scanning electron microscopy
SiC	Silicon carbide
SPPC	Sierra Pacific Power Company
STC	Science and Technology Center
SWPC	Siemens Westinghouse Power Corporation
USF	U.S. Filter/Fluid Dynamics

# TABLE OF CONTENTS

ABSTRACT

EXECUTIVE SUMMARY

1. INTRODUCTION.....	1
2. POROUS CERAMIC FILTER MATRICES .....	4
2.1. Monolithic Oxide-Based Ceramic Matrices.....	4
2.2 Monolithic Nonoxide-Based Ceramic Matrices.....	15
2.3 Second-Generation Oxide-Based Ceramic Matrices.....	26
2.4 Second-Generation Nonoxide-Based Ceramic Matrices.....	31
3. FIELD TESTING.....	38
3.1 Overview .....	38
3.2 Foster Wheeler PCFBC Test Campaigns .....	39
4. FILTER FAILURE MECHANISMS .....	44
5. ACCELERATED LIFE TESTING PROGRAMS .....	54
5.1 Assessment of Advanced Second Generation Candle Filters — Phase I.....	54
5.2 Extended Accelerated Life Testing — Phase II .....	58
5.2.1 Accelerated Pulse Cycle Exposure.....	59
5.2.2 Thermal Transient Testing .....	60
5.2.3 Material Characterization .....	61
5.3 Accelerated Life Testing and High Temperature Corrosion Studies — Phase III .....	67
6. SUMMARY AND CONCLUSIONS .....	78
7. REFERENCES.....	86
8. ACKNOWLEDGMENTS.....	88

APPENDIX A — FILTER MATERIAL STRENGTH

## TABLES

1. Hot Gas Filter Materials .....	2
2. Porous Filter Technology Development.....	3
3. Field and Extended Life Testing .....	39
4. Summary of PCFBC Testing in 1995-1996 .....	40
5. Summary of PCFBC Testing in 1997.....	42
6. Advanced Second Generation Candle Filter Material Stability and Performance Evaluation ....	54
7. Summary of the Extended Filter Life Test Program — Phase I.....	56
8. Extended Filter Life Testing — Phase II.....	60
9. Residual Filter Element Room and High Temperature Strength.....	62
10. Residual Filter Element Room and High Temperature Load Bearing Capabilities .....	63
11. Residual Filter Element Room and High Temperature Material Diametral Strength and Load Bearing Capabilities .....	64
12. Candle Filter Array — Steady State, Accelerated Pulse Cycling and Thermal Transient Testing — Phase III.....	68
13. Candle Filter Array — High Temperature Corrosion Testing — Phase III .....	71
14. Porous Ceramic Filter Failure Mechanisms.....	81
A-1 Residual Room and High Temperature Strength after PFBC/PCFBC and Accelerated Life Testing	

## FIGURES

1. Porous candle and cross flow filter elements .....	1
2. Variation in the candle filter flange geometry .....	5
3. Variations in the candle flange and filter wall thickness .....	6
4. Variation in the candle filter closed end geometry .....	7
5. Hot gas filter development — Geometric design concepts .....	8
6. High temperature particulate filtration .....	8
7. As-manufactured Coors P-100A-1 alumina/mullite filter matrix .....	9
8. Extensive mullitization within the Coors P-100A-1 filter matrix with extended operation in PFBC/PCFBC applications .....	9
9. Crystallization of the Coors P-100A-1 alumina/mullite filter matrix resulted during PFBC/PCFBC operation leading to extensive mullite formation along the surface of pore cavities within the filter element .....	10
10. Anorthite formation along the surface of the pore cavities, and mullitization within the ligaments of the PFBC/PCFBC-exposed Coors P-100A-1 alumina/mullite filter matrix .....	11
11. Silica phase enrichment at the tips of the blunted mullite rods along the pulse cycled surface of the PFBC/PCFBC-exposed Coors P-100A-1 alumina/mullite filter matrix .....	11
12. As-manufactured Blasch mullite bonded alumina filter matrix .....	12
13. Mullitization resulting within the Blasch filter media with extended PFBC/PCBFC operation .....	13
14. As-manufactured Ensto mullite bonded alumina filter matrix .....	13
15. Mullite formation along the outer surface of the alumina grains contained within the as-manufactured Ensto filter matrix .....	14
16. Mullite ligament formation bonding adjacent alumina grains together within the as-manufactured Ensto filter matrix .....	14
17. Vacuum infiltrated chopped fibers contained within the IF&P Fibrosic™ filter matrix .....	15
18. Morphology of the as-manufactured Schumacher Dia Schumalith clay bonded silicon carbide filter matrix .....	16
19. Residual strength of the PFBC/PCFBC-aged and extended life-tested porous ceramic filter elements .....	17
20. Coalescence and crystallization of the binder coating that encapsulated the silicon carbide grains within the Schumacher filter matrix after 3038 hours of PFBC operation .....	18
21. Micrograph montage illustrating coalescence and crystallization of the binder coating along the surface of the silicon carbide grains, as well as within the ligament bond posts of the PFBC-exposed Pall clay bonded silicon carbide filter matrix .....	18
22. Micrograph montage illustrating the thickness of the silica-enriched layer that formed along the outer surface of the silicon carbide grains within the Pall filter matrix after PFBC operation .....	19
23. Formation of mullite and silica within the aluminosilicate binder phase that encapsulated the silicon carbide grains within the PFBC/PCFBC-exposed Schumacher filter matrix .....	19
24. Morphology of the fresh fractured Pall filter matrix after PFBC/PCFBC operation .....	20
25. Formation of a silica-enriched phase along the surface of the silicon carbide grains, as well as at the base of the filter ligaments within the PFBC/PCFBC-exposed Pall and Schumacher filter matrices .....	21
26. Crystallization resulting at the base of the fresh fractured ligament in the PFBC-exposed Schumacher filter matrix .....	22
27. Outgassing of species along the surface of the PFBC/PCFBC-exposed Pall filter matrix leading to the formation of voids along the silica-enriched crystallized surface .....	22
28. As-manufactured IF&P recrystallized silicon carbide filter matrix .....	23
29. Formation of silica along the outer surface of the IF&P recrystallized silicon carbide filter matrix .....	23

30. Dendritic mullite formation along the surface of the simulated PFBC-exposed IF&P recrystallized silicon carbide grains.....	24
31. As-manufactured Ultramet CVI-SiC reticulated foam.....	25
32. DuPont PRD-66 filament wound filter matrix.....	26
33. Filaments contained within the as-manufactured DuPont PRD-66 filter matrix.....	26
34. Cross-sectioned filament within the DuPont PRD-66 filter matrix.....	27
35. Crystalline features along the outer surface of the fiber replicas of the DuPont filter matrix.....	28
36. Nextel™ filament bundles contained within the McDermott CFCC candle filter.....	29
37. Filament fiber bundles embedded within the chopped fiber matrix along the o.d. surface of the as-manufactured McDermott CFCC filter element.....	29
38. As-manufactured Techniweave CFCC filter element.....	30
39. 3M CVI-SiC filter matrix.....	31
40. CVI-SiC layer deposited along the outer surface of the 3M Nextel™ 312 structural support triaxial braid.....	32
41. Sections of the 3M CVI-SiC composite candle filter after PFBC or PCFBC operation.....	32
42. Crack formations along the silica-enriched infiltrated layers that surrounded the Nextel™ 312 fibers in the triaxial support braid of the 3M composite filter matrix after 2815 hours of exposure above the Siemens Westinghouse APF system tubesheet at AEP.....	33
43. Morphology of the cross-sectioned 3M CVI-SiC composite filter material after 400 hours of exposure at 870°C (1600°F) to 20 ppm NaCl/5-7% steam/air.....	34
44. DuPont SiC-SiC CFCC filter architecture.....	35
45. Morphology of the DuPont SiC-SiC CFCC hybrid filter matrix after accelerated pulse cycle testing in SWPC's PFBC simulator test facility.....	36
46. SWPC APF system at the AEP PFBC Tidd demonstration plant in Brilliant, OH.....	38
47. Thermal fatigue of the Coors P-100A-1 alumina/mullite filter matrix.....	44
48. Coors P-100A-1 alumina/mullite closed end cap.....	44
49. Crack formations at the base of the Pall Vitropore filter flange as a result of high temperature creep during operation at AEP.....	45
50. Failure of the porous ceramic filter elements as the result of ash bridging within the filter array.....	46
51. Failure of the vacuum infiltrated chopped fibrous candle filters.....	46
52. Failure of the thinner walled 3M CFCC filter element flange.....	47
53. Failure of the DuPont PRD-66 filter element.....	48
54. Failure of the Techniweave CFCC filter element after operation in the PCFBC test facility in Karhula, Finland.....	48
55. Failure of the 3M oxide-based CFCC filter elements.....	49
56. Removal of fibers along the outer surface of the McDermott CFCC filter element.....	49
57. Critical inserts within the McDermott CFCC filter element.....	50
58. Crystallization of the Nextel™ fibers within the oxide-based CFCC filter matrices.....	51
59. Failure of the 3M nonoxide-based CFCC filter element.....	52
60. Failure of the DuPont SiC-SiC CFCC filter matrix.....	53
61. Residual room and process temperature compressive strength of the various ceramic candle filter materials as a function of field and extended simulated PFBC accelerated life testing.....	65
62. Residual room and process temperature tensile strength of the various ceramic candle filter materials as a function of field and extended simulated PFBC accelerated life testing.....	66
63. Ceramic and metal candle filter array.....	67
64. Temperature profile during thermal transient testing.....	69
65. Filter elements at the conclusion of steady state, accelerated pulse cycling and thermal transient testing.....	70
66. Failure of the Blasch mullite bonded alumina candle filter after 282 hours of operation in the 840°C (1550°F), simulated PFBC process gas environment containing gas phase sulfur and alkali (Test Segment No. 1).....	71

67. Candle filters at the conclusion of Test Segment No. 2 — 486 hours of exposure at 840°C (1550°F) in the simulated PFBC process gas environment containing gas phase sulfur and alkali...	72
68. Room temperature gas flow resistance through the porous filter elements.....	73
69. Schumacher clay bonded silicon carbide FT20 filter matrix after 204 hours of operation in the gas phase alkali and sulfur-laden, 840°C (1550°F), simulated PFBC process gas environment.....	74
70. Morphology of the Filtros recrystallized silicon carbide filter matrix after 486 hours of operation in the gas phase alkali and sulfur-laden, 840°C (1550°F), simulated PFBC process gas environment.....	74
71. Morphology of the Blasch filter matrix after 282 hours of exposure to the 840°C (1550°F), gas phase alkali and sulfur-laden, simulated PFBC process gas environment .....	75
72. Microstructure of the DuPont PRD-66 filter matrix after 486 hours of exposure to the gas phase alkali and sulfur-laden, 840°C (1550°F), simulated PFBC process gas environment.....	76
73. Microstructure of the McDermott CFCC filter matrix after 486 hours of operation in the gas phase alkali and sulfur-laden, 840°C (1550°F), simulated PFBC process gas environment.....	76
74. Microstructure of the Techniweave CFCC filter matrix after 486 hours of operation in the gas phase alkali and sulfur-laden, 840°C (1550°), simulated PFBC process gas environment.....	77
75. Microstructure of the Pall FeAl filter matrix after 204 hours of operation in the gas phase alkali and sulfur-laden PFBC process gas environment.....	77
76. Porous hot gas filter material technology development .....	78
77. Porous monolithic nonoxide-based ceramics used for hot gas filter technology development.....	79
78. Porous monolithic oxide-based ceramics used for hot gas filter technology development.....	80
79. Porous second-generation oxide-based ceramics used for hot gas filter technology development....	82
80. Porous second-generation nonoxide-based ceramics used for hot gas filter technology development .....	83
81. Recommended maximum operating temperatures for hot gas filter material stability.....	84

## EXECUTIVE SUMMARY

As a key component in advanced coal or biomass-based power applications, hot gas filtration systems protect the downstream gas turbine components from particle fouling and erosion, cleaning the process gas to meet emission requirements. When installed in either pressurized fluidized-bed combustion (PFBC) or integrated gasification combined cycle (IGCC) plants, lower downstream component costs are projected, in addition to improved energy efficiency, lower maintenance, and elimination of additional and expensive fuel or flue gas treatment systems. As a critical component, long-term performance, durability and life of the porous filter elements are essential to the successful operation of hot gas filtration systems in advanced combustion and gasification applications.

Development of the porous ceramic hot gas filter technology began with the use of monolithic clay bonded silicon carbide materials, where silicon carbide particles were bonded together via a binder phase, forming the basic 1.0 m long, 60 mm diameter candle filter architecture. For use in 800-900°C (1470-1650°F) PFBC systems, monolithic oxide-based materials were introduced in order to limit high temperature oxidation of the silicon carbide grains, and to mitigate potential reactions with gas phase alkali released during coal processing. The monolithic oxide-based filters exhibited thermal fatigue failure when operated in Siemens Westinghouse Advanced Particulate Filtration (APF) systems at the American Electric Power (AEP) Tidd demonstration plant in Brilliant, OH, and at the Foster Wheeler pressurized circulating fluidized-bed combustion (PCFBC) test facility in Karhula, Finland. When similarly tested, the nonoxide-based clay bonded silicon carbide elements, exhibited elongation and failure that ultimately led to technology developments for improvement and stabilization of the clay binder. Oxidation of the silicon carbide grains and volume expansion of the filter element were addressed through the application of oxidation resistant grain and/or binder additives.

To provide a more “ruggedized” filter system, emphasis in the mid-1990’s was focused on the development and manufacture of advanced nonoxide- and oxide-based, porous second-generation, continuous fiber ceramic composite (CFCC) and filament wound filter elements which were projected to have significantly improved fracture toughness characteristics over that of the first-generation monolithic ceramic filter materials. When tested in Siemens Westinghouse filter systems, oxidation of the nonoxide-based elements led to brittle failure of the candles, while debonding of external particulate filtration membranes, and failure initially occurred along seams and non-integral flanges and end caps of the advanced second-generation oxide-based candle filters. Many of these issues were resolved with appropriate design and manufacturing modifications.

At the peak of the hot gas filter development program, nearly twenty suppliers were involved in the development, manufacture and supply of 1-1.5 m porous ceramic candle filter elements. Today, a maximum of six filter suppliers are available. However, during the years between 1980 and 2000, significant improvements were made not only to the materials themselves, but also to component design, architecture and manufacturing of the filter elements. These improvements resulted in production of elements that met quality assurance and control criteria, as well as filter geometry and process operating design specifications, and were readied for extended long-term use in advanced PFBC/PCFBC applications. In the Filter Component Assessment program, Siemens Westinghouse demonstrated the viability of the select porous ceramic materials and components to achieve  $\geq 3$  years of equivalent filter operating life under accelerated simulated PFBC operating conditions. Siemens Westinghouse similarly demonstrated the capability of suppliers to manufacture 2.0 m porous ceramic filter elements, and the capability of the elements to be successfully tested in our bench-scale PFBC filter vessel. As a result of

conduct of the Filter Component Assessment program and participation in numerous field surveillance programs, the McDermott oxide-based CFCC filter elements are recommended as the hot gas filter material technology for extended ~800-900°C (~1470-1650°F) PFBC/PCFBC field service use. In addition, the Schumacher/Pall clay bonded silicon carbide filter elements are recommended for PFBC/PCFBC field service operations not exceeding ~750-800°C (~1380-1470°F).

## 1. INTRODUCTION

Siemens Westinghouse Power Corporation (SWPC)<sup>1</sup> has been involved in the development of the hot gas filter material technology since 1988. Emphasis was initially focused on the development and use of oxide- and nonoxide-based ceramic monolithic filter materials in bench-scale test programs and field applications (Figure 1, Table 1) [1,2]. With thermal fatigue issues being encountered by the oxide-based monoliths, and oxidation and/or high temperature creep issues resulting in the nonoxide-based filter matrices during pressurized fluidized-bed combustion (PFBC) and/or pressurized circulating fluidized-bed combustion (PCFBC) operation (Table 2) [3-9], development of fracture toughened, continuous fiber reinforced ceramic composites (CFCC) filters was undertaken in 1994 [10-18]. Several issues were identified with respect to the long-term durability, response, and performance of the CFCC filter elements during extended service life. These included manufacturing and structural integrity, load bearing capability, and ease of fixturing within the filter system.

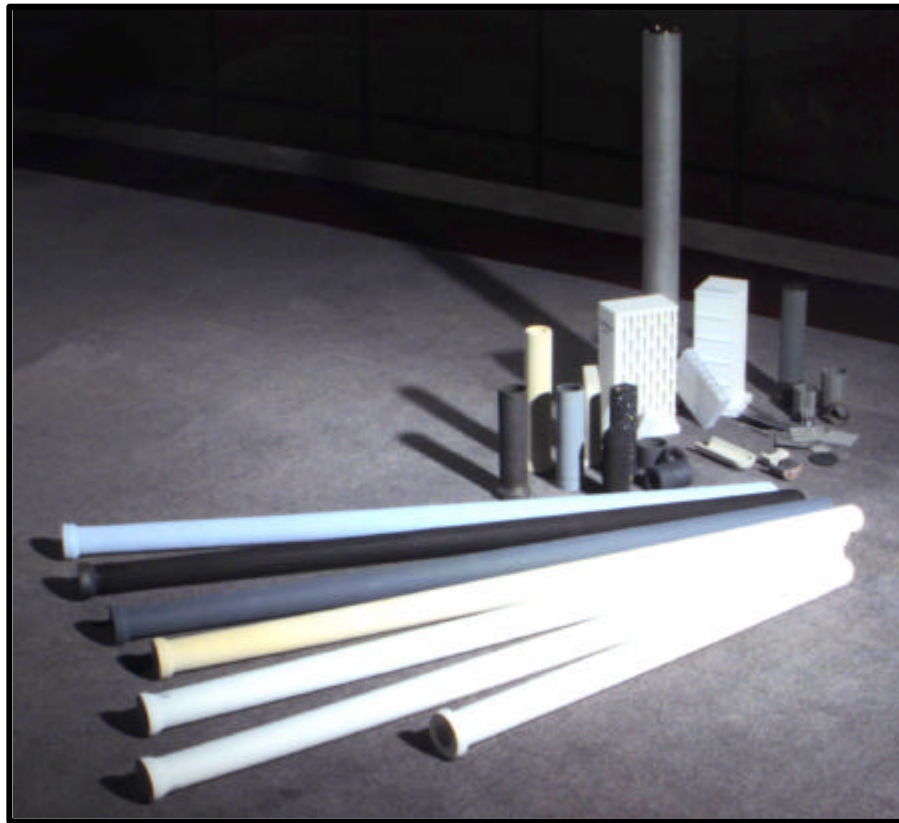


Figure 1 — Porous candle and cross flow filter elements.

Numerous advancements were made since initiating development and manufacture of the monolithic and composite ceramic filters in 1988 and 1994, respectively. These have included:

---

<sup>1</sup> Formerly Westinghouse Electric Corporation.

- Development and use of high temperature, creep resistant binders in the clay bonded silicon carbide filter materials.
- Efforts by numerous domestic and offshore suppliers to provide potentially viable filter materials and/or filter elements manufactured by alternate processes and production techniques.
- Development of alternate filter concepts (i.e., sheet filter, inverted candle filter, etc.).
- Development of oxidation resistance coatings for nonoxide matrices.
- Incorporation of a membrane along the o.d./i.d. surfaces of the filter elements.
- Enhanced flange strength and surface abrasion resistance.

**TABLE 1  
HOT GAS FILTER MATERIALS**

Monolithic Ceramics	Continuous Fiber Reinforced Ceramic Composites	Metal, Advanced Alloys and Intermetallics
Coors P-100A-1 Alumina/ Mullite Pall Clay Bonded Silicon Carbide (442T, 326, 181) Schumacher Clay Bonded Silicon Carbide (F40, FT20) GTE Cordierite and Cordierite-Silicon Nitride AiResearch Reaction Bonded and/or Sintered Silicon Nitride Ensto Alumina Blasch Mullite Bonded Alumina Specific Surface Cordierite IF&P Recrystallized SiC	McDermott Oxide-Based CFCC Techniweave Oxide-Based CFCC  3M CVI-SiC DuPont SiC-SiC Textron Nonoxide-Based CFCC  Americom Oxide-Based CFCC 3M Oxide-Based CFCC  <b>Filament Wound</b> DuPont PRD-66	310S Inconel 600 Hastelloy X Iron Aluminide Fecralloy Haynes 230 Haynes 214 Haynes 556 Haynes 188
<b>Vacuum Infiltrated Chopped Fibers</b>	<b>Technology Development and Commercialization Goals</b>	
IF&P (Fibrosic™) Scapa (Foseco)	<ul style="list-style-type: none"> <li>• System Retrofit Capabilities</li> <li>• Achievement of Design and Material Specifications</li> <li>• Achievement of Performance Specifications</li> <li>• Matrix and Component Operational Stability</li> <li>• QA/QC Manufacturing Capabilities</li> <li>• Commercial Production Capabilities</li> <li>• Initial and Life Cycle Cost Effectiveness</li> <li>• 3 Years Warranted Life</li> </ul>	
<b>Reticulated Foam</b> Ultramet CVI-SiC Selee Oxide-Based Foam		

Following the CFCC programs, DOE/NETL efforts were then directed in 1998 to development of metallic, advanced alloy, and intermetallic, porous filter media [19,20]. In conjunction with various metal filter suppliers, SWPC demonstrated that the iron aluminide and Fecralloy porous sinter bonded metal media were candidate materials for use in 840°C (1550°F), gas phase sulfur-containing but alkali-free, PFBC applications. In the presence of 1 ppm gas phase alkali at 840°C (1550°F), all porous metal filter media underwent accelerated oxidation, limiting gas permeability through the filter matrix and ultimately filter life.

**TABLE 2**  
**POROUS FILTER TECHNOLOGY DEVELOPMENT**

<b>Porous Ceramic Matrices</b>			<b>Metals/Intermetallics</b>
<b>Monoliths</b>	<b>CFCC/Filament Wound</b>		
<b>Advantages</b>			
<ul style="list-style-type: none"> <li>• Ease of Fabrication</li> <li>• Low Component Cost</li> <li>• Chemical Stability of Oxide-Based Materials in PFBC/PCFBC Applications</li> </ul>	<ul style="list-style-type: none"> <li>• Expected Improved Fracture Toughness</li> <li>• Light Weight</li> <li>• Chemical Stability of Oxide-Based Materials in PFBC/PCFBC Applications</li> </ul>	<ul style="list-style-type: none"> <li>• Ductility</li> <li>• Ease of Manufacturing Various Shapes</li> </ul>	
<b>Critical Issues</b>			
<ul style="list-style-type: none"> <li>• Thermal Fatigue/Shock of Oxide-Based Materials</li> <li>• Thermal Shock of Nonoxides during Auto-Ignition Events</li> <li>• Oxidation of Nonoxide-Based Materials</li> <li>• Potential High Temperature Creep of Exposed Nonoxides</li> <li>• Alkali Silicate Eutectic Formation during Exposure of Nonoxides to Na/K Species</li> <li>• Development of Advanced Materials/Architecture</li> </ul>	<ul style="list-style-type: none"> <li>• Higher Cost (CFCC)</li> <li>• Potential Oxide Fiber Embrittlement with Time</li> <li>• Low Load Bearing Capability</li> <li>• Low Flange Strength</li> <li>• Outer Surface Abrasion</li> <li>• Oxidation/Embrittlement of Nonoxides (No Longer Considered for PFBC/PCFBC Applications)</li> </ul>	<ul style="list-style-type: none"> <li>• Oxidation/Accelerated Oxidation in the Presence of Gas Phase Alkali and Sulfur</li> <li>• Metal Blinding in Gasification Applications</li> <li>• Mechanical Properties; Retention of Ductility</li> <li>• Weld and Seam Integrity</li> <li>• Component Cost</li> </ul>	

## 2. POROUS CERAMIC FILTER MATRICES

Throughout the development of porous ceramic candle filters, phase and matrix composition have been critical to establishing long-term thermal and chemical stability of the component during operation in either high temperature combustion or gasification applications. Similarly the overall geometry and dimensional specifications, as well as component manufacturing criteria have significantly impacted the overall integrity and operational life of the filter elements. Architecturally the porous ceramic filter matrices are classified as:

- Monolithic oxides and nonoxides
- Oxide- and nonoxide-based continuous fiber ceramic composites (CFCC)
- Filament wound oxides
- Vacuum infiltrated chopped fibers
- Oxide and nonoxide reticulated foams.

With variations in the matrix architecture, differences resulted in the contour of the flange (Figure 2), flange and filter wall thickness (Figure 3), as well as the closed end cap (Figure 4) during manufacturing of the filter elements. Significant differences resulted in the weight of the elements, ranging from ~3632-5448 gm (~8-12 lb) for the 1.5 m monolithic candles, to ~908-2270 gm (~2-5 lb) for the chopped fiber, filament wound, and CFCC matrices. Differences also resulted in the manner by which the individual candle filters were held and sealed within the filter array. Particular focus was directed to the design and positioning of the gasket seals, and the load bearing capabilities and ultimate process temperature strength of the filter flange. During development of the filter technology, efforts also addressed the critical design issues of the monolithic matrix closed end cap in order to eliminate internal stress risers (crack initiators) which ultimately failed many of the initially manufactured, porous, monolithic oxide-based elements (i.e., Coors P-100A-1 alumina/mullite candle filters). Before addressing the critical failure modes of the various ceramic matrices and filter elements in this report, the following sections describe the composition and microstructure of the various porous ceramic filter materials, and illustrate changes that occurred during operation in SWPC's bench-scale and demonstration plant test facilities.

### 2.1 Monolithic Oxide-Based Ceramic Matrices

The first porous monolithic oxide-based ceramic filter matrix was manufactured by Coors Ceramics Company in the 1980's. Technology was initially directed to development of the cross flow filter architecture [21], prior to transitioning production to the candle and sheet filter geometries in the 1990's (Figure 5). Irrespective of the hot gas filter geometry, particulate fines resulting as a product of combustion or gasification were collected on the outside surface of the filter element, permitting "cleaned" gas to pass through the porous filter media which was then directed to either the stack or gas turbine (Figure 6). As fines collected along the outer surface of the filter element, the pressure drop across the system increased. In order to continue operation and clean the dust cake layer from the filter element, a pulse of air (PFBC/PCFBC) or nitrogen (IGCC) was directed along the "clean" gas channels of each element which in turn permeated through the porous filter media, forcing the dust cake to be removed from the surface of the filter element. In more robust SWPC filter system designs, an inverted candle filter system was developed, whereby the particulate-laden gas initially contacts the i.d. surface of the element, directing "clean" gas flow through the porous filter wall, with subsequent release from the o.d. filter element surface into the filter holder or containment plenum [22].

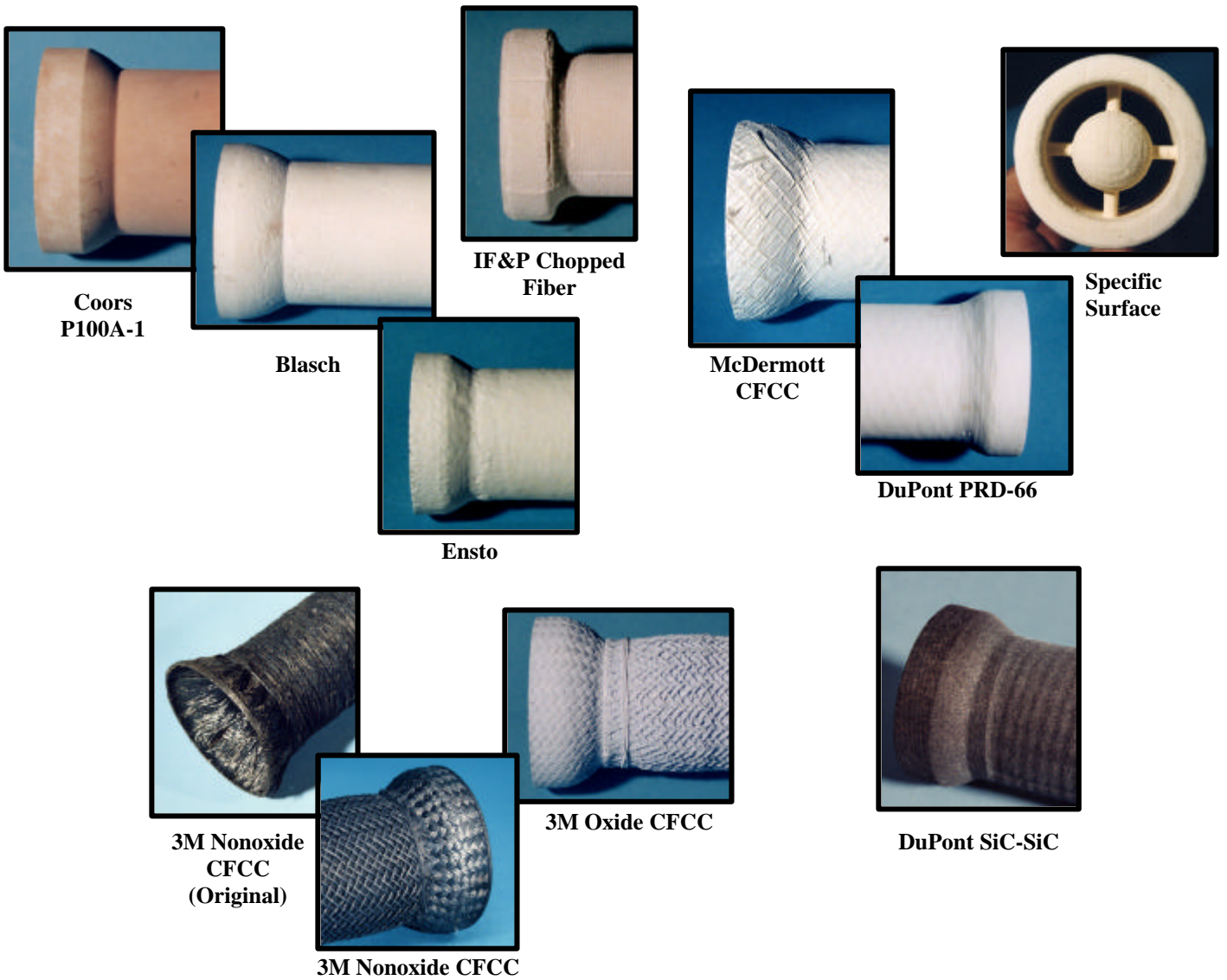


Figure 2 — Variation in the candle flange geometry.

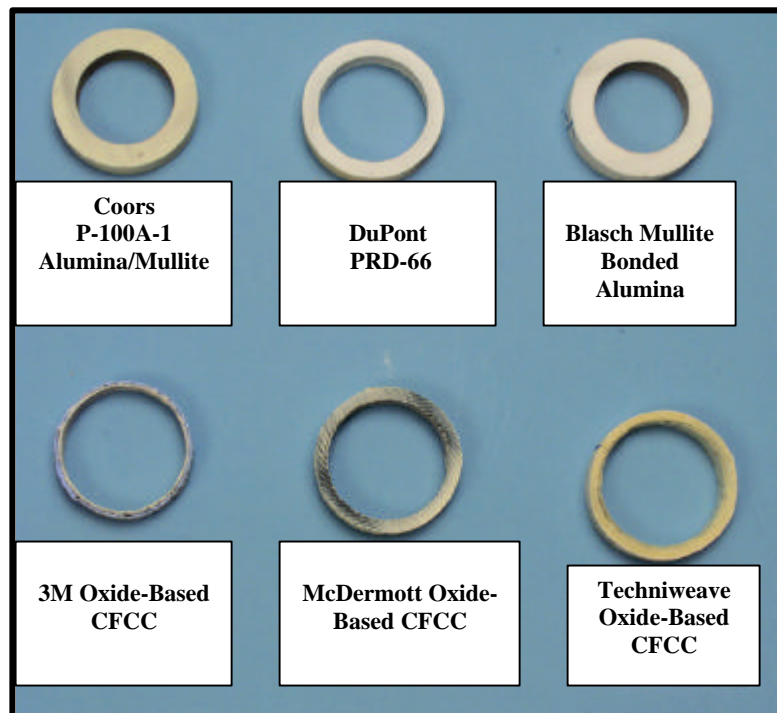
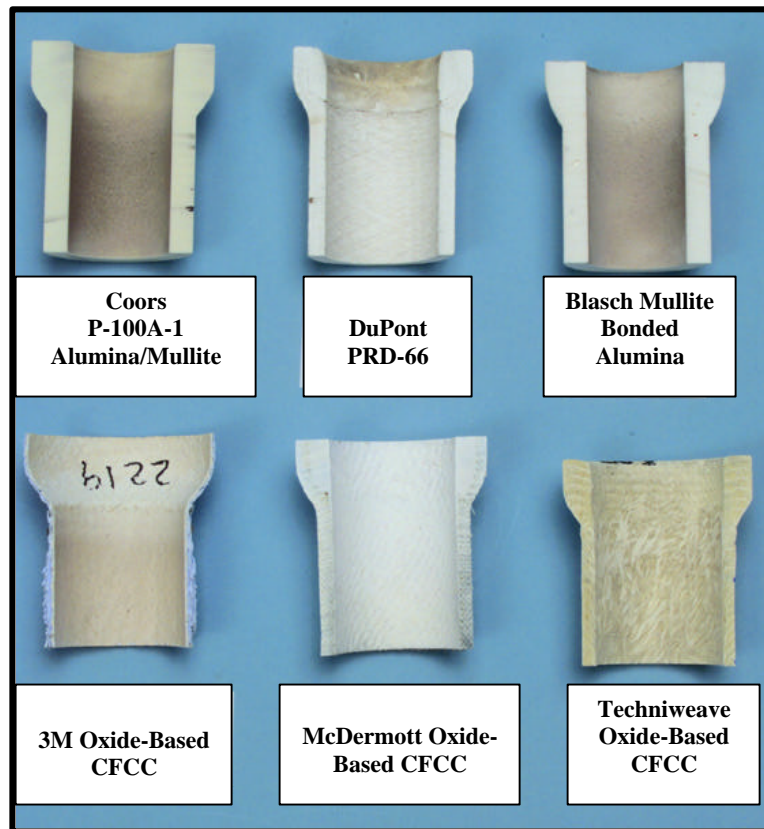
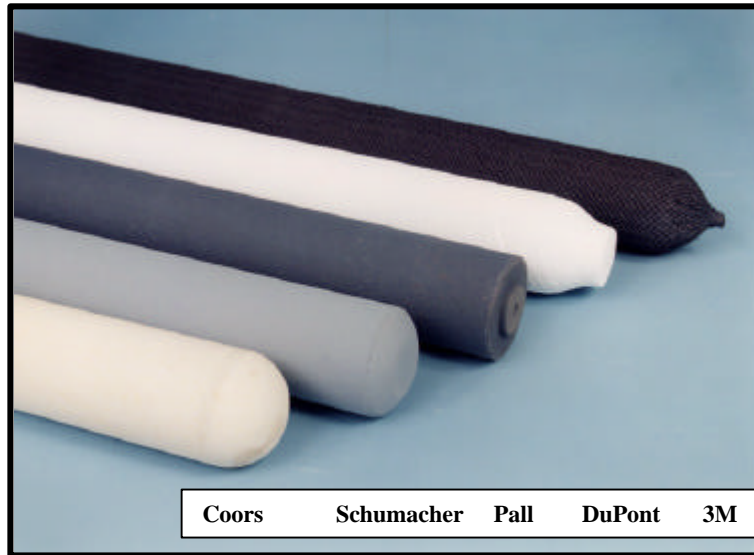


Figure 3 — Variations in the candle flange and filter wall thickness.



Coors  
P100A-1



DuPont PRD-66



3M Nonoxide  
CFCC



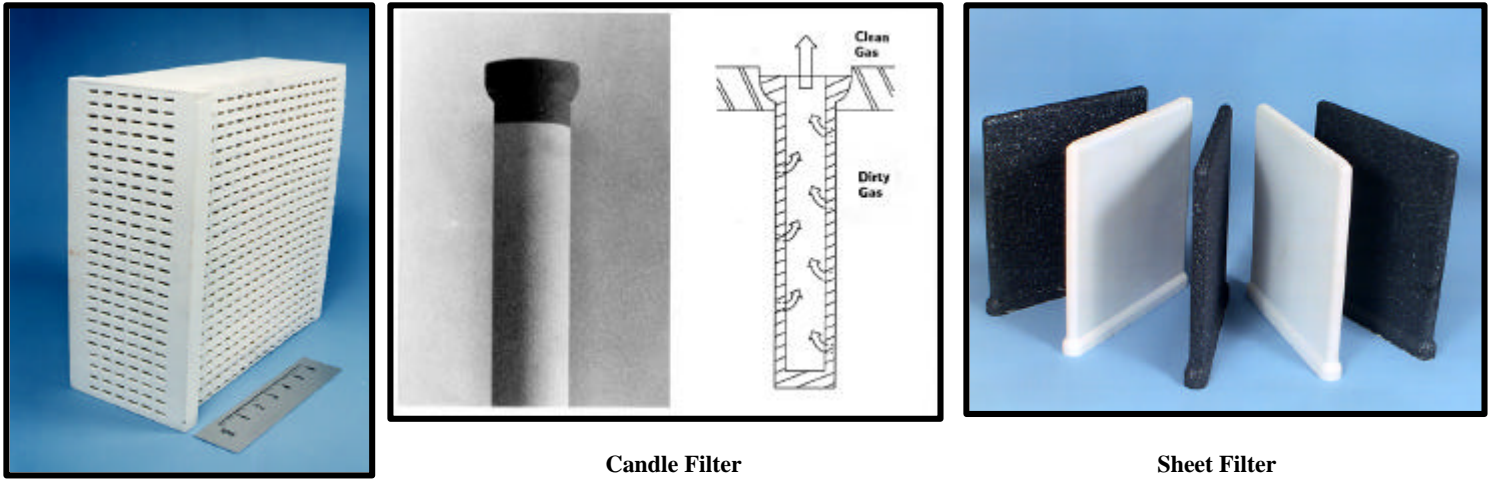
3M Oxide CFCC



Specific Surface



Figure 4 — Variation in the candle filter closed end cap geometry.



Cross Flow Filter

Candle Filter

Sheet Filter

Figure 5 — Hot gas filter development — Geometric design concepts.

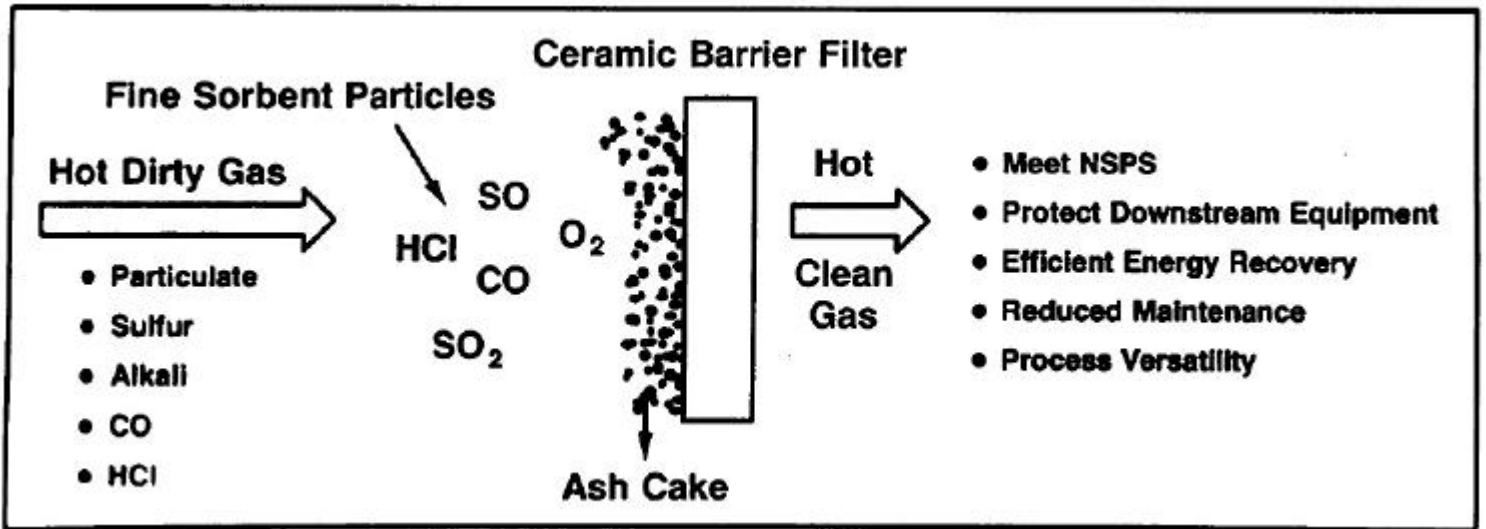


Figure 6 — High temperature particulate filtration.

The Coors P-100A-1 alumina/mullite filter matrix consisted of mullite rods that were embedded within an amorphous phase that contained corundum ( $Al_2O_3$ ) and anorthite ( $CaAl_2Si_2O_8$ ) (Figure 7). The ~10 mm thick Coors filter wall was manufactured without application of an external surface membrane. The Coors candles were 1.0 m and 1.5 m in length, with a 60 mm o.d. along the length of the filter body. With extended operation in PFBC/PCFBC applications, continued mullitization of the matrix resulted leading to the extension of mullite rods across pore cavities (Figure 8). Extensive mullitization similarly resulted along the surface of the pore cavities (Figure 9).

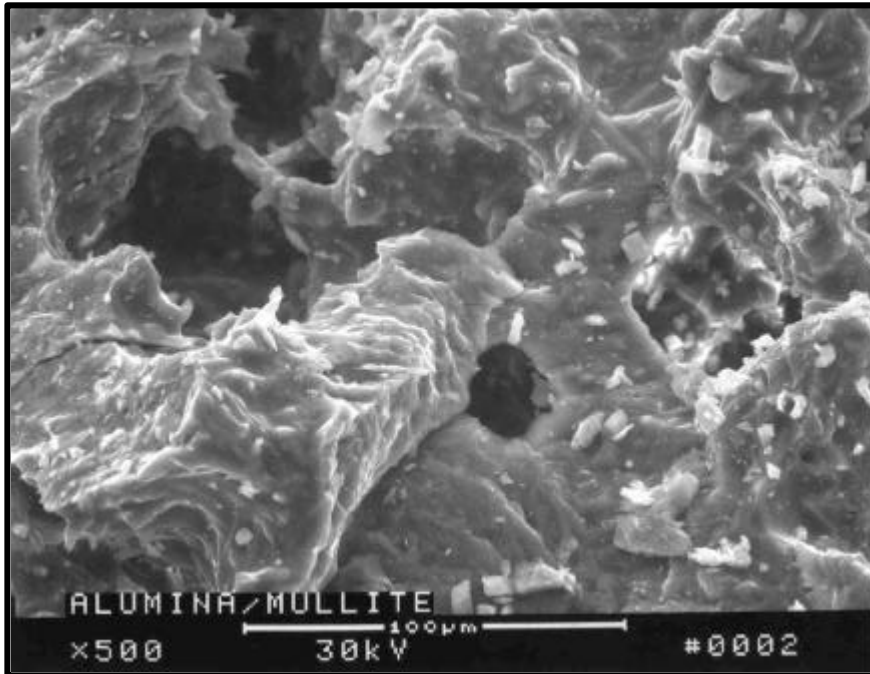


Figure 7 — As-manufactured Coors P-100A-1 alumina/mullite filter matrix.

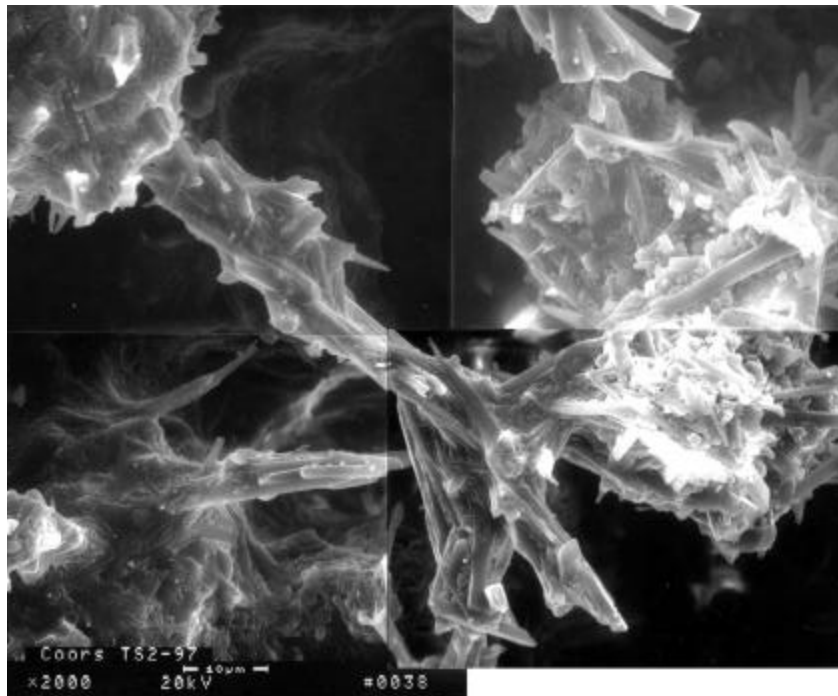


Figure 8 — Extensive mullitization within the Coors P-100A-1 filter matrix with extended operation in PFBC/PCFBC applications.

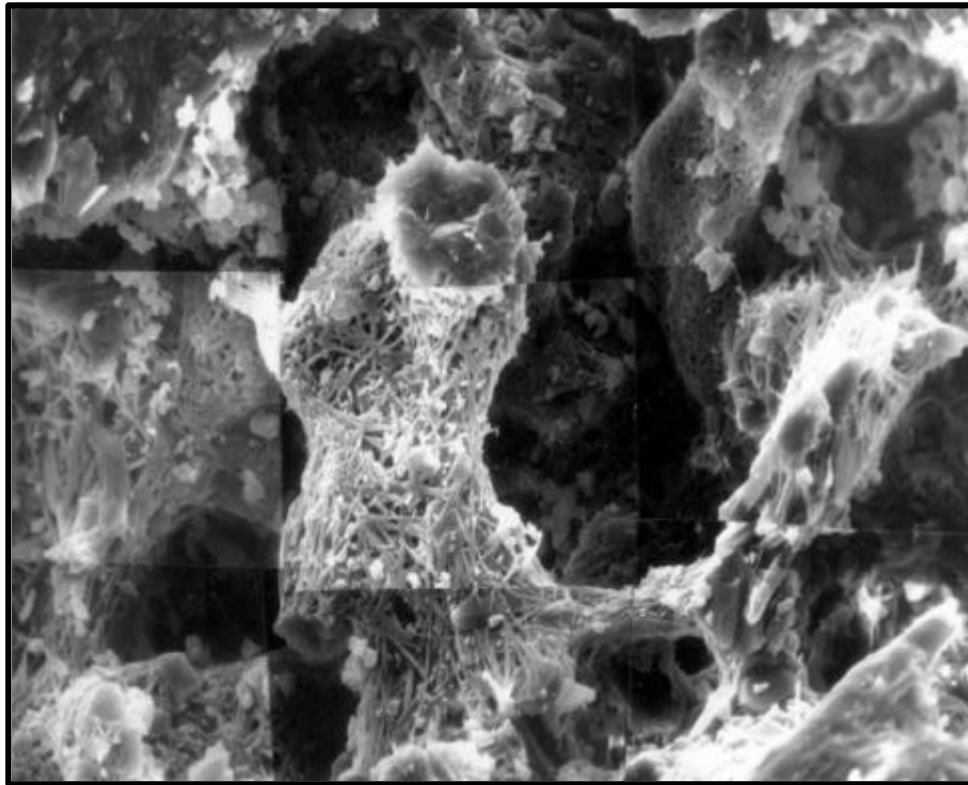


Figure 9 — Crystallization of the Coors P-100A-1 alumina/mullite filter matrix resulted during PFBC/PCFBC operation leading to extensive mullite formation along the surface of pore cavities within the filter element.

Crystallization within the pore ligaments similarly led to pronounced mullite formation, as well as the formation of fine grained anorthite along the surface of the pore cavity walls (Figure 10). Along the pulse cycled surface of the filter wall, nearly spherical,  $\sim 2\text{-}4\ \mu\text{m}$  diameter, silica-enriched features formed at the tips of the blunted mullite-enriched rods which extended into the pore cavities of the filter matrix (Figure 11).

In addition to Coors Ceramics, Blasch Precision Ceramics and Ensto Ceramics OY manufactured 1.5 m, monolithic, oxide-based candle filters. Blasch utilized an injection molding technique to produce the hot gas filter elements. The wall thickness of the Blasch filter element was  $\sim 10\ \text{mm}$ , and the filter elements were typically fabricated without a finer porosity external surface membrane.

The Blasch filter matrix consisted of alumina particles that were held together by striated, flat, plate-like, ligament features which contained a silica and an aluminosilicate or mullite phase (Figure 12). Directionality of the striated mullite containing ligaments was frequently observed within the cross-sectioned filter matrix. Limited crystallization was initially evident within the mullite phase that was present in the as-manufactured filter matrix. Similar to the Coors Ceramics filter matrix, extensive mullitization of the ligament or bond phase resulted (Figure 13) within the Blasch filter media during extended PFBC/PCFBC operation.

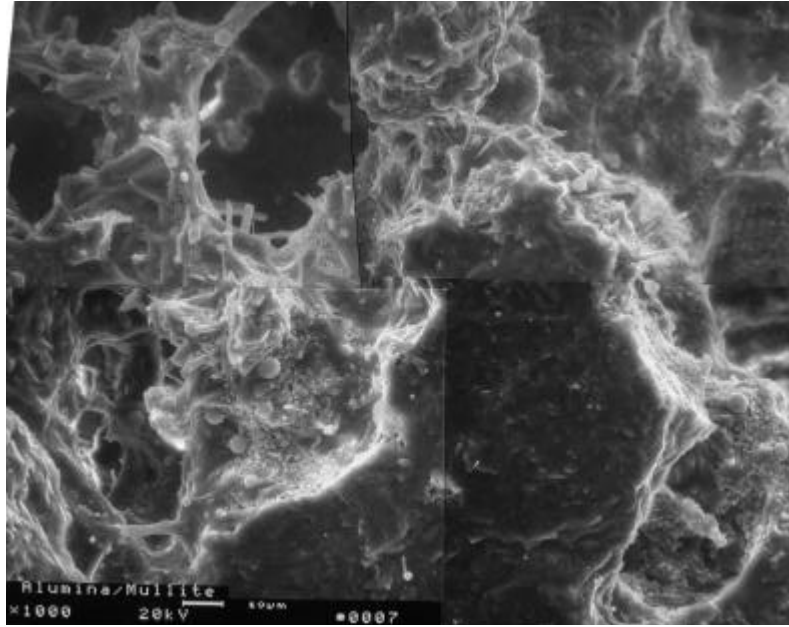


Figure 10 — Anorthite formation along the surface of the pore cavities, and mullitization within the ligaments of the PFBC/PCFBC-exposed Coors P-100A-1 alumina/mullite filter matrix.

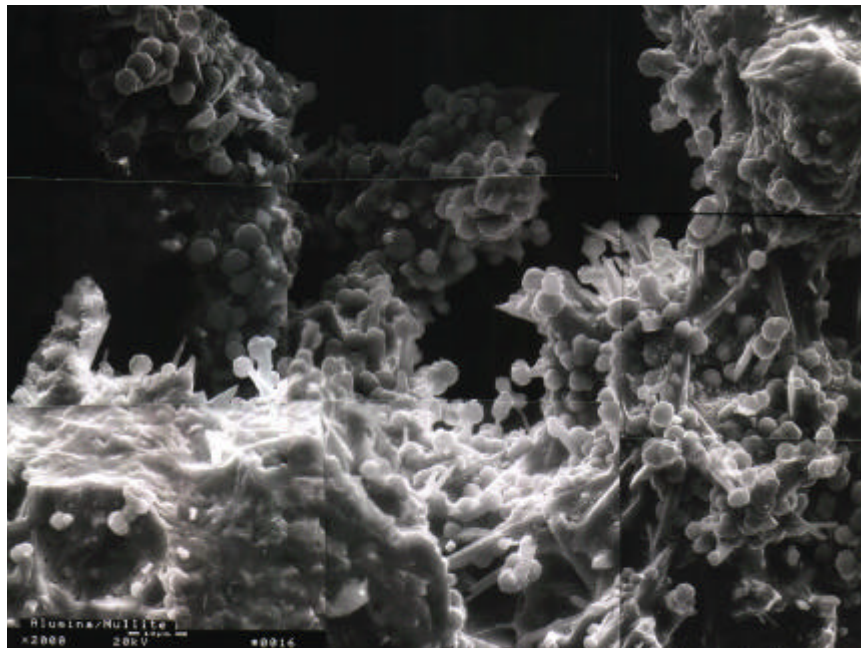


Figure 11 — Silica phase enrichment at the tips of the blunted mullite rods along the pulse cycled surface of the PFBC/PCFBC-exposed Coors P-100A-1 alumina/mullite filter matrix.

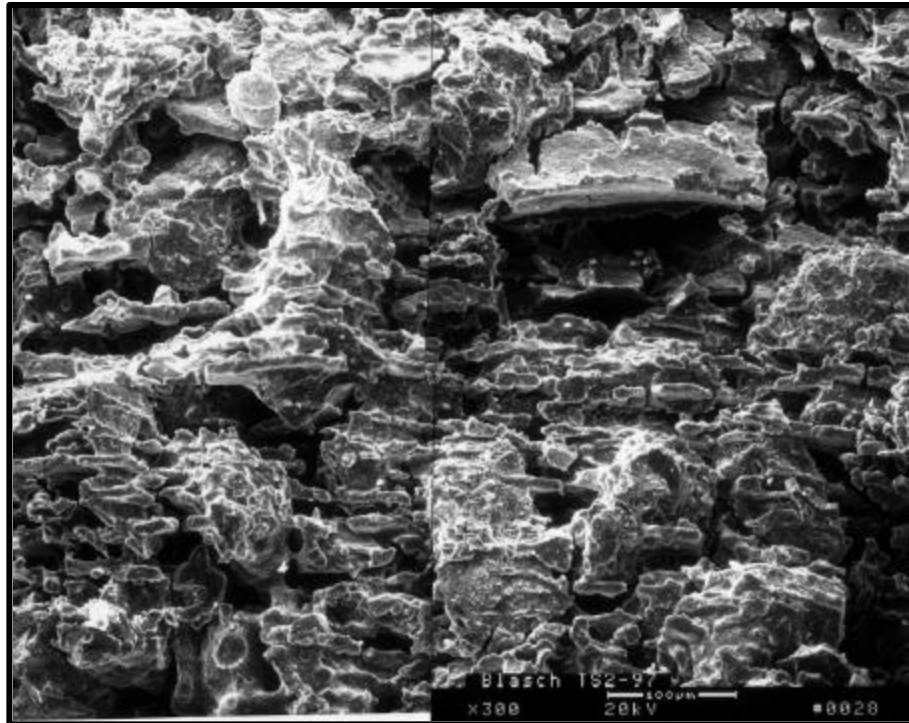


Figure 12 — As-manufactured Blasch mullite bonded alumina filter matrix.

In the as-manufactured Ensto filter matrix, ~20-60  $\mu\text{m}$ , irregularly shaped, alumina-enriched grains were used to form the porous outer surface membrane of the filter element. The thickness of the outer surface membrane was ~100  $\mu\text{m}$  (Figure 14). Directly below the porous outer surface membrane was an ~10 mm thick structural support layer which contained ~400-600  $\mu\text{m}$  alumina-enriched grains.

Within the outer surface membrane, minor concentrations of silicon and/or calcium were detected along the bonding surface of the alumina-enriched ligaments. Within the structural support wall, as well as along the i.d. surface of the as-manufactured Ensto filter elements, the alumina grains were encapsulated with a mullite phase (Figure 15). Frequently mullite formations bridged across the open pores in the as-manufactured Ensto filter matrix. Mullite was considered to serve as the bonding phase or ligament structure that held adjacent alumina-enriched grains together within the structural support wall of the Ensto filter matrix (Figure 16).

Additional suppliers participated during the 1980's in the development of the porous, monolithic, oxide-based, filter technology. These included:

- GTE — Cordierite cross flow filter architecture. The GTE matrix primarily consisted of cordierite ( $\text{Mg}_2\text{Al}_4\text{Si}_5\text{O}_{18}$ ) with the presence of an amorphous phase.
- CeraMem — Cordierite honeycomb or cross flow architecture with a zirconia-enriched silicate membrane.
- Specific Surface — Cordierite candle filter architecture.

- Didier — Pentel P20 consisted of a single coarse size fireclay grain that was bonded together via a fireclay matrix.
- Selee — Alumina-based reticulated foam.

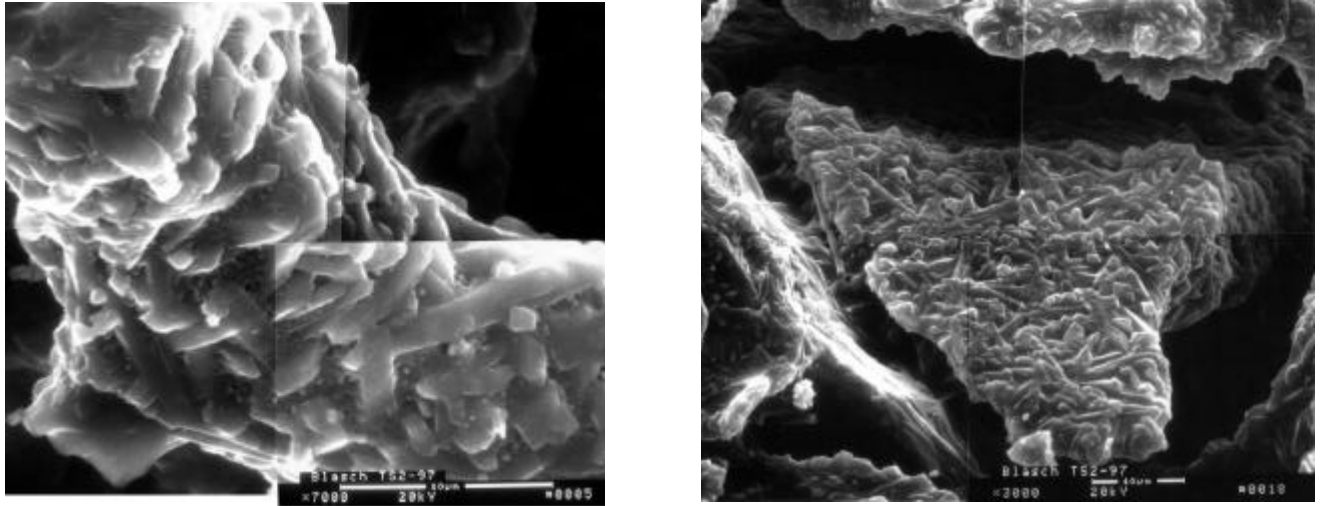


Figure 13 — Mullitization resulting within the Blasch filter media with extended PFBC/PCFBC operation.

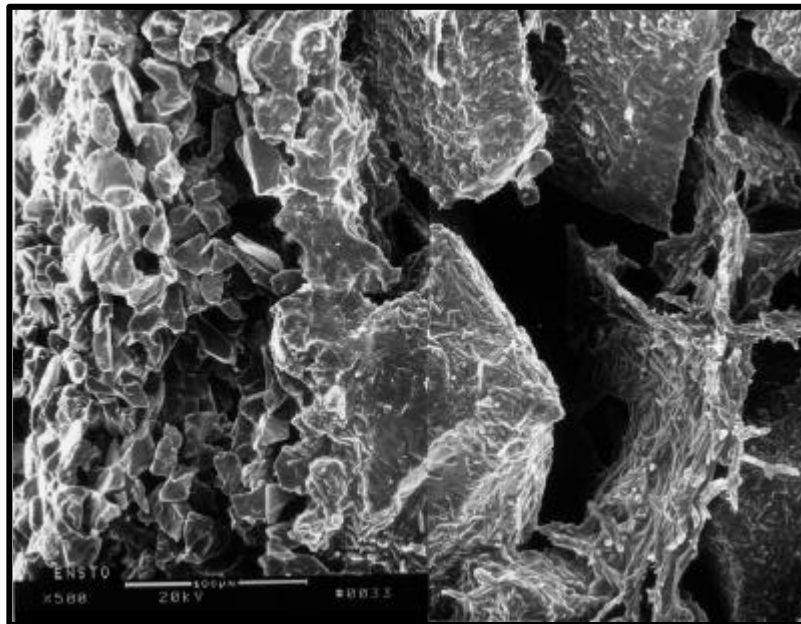


Figure 14 — As-manufactured Ensto mullite bonded alumina filter matrix.

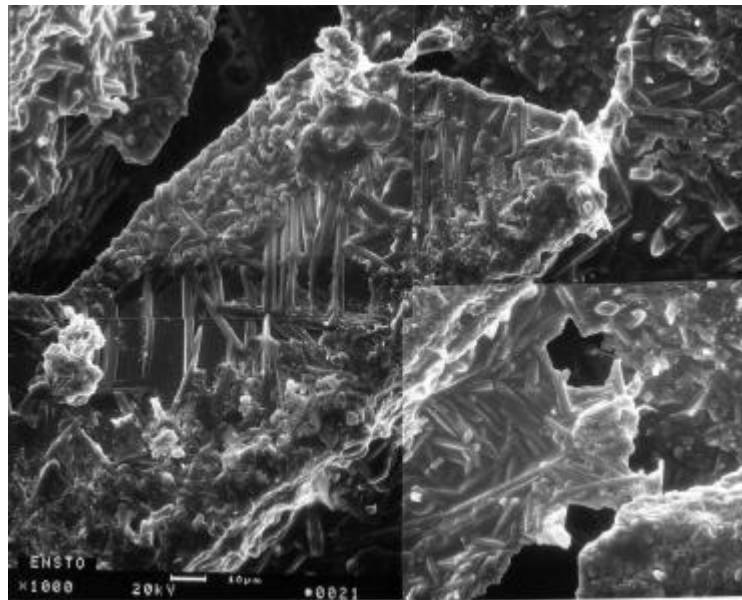


Figure 15 — Mullite formation along the outer surface of the alumina grains contained within the as-manufactured Ensto filter matrix.

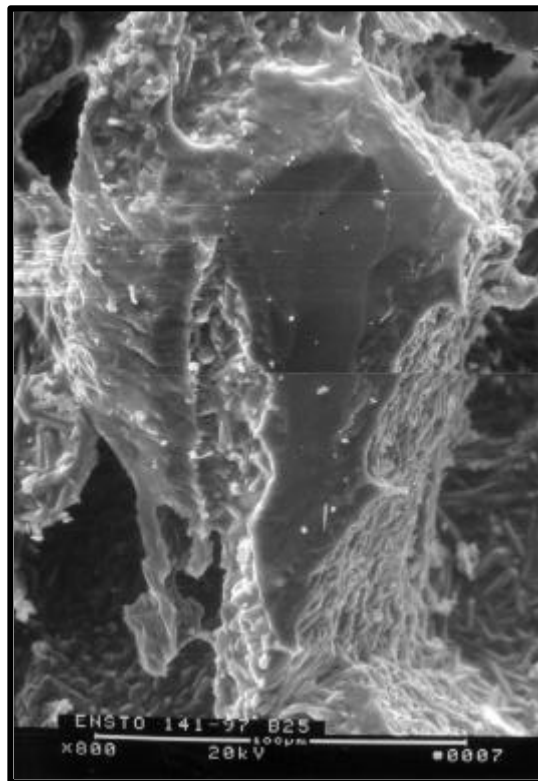


Figure 16 — Mullite ligament formation bonding adjacent alumina grains together within the as-manufactured Ensto filter matrix.

In contrast to the structurally “harder” monolithic oxides, “softer” chopped fiber oxide-based matrices were manufactured by Industrial Filter & Pump, Inc. (IF&P) and Foseco. As shown in Figure 17, the IF&P Fibrosic™ Hi-Perm filter matrix consisted of a blend of 3 μm diameter aluminosilicate fibers, and a silica and alumina binder. The 1.0 m and 1.5 m Fibrosic™ candle filter surface was vacuum infiltrated or impregnated with alumina to normalize the pore size and to toughen the skin along the outer surface of the filter element.

The Foseco<sup>2</sup> filter element consisted of glass fibers that were coated and held together by a mullite wash. Similar to the IF&P filter matrix, uncoated fibers are susceptible to devitrification in the presence of alkali species. During devitrification, the fibers shrink and crack.

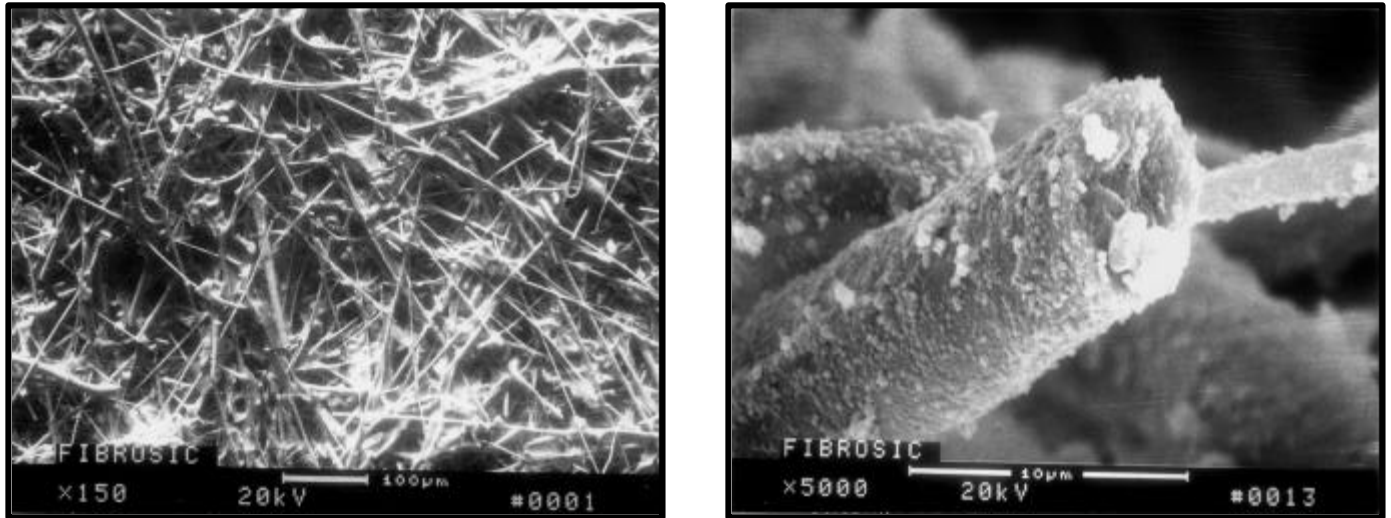


Figure 17 — Vacuum infiltrated chopped fibers contained within the IF&P Fibrosic™ filter matrix.

## 2.2 Monolithic Nonoxide-Based Ceramic Matrices

The as-manufactured 10 mm thick structural support wall of the monolithic Schumacher Dia Schumalith filter matrix consisted of silicon carbide grains that were held together by a clay binder phase (Figure 18). The clay binder not only coated or encapsulated the individual silicon carbide grains, but also formed the ligaments or bond posts between grains within the Schumacher filter matrix. As bench-scale qualification and pilot-scale testing identified the need for modification of the clay binder within the F40 Schumacher filter media, the FT20 binder was developed which consisted of a high temperature, creep resistant, aluminosilicate phase. An ~100 μm thick membrane layer was applied to the outer surface of the Schumacher filter element. The membrane of the FT20 filter matrix consisted of alumina fibers and fine silicon carbide grains that were held together via the aluminosilicate binder.

<sup>2</sup> Acquired by Scapa which produced the Cerafil vacuum infiltrated fibrous filter element.

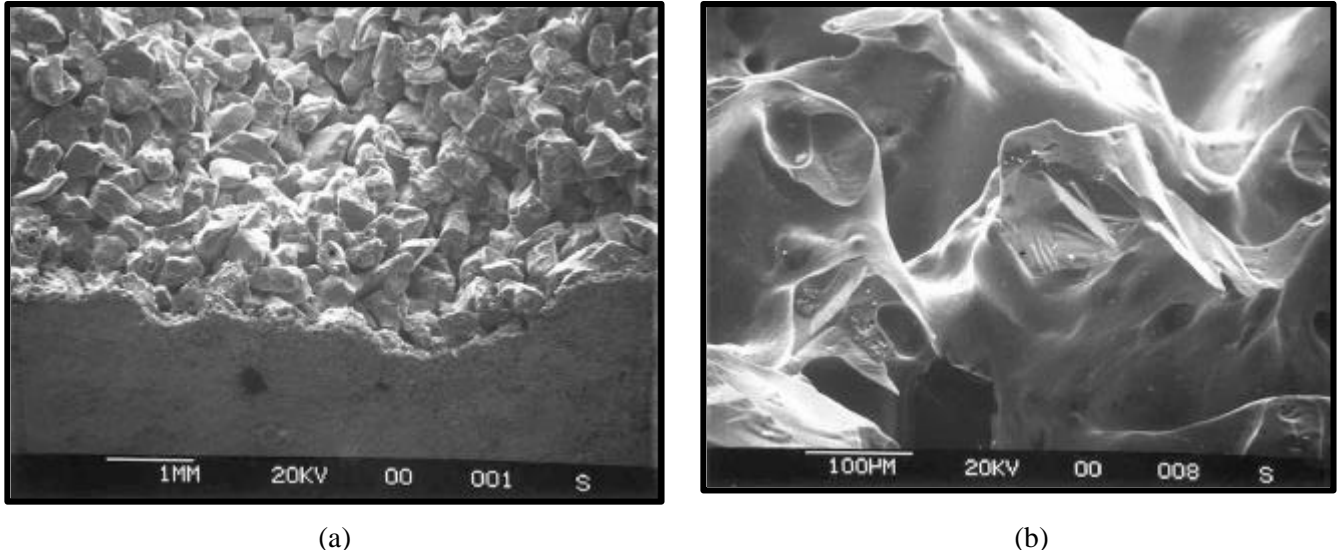


Figure 18 — Morphology of the as-manufactured Schumacher Dia Schumalith clay bonded silicon carbide filter matrix. (a) Fresh fractured cross-sectioned filter surface illustrating membrane coated outer surface and interior coarse silicon carbide grains within the filter element; (b) Higher magnification of the structural support clay bonded silicon carbide grains.

A series of microstructural changes resulted within the clay bonded silicon carbide filter matrix as a function of time during operation in the PFBC/PCFBC environment. These included:

- Coalescence and crystallization of the binder coating along the surface of the silicon carbide grains.
- Oxidation of the silicon carbide grains resulting from diffusion of the process gas through the binder coating. Subsequent reaction with the silicon carbide grain led to the release of  $\text{CO}_2$ , mottling of the silicon carbide grains, and the formation of silica below the partially or fully crystallized binder coating.
- Crystallization along the outer surface of the binder-enriched bond posts or ligaments.
- Enhanced oxidation of the silicon carbide grains leading to a volume expansion of the matrix, and the formation of a thicker oxide scale.
- Crystallization of the silica-enriched layer, leading to separation from the residual underlying mottled surface of the silicon carbide grains.
- Continued oxidation and diffusion of elements along the surface of the silicon carbide grains, leading to the formation of areas enriched with crystallized silica, amorphous silica, and mullite-enriched aluminosilicate rods.
- Enhanced crystallization throughout the binder-enriched bond posts or ligaments.
- Coalescence of the silica-enriched grains, leading to the initiation of a secondary oxide phase formation between the silica-enriched grains along the surface of the silicon carbide structural support grains.

During process operation, initial coalescence and crystallization of the binder or oxide-enriched coating, as well as crystallization along the surface of the bond posts or ligaments were expected to increase the high temperature strength of the clay bonded filter matrix. Similarly with extended time,

the thickness of the crystalline silica-enriched layer increased, encapsulating the silicon carbide grains, and extended into the crystallized aluminosilicate ligaments or bond posts. With extended service operation, thermal fatigue at the junction of the crystallized silica-enriched encapsulating layer and the crystallized binder ligaments was considered to occur, reducing the bulk strength of the filter matrix, exposing the underlying silicon carbide grains to further oxidation (Figure 19).

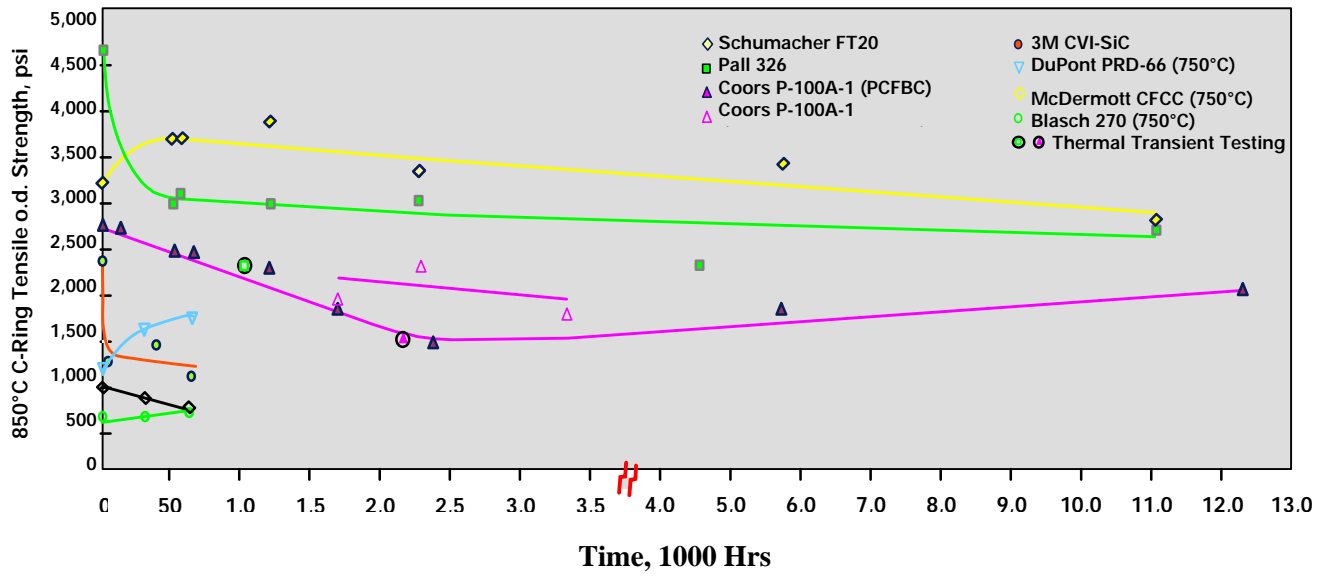


Figure 19 — Residual strength of the PFBC/PCFBC-aged and extended life-tested porous ceramic filter elements.

Removal of the crystallized binder and oxide-enriched coating that encapsulated the silicon carbide grains along the pulse cycled surface of the clay bonded silicon carbide filter elements was observed after extended accelerated pulse cycling and thermal transient testing. Edge abrasion of the grains, particularly in areas associated with bond posts or ligaments was expected to decrease bulk strength of the matrix along the i.d. surface of the filter element.

Similar to the Schumacher Dia Schumalith FT20 candle filters, the as-manufactured monolithic Pall 326 filters consisted of silicon carbide grains that were bonded together via a high temperature creep resistant binder. Initially a finer grained silicon carbide layer was applied to the outer surface of the 10 mm thick structural support wall of the filter element, forming the external membrane required for particulate removal. In addition to the morphology changes that resulted within the Schumacher filter matrix as a function of extended operating time, outgas void or hole formations were frequently observed along the outer surface of the silica-enriched layer that encapsulated the surface of the silicon carbide grains within the Pall filter matrix. Figures 20-27 illustrate many of the microstructural changes resulting within the Schumacher and Pall clay bonded silicon carbide filter matrices after extended operation in the PFBC/PCFBC environment.

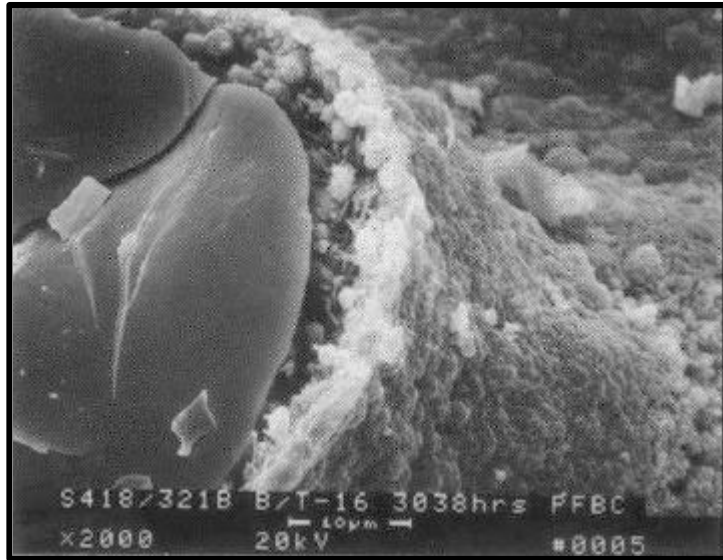


Figure 20 — Coalescence and crystallization of the binder coating that encapsulated the silicon carbide grains within the Schumacher filter matrix after 3038 hours of PFBC operation. The outer surface of the encapsulating layer was enriched with silica while an underlying crystalline aluminosilicate whisker or needle-like formation was evident.

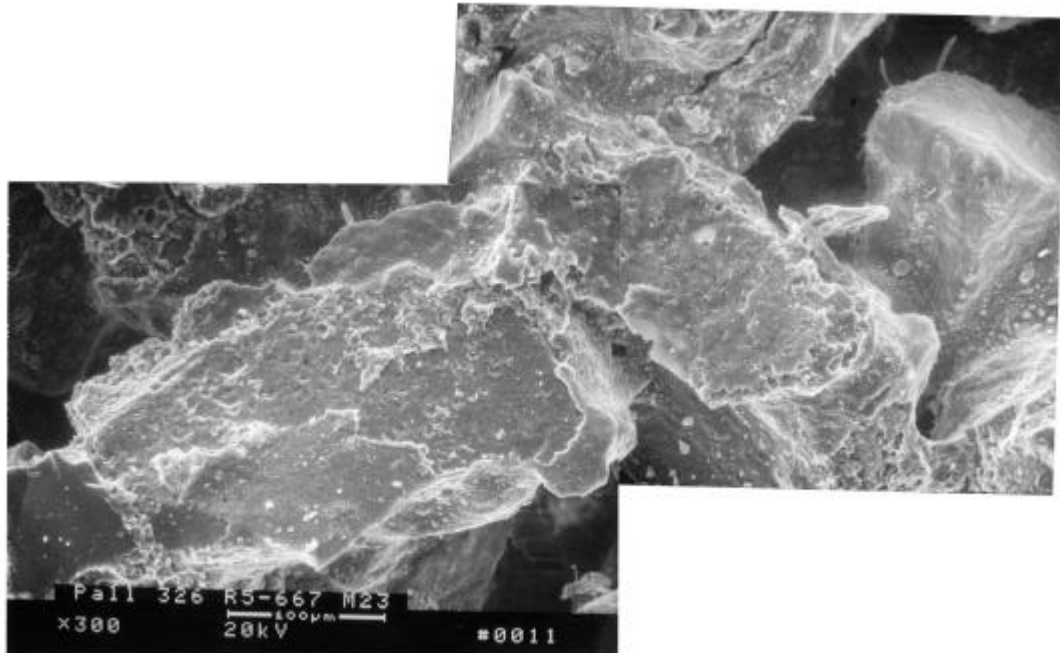


Figure 21 — Micrograph montage illustrating coalescence and crystallization of the binder coating along the surface of the silicon carbide grains, as well as within the ligament bond posts of the PFBC-exposed Pall clay bonded silicon carbide filter matrix.

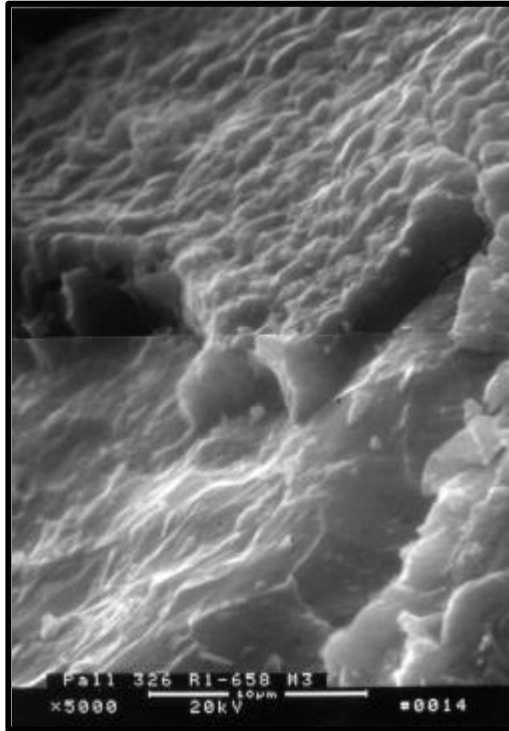


Figure 22 — Micrograph montage illustrating the thickness of the silica-enriched layer that formed along the outer surface of the silicon carbide grains within the Pall filter matrix after PFBC operation.

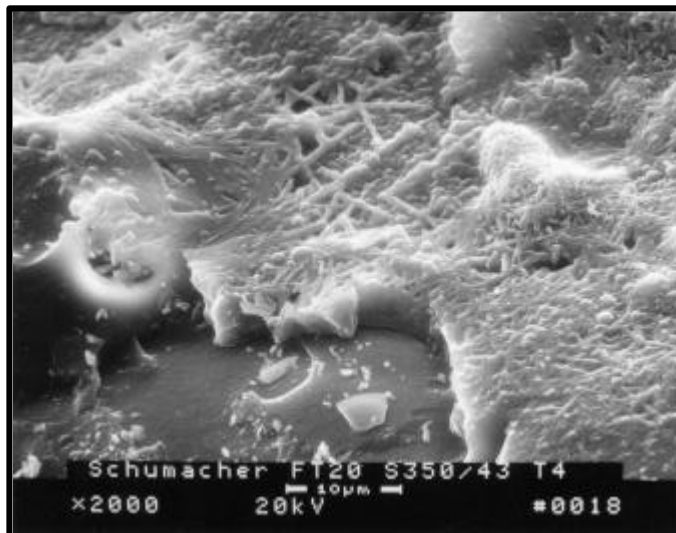


Figure 23 — Formation of mullite and silica within the aluminosilicate binder phase that encapsulated the silicon carbide grains within the PFBC/PCFBC-exposed Schumacher filter matrix.

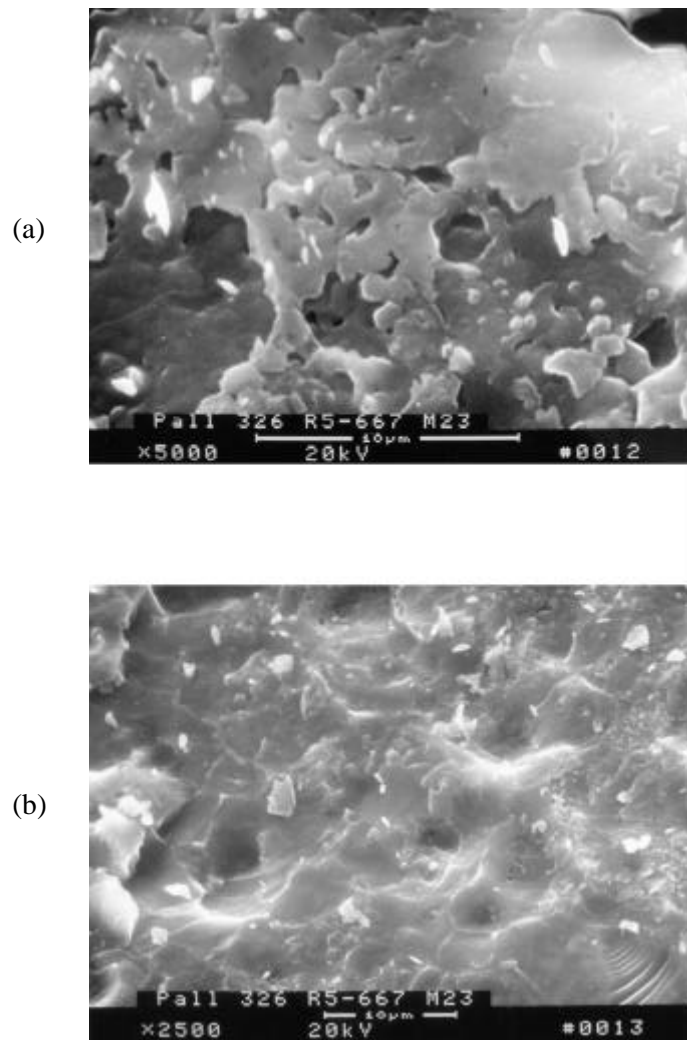


Figure 24 — Morphology of the fresh fractured Pall filter matrix after PFBC/PCFBC operation. (a) Residual silica remaining along the surface of the silicon carbide grains; (b) Pitted surface of the underlying silicon carbide grain after removal of the encapsulating silica-enriched surface layer.

In contrast to the clay bonded silicon carbide filter matrix, Industrial Filter& Pump (IF&P) in conjunction with Filtros Ceramic Products manufactured a recrystallized silicon carbide filter matrix (Figure 28), eliminating the use of a binder phase for holding adjacent grains to each other. When exposed to a simulated PFBC environment during bench-scale testing at SWPC in Pittsburgh, PA, silica once again formed along the outer surface of the recrystallized silicon carbide grains (Figure 29). In localized areas, dendritic mullite features were infrequently observed to have formed along the surface of the simulated PFBC-exposed recrystallized silicon carbide grains (Figure 30).

Alternately Ultramet Inc. developed a chemical vapor deposition (CVD) process for infiltration of silicon carbide along the surface of carbonaceous foams. The Ultramet CVI-SiC open cell reticulated foams consisted of a tortuous path of thin ligaments that formed a three-dimensional interconnected cell structure that had high surface area and minimal backpressure (Figure 31). When initially exposed within the plenum above the SWPC filter array at the American Electric Power (AEP) Tidd demonstration plant in Brilliant, OH, oxidation of the outer surface of the silicon carbide

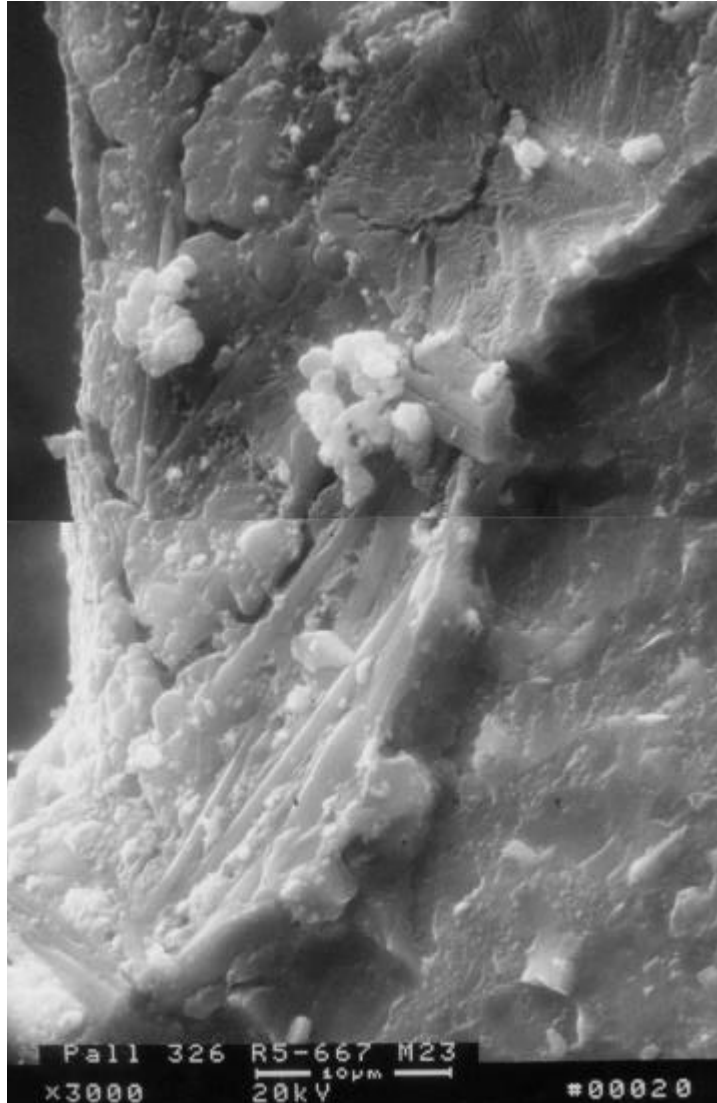


Figure 25 — Formation of a silica-enriched phase along the surface of the silicon carbide grains, as well as at the base of the filter ligaments within the PFBC/PCFBC-exposed Pall and Schumacher filter matrices. Separation or crack formations within the surface silica-enriched phase generally resulted in hexagonal platelets. Once removed, replicate hexagonal features remained along the surface of the underlying silicon carbide grain.

reticulated foam ligaments resulted, leading to the formation of an  $\sim 1 \mu\text{m}$  thick layer of silica. Spalling of the silica-enriched layer subsequently leading to thinning of the reticulated foam ligament during thermal cycling was considered as a potential degradation mechanism of the Ultramet reticulated foam. In order to mitigate oxidation, Ultramet developed a lanthanum aluminate ( $\text{LaAlO}_3$ ) oxidation resistant coating that was applied to the porous foam prior to the addition of the outer surface particulate filtration membrane. Initially the membrane consisted of carbon fibers, but was subsequently changed to mullite that was infiltrated to approximately one pore layer into the filter matrix.

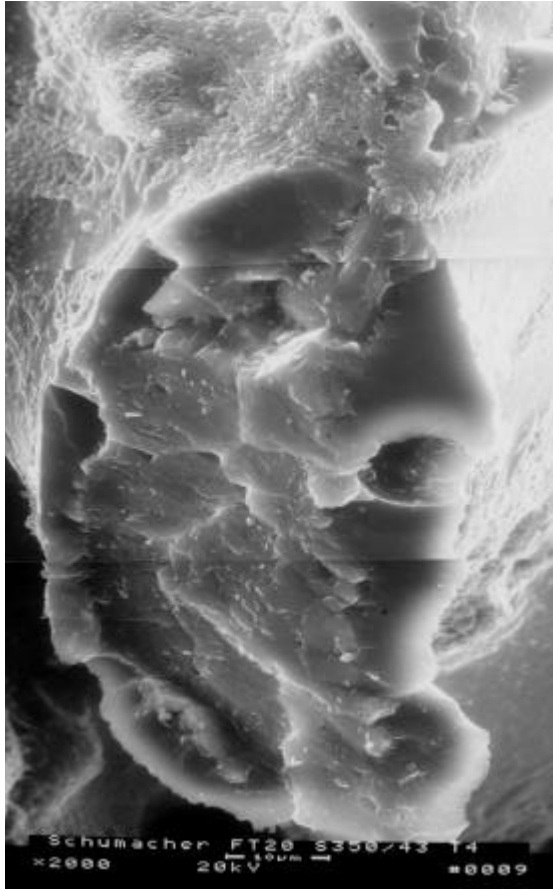


Figure 26 — Crystallization resulting at the base of the fresh fractured ligament in the PFBC-exposed Schumacher filter matrix. Hexagonal silica-enriched platelets formed along the surface of the fresh fractured ligament adjacent to the surface of the underlying silicon carbide grain.

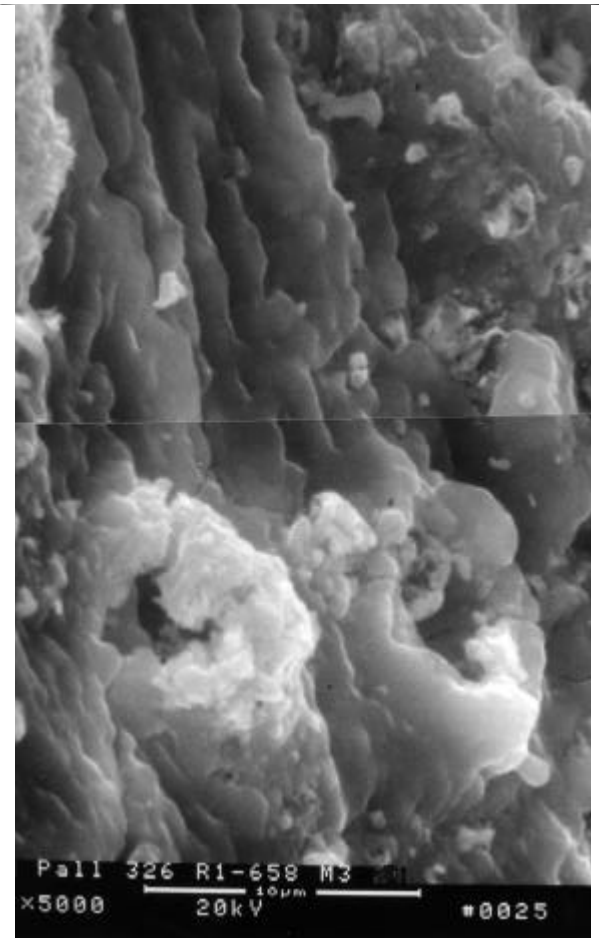


Figure 27 — Outgassing of species along the surface of the PFBC/PCFBC-exposed Pall filter matrix leading to the formation of voids along the silica-enriched crystallized surface.

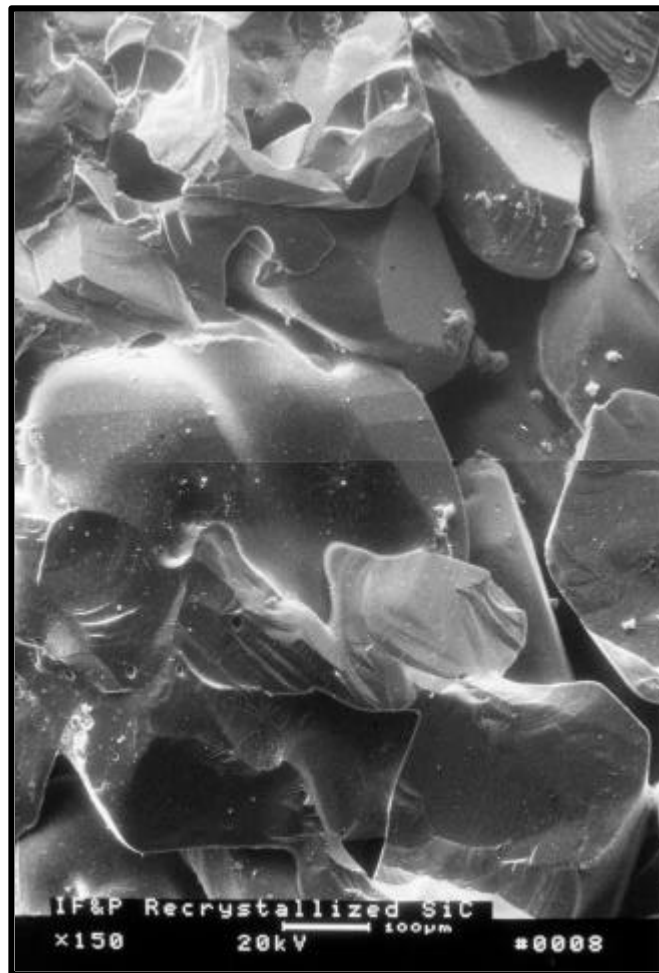


Figure 28 — As-manufactured IF&P recrystallized silicon carbide filter matrix.

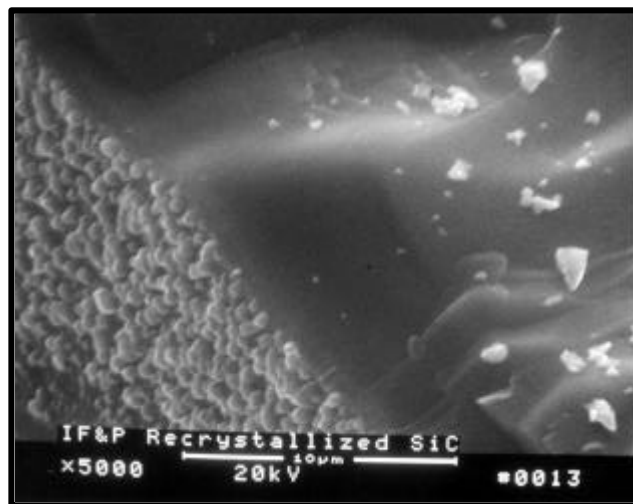


Figure 29 — Formation of silica along the outer surface of the IF&P recrystallized silicon carbide filter matrix.

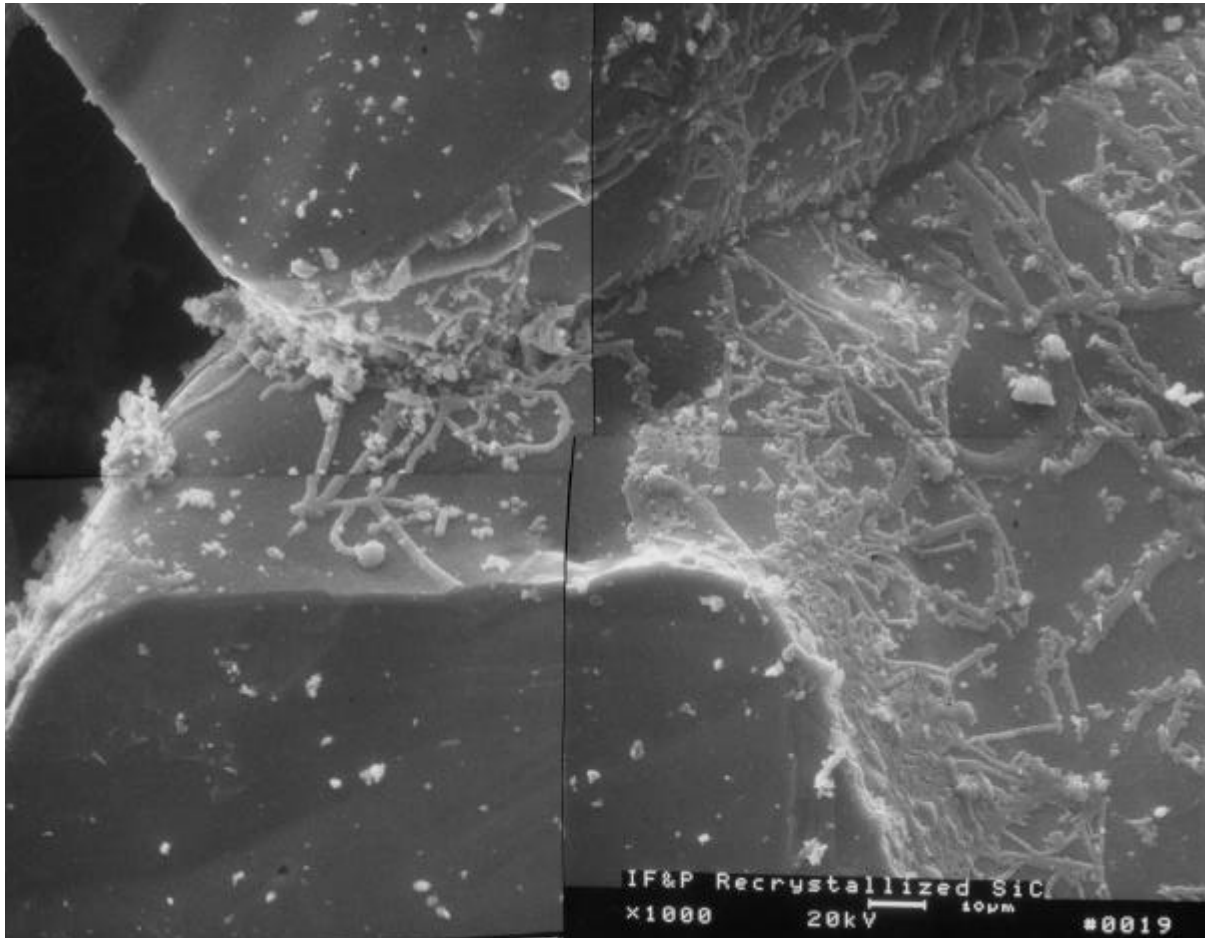


Figure 30 — Dendritic mullite formation along the surface of the simulated PFBC-exposed IF&P recrystallized silicon carbide grains.

Additional suppliers participated during the 1980's in the development of the porous, monolithic, nonoxide-based, filter technology. These included:

- Didier — Clay bonded silicon carbide filter matrix.
- Norton — Recrystallized silicon carbide (Crystar).
- GTE — Cordierite-silicon nitride. The matrix consisted of 25% cordierite ( $\text{Mg}_2\text{Al}_4\text{Si}_5\text{O}_{18}$ ) to enhance densification of the  $\text{Si}_3\text{N}_4$  through liquid phase sintering. X-ray analysis of the matrix identified the presence of  $\beta\text{-Si}_3\text{N}_4$ , secondary contributions of silicon oxynitride ( $\text{Si}_2\text{ON}_2$ ), and traces of cordierite ( $\text{Mg}_2\text{Al}_4\text{Si}_5\text{O}_{18}$ ). Approximately 10  $\mu\text{m}$  pores were present within the filter matrix.
- AiResearch — Reaction bonded silicon nitride (RBSN). This matrix was produced by nitriding silicon powder. Grain boundary phases were not formed within the densely packed 1-20  $\mu\text{m}$  particles in the RBSN filter matrix. Whisker-like needle formations of

$\alpha$ - $\text{Si}_3\text{N}_4$  resulted between the  $\beta$ - $\text{Si}_3\text{N}_4$  grains. X-ray diffraction analysis identified the presence of both phases, as well as minor contributions of  $\alpha$ -iron and possibly an amorphous phase.

- AiResearch — Sintered silicon nitride (SSN). Porosity within the high purity SSN filter matrix was achieved through the formation of nearly spherical  $>50$ - $150\ \mu\text{m}$  pores that were filled with the whisker-like  $\alpha$ - $\text{Si}_3\text{N}_4$  phase.

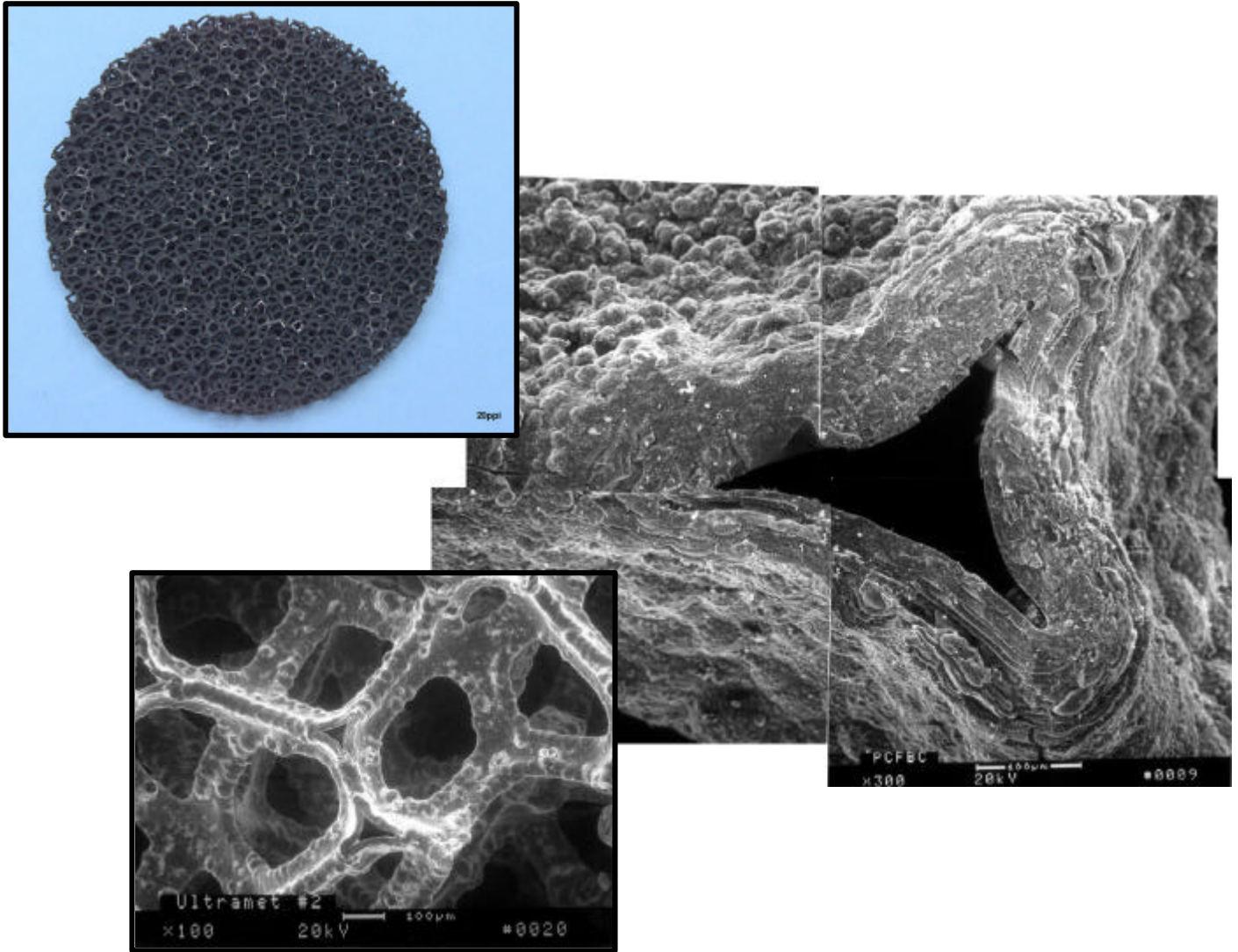


Figure 31 — As-manufactured Ultramet CVI-SiC reticulated foam.

### 2.3 Second-Generation Oxide-Based Ceramic Matrices

DuPont<sup>3</sup> PRD-66 candle filters consisted of an ~7 mm thick structural support filament wound filter wall. An open filament winding process was typically used to form the diagonal weave or chevron pattern in the structural support filter matrix (Figure 32). Each polycrystalline, refractory, oxide-based, filament in the structural support wall was ~200  $\mu\text{m}$  in diameter, and contained numerous ~7-17  $\mu\text{m}$  diameter fiber replicas (Figure 33). A thin single filament membrane layer was wrapped along the outer surface of the support matrix, producing a lightweight, bulk or depth vs barrier filter element.

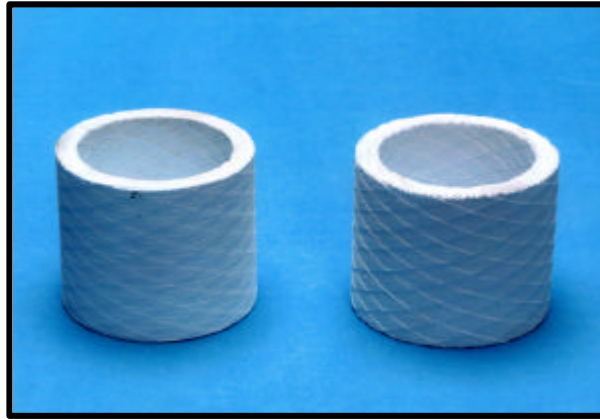


Figure 32 — DuPont PRD-66 filament wound filter matrix.

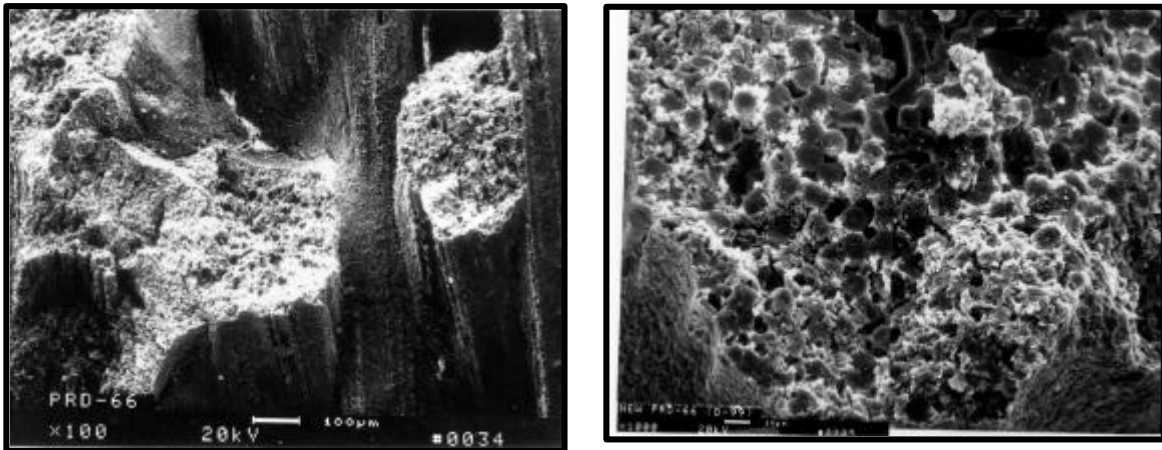


Figure 33 — Filaments contained within the as-manufactured DuPont PRD-66 filter matrix.

A coarse slurry of alumina-enriched grains (i.e., ~75-100  $\mu\text{m}$ ) was used to sinter bond adjacent filament bundles together along the outer surface membrane of the as-manufactured DuPont PRD-66 filter elements. A finer slurry of alumina-enriched grains (i.e.,  $\leq 5-7$   $\mu\text{m}$ ) was used in the structural support filament winding process to

<sup>3</sup> Currently GE Power Systems.

- Coat and fill the voids along and between the outer surface of fiber replicas in the filament bundles.
- Sinter bond adjacent fiber replicas to each other.
- Assist in bonding the external single filament to the underlying structural support filaments.

The intersecting wound filaments in the structural support filter wall were sinter bonded to each other via slurry matrix grains, thus providing strength to the filter matrix. As along the outer surface membrane, slurry generally filled the crevices between intersecting filaments, and infiltrated into the filament bundles, bonding adjacent fiber replicas to each other. When the as-manufactured DuPont PRD-66 filter wall was cross-sectioned, discrete and coalesced fiber replicas were seen to be present within the filament support matrix (Figure 34). Discrete fiber replicas tended to be surrounded by the infiltrated alumina-enriched slurry matrix. Where the infiltrated slurry matrix was absent, coalescence of the fiber replicas tended to result. Crystalline features were generally observed along the outer surface of the fiber replicas, as well as along their fresh fractured surfaces (Figure 35).

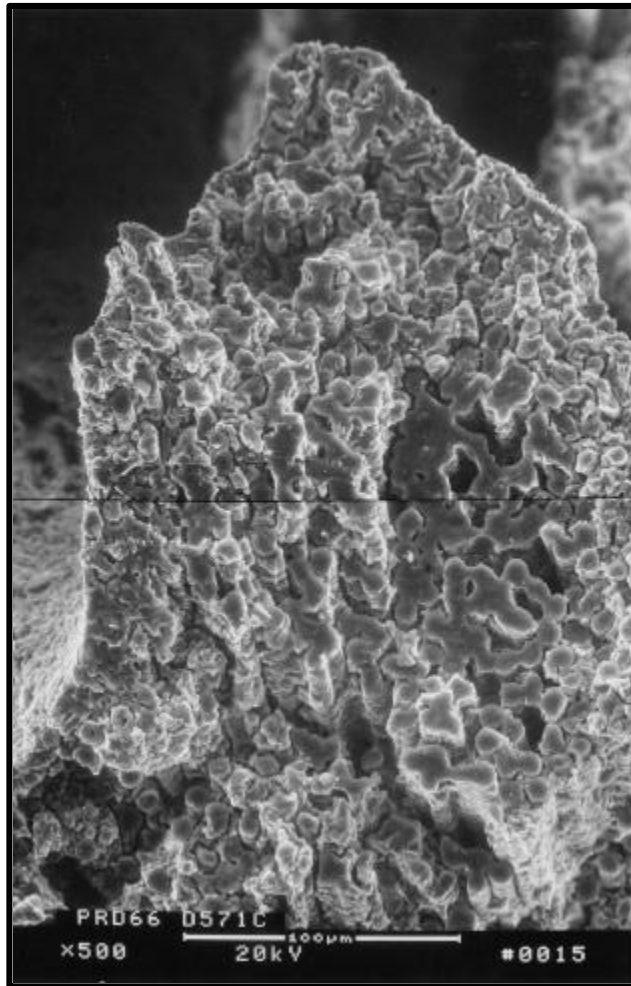


Figure 34 — Cross-sectioned filament within the DuPont PRD-66 filter matrix.

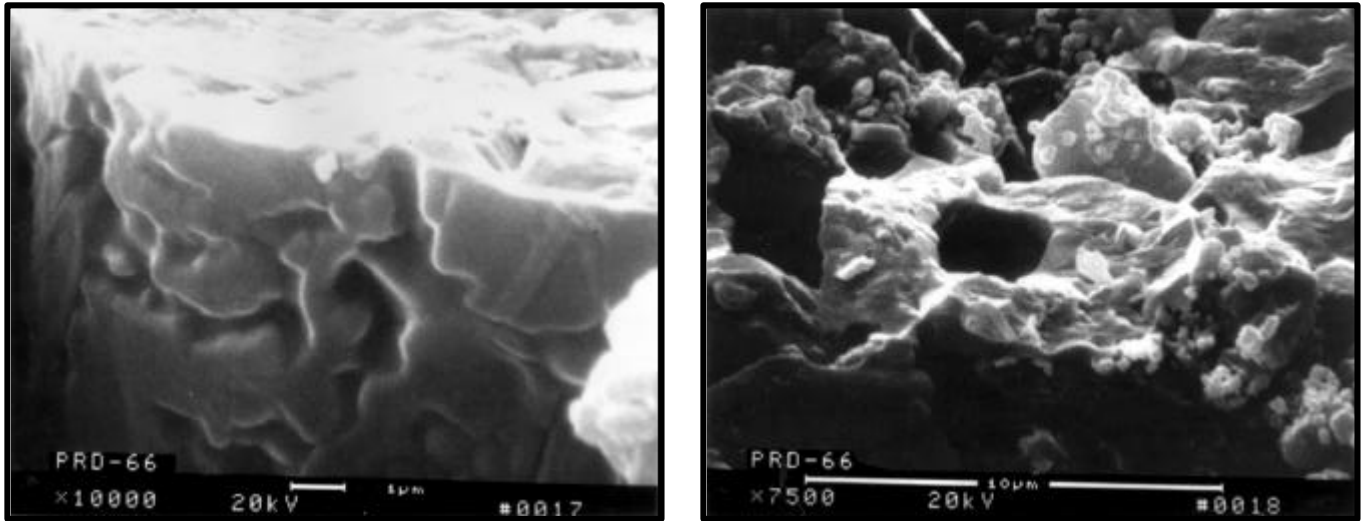


Figure 35 — Crystalline features along the outer surface of the fiber replicas of the DuPont filter matrix. Void formations along the center of the fiber replicas were observed.

X-ray diffraction analysis identified the composition of the as-manufactured DuPont PRD-66 filter matrix as ~30% cordierite ( $Mg_2Al_4Si_5O_{18}$ ), 50% corundum ( $Al_2O_3$ ), with secondary and minor concentrations of cristobalite ( $SiO_2$ ), mullite ( $3Al_2O_3 \cdot 2SiO_2$ ), and an amorphous phase. Due to the differences in thermal expansion of corundum, cordierite and mullite, a microcracked structure formed during high firing of the filter matrix.

As part of the hot gas filter development effort during the mid 1990's, McDermott<sup>4</sup> manufactured a continuous fiber ceramic composite (CFCC) via a filament winding process using Nextel™ 610 fiber (alumina filament bundles), Saffil chopped fibers (i.e., 95-96% alumina; silica), and an  $Al_2O_3$  matrix. The diagonally wound Nextel™ 610 filament fiber bundles served as the structural support matrix through the ~5 mm thick McDermott CFCC filter wall (Figure 36). Interspersed throughout the filter wall were chopped fibers and a bonding matrix that provided the surface and bulk filtration characteristics of the filter element. As a result of the manufactured architecture of the chopped fiber and bonding matrix, a membrane was not required in order to achieve particulate removal specifications.

When characterized, the diagonally wound filament fiber bundles were generally seen to be embedded within a chopped fiber matrix along the outer surface of the as-manufactured McDermott CFCC candle filter (Figure 37). A mud cracked alumina matrix was also present along the outer surface of the Nextel™ 610 and chopped Saffil fibers. Typically there appeared to be a higher concentration of the bonding matrix along the chopped fibers that were present along the o.d. surface of the McDermott CFCC filter element in comparison to the limited quantity of bonding matrix that was present along the chopped fibers along the i.d. wall of the candle filter. The chopped fibers along the i.d. wall appeared to be randomly held together through packing and/or limited bonding via submicron particles or agglomerates. Along the i.d. wall of the candle filter, chopped fibers were present as a felt-like layer that primarily covered the underlying wound filament fiber bundles.

<sup>4</sup> Formerly Babcock and Wilcox.



Figure 36 —Nextel™ filament bundles contained within the McDermott CFCC candle filter.

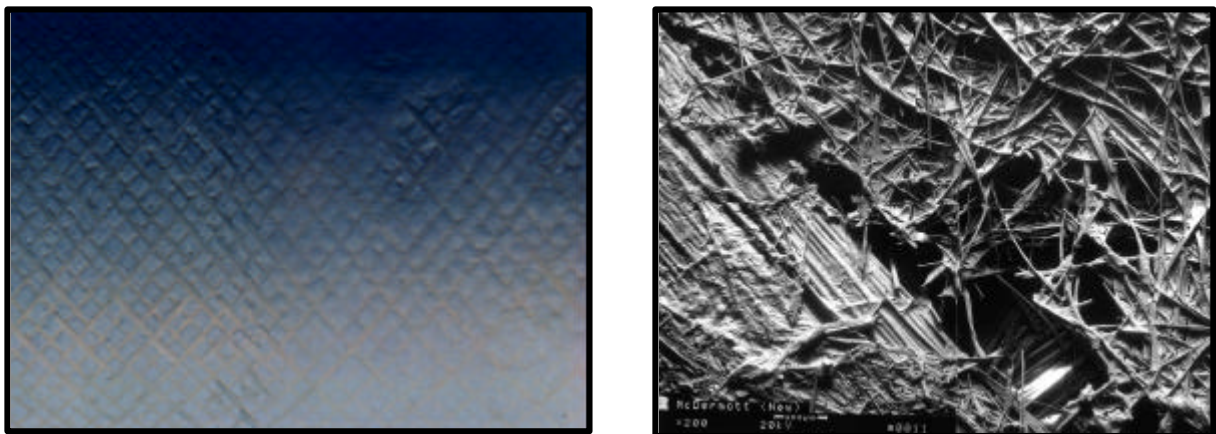


Figure 37 — Filament fiber bundles embedded within the chopped fiber matrix along the o.d. surface of the as-manufactured McDermott CFCC filter element.

The Techniweave<sup>5</sup> CFCC filter element consisted of Nextel™ 610 (30-40% mullite; 60-70%  $\alpha$ -Al<sub>2</sub>O<sub>3</sub>) or Nextel™ 720 (70-80% mullite;  $\alpha$ -Al<sub>2</sub>O<sub>3</sub>; trace ternary silicate) fibers that were woven into a two dimensional architecture. In order to achieve a high particulate filtration collection efficiency, an alumina slurry was infiltrated into the porous structure, forming a low porosity external outer surface membrane (Figure 38). In contrast, discrete filament bundles were evident along the inner or pulse cycled surface of the Techniweave CFCC filter element.

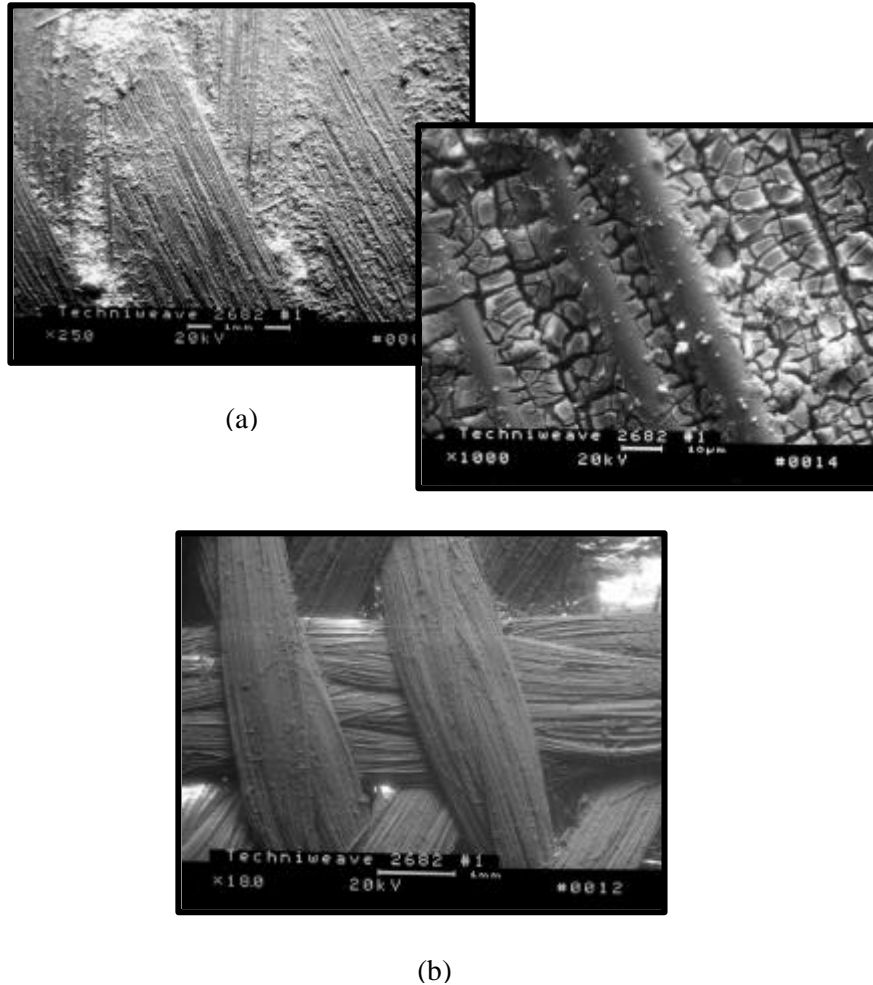


Figure 38 — As-manufactured Techniweave CFCC filter element. (a) Outer surface; (b) Inner or pulse cycled surface of the filter element.

Additional suppliers participated during the 1990's in the development of porous, 2<sup>nd</sup> generation, oxide-based CFCC filter elements. These included:

- 3M — Infiltration of an aluminosilicate phase on an aluminosilicate Nextel™ 610 or Nextel™ 720 triaxial braid perform; Chopped alumina-enriched filtration mat layer; Open mesh Nextel™ 610 or Nextel™ 720 outer confinement layer (Figure 39).
- Americom — Nextel™ filament with oxide infiltrate.

<sup>5</sup> Currently Albany International Techniweave, Inc.

## 2.4 Second-Generation Nonoxide-Based Ceramic Matrices

The 3M CVI-SiC continuous ceramic fiber composite (CFCC) filter elements consisted of three layers — an open mesh outer confinement layer, a middle filtration layer, and an inner structural support triaxial braided layer (Figure 39). Within the confinement and filtration mat layers, an  $\sim 1\text{-}2\ \mu\text{m}$  thick layer of silicon carbide was chemically infiltrated along the surface of Nextel™ 312 or alumina-based fibers, while an  $\sim 100\ \mu\text{m}$  thick layer of silicon carbide was deposited along the Nextel™ 312 triaxial braid in the support matrix (Figure 40).

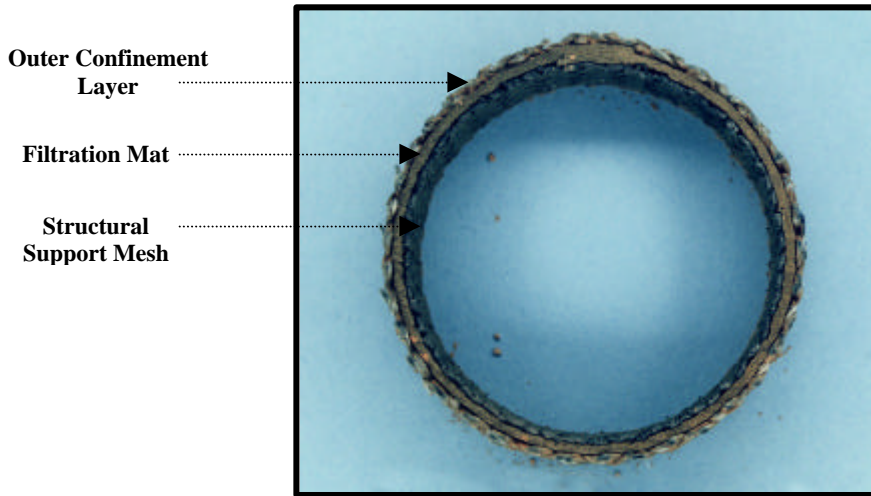


Figure 39 — 3M CVI-SiC filter matrix.

When the 3M CVI-SiC filter element was installed and operated in either the  $825^{\circ}\text{C}$  ( $1520^{\circ}\text{F}$ ) PFBC filter array at the AEP Tidd demonstration plant in Brilliant, OH, or in the  $850^{\circ}\text{C}$  ( $1560^{\circ}\text{F}$ ) PCFBC filter array at the Foster Wheeler Karhula test facility, a color change was readily evident along the outer confinement and filtration mat layers (Figure 41). After 387 hours of PCFBC operation, the outer confinement layer appeared to be white (excluding the presence of ash fines), while the filtration mat layer appeared to be a light to medium gray. The triaxial support braid retained its as-manufactured dark black appearance. Scanning electron microscopy/energy dispersive x-ray analysis (SEM/EDX) characterization of the PCFBC-exposed 3M CVI-SiC composite filter matrix confirmed that removal of the SiC layer which initially encapsulated the Nextel™ 312 fibers in the outer confinement layer had occurred. Characterization of the lapped filtration mat indicated that oxidation of the  $2\ \mu\text{m}$  thick CVI-SiC shell had also occurred. As a result, an  $\sim 1\ \mu\text{m}$  thick oxygen-enriched region formed along the inner surface of the CVI-SiC shell, bonding the shell to the filtration mat fibers. Bonding of the oxygen-enriched CVI-SiC shell to the fibers ultimately reduced the fracture toughness of the composite matrix layer. After 2815 hours of PFBC operation at Tidd, the  $2\ \mu\text{m}$  CVI-SiC layer that infiltrated into the triaxial braid, coating individual fibers, similarly formed an outer  $\sim 1\ \mu\text{m}$  thick  $\text{SiO}_2$ -enriched layer that frequently contained cracks (Figure 41). After 2815 hours of exposure to the PFBC process gas environment, only  $\sim 21\%$  of the initial strength of the triaxial support braid remained. Neither the filtration mat nor the outer confinement layers were expected to significantly contribute to the overall strength of the 3M CVI-SiC composite filter matrix.



Figure 40 — CVI-SiC layer deposited along the outer surface of the 3M Nextel™ 312 structural support triaxial braid.



Figure 41 — Sections of the 3M CVI-SiC composite candle filter after PFBC or PCFBC operation.

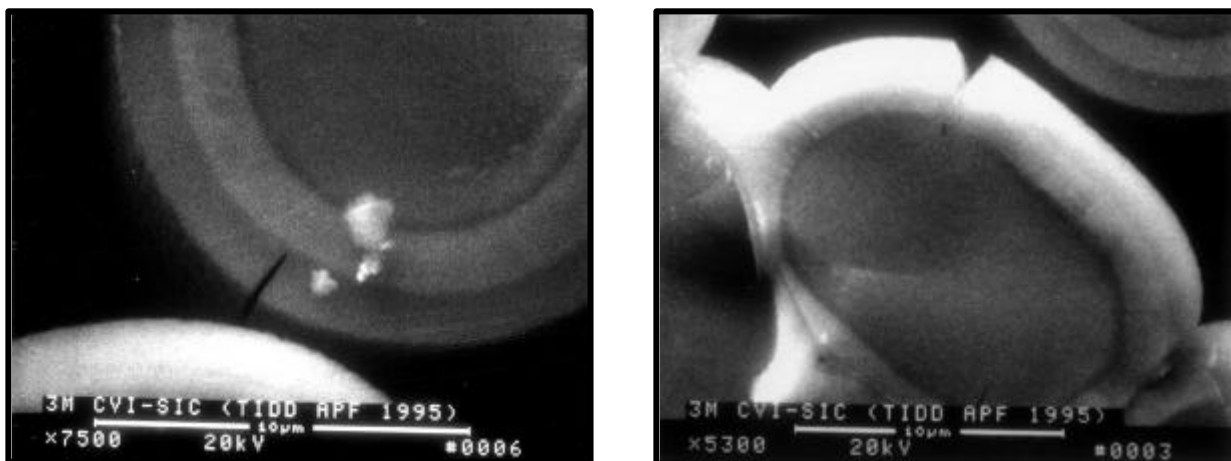
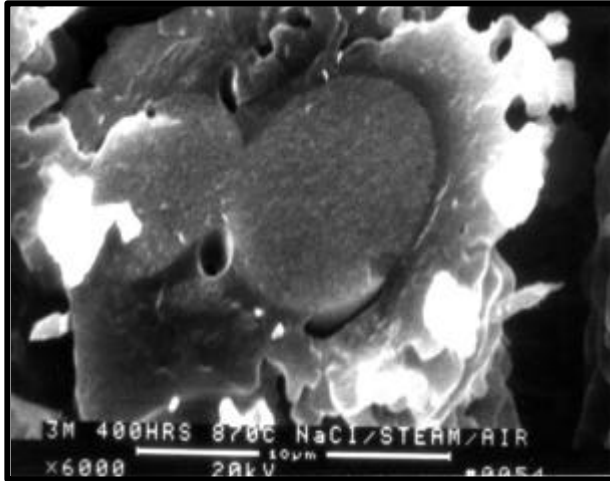


Figure 42 — Crack formations along the silica-enriched infiltrated layers that surrounded the Nextel™ 312 fibers in the triaxial support braid of the 3M composite filter matrix after 2815 hours of exposure above the Siemens Westinghouse APF system tubesheet at AEP. Cracks formations resulted from volume expansion of the silica, thermal mismatch with the underlying SiC layer, and plant startup/shutdown cyclic operation.

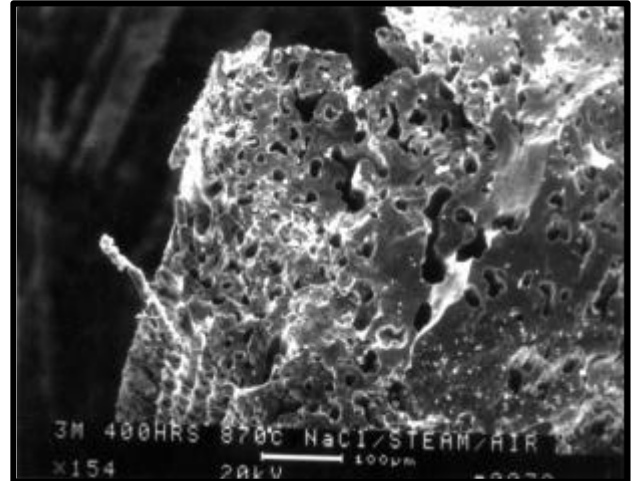
Bench-scale testing conducted at SWPC Science and Technology Center (STC) exposed 3M CVI-SiC mini-candles to either an 870°C (1600°F) 5-7% steam/air or a 20 ppm alkali/5-7% steam/air flow-through environment. Although the mini-candles were intact after 400 hours of bench-scale testing, the outer confinement layer was very brittle, and in several locations, the fiber bundles were broken or missing. SEM/EDX analysis indicated that the ~1-2 µm thick SiC layer that had been deposited along the outer surface of the filtration mat fibers had been removed. Exposure of the 3M CVI-SiC composite filter matrix to 20 ppm NaCl/5-7% steam/air environment led to the formation of a “melt-like” phase between the alumina filtration mat fibers and the remaining encapsulating CVI-SiC shell (Figure 43). Within the fiber bundles in the outer confinement layer and triaxial braid, similar oxidation of the infiltrated CVI-SiC layer led to bonding and coalescence of adjacent Nextel™ fibers, ultimately leading the loss of fracture toughness and embrittlement of the 3M CVI-SiC architecture.

In contrast to the 3M CVI-SiC composite filter element, the DuPont SiC-SiC candle was fabricated from a two-ply Nicalon™ felt that was formed into an ~1.4 m cylindrical tube. A plug as inserted into one end of the cylinder to form a closed end cap, while additional felt was wrapped around the other open end of the cylindrical tube to form the flange. Silicon carbide was chemically vapor infiltrated (CVI) through both Nicalon™ felt layers, forming a strengthened matrix, as well as bonding the felt wrap and/or plug to the filter body. Fine grain silicon carbide grit was applied with a polymeric resin slurry along the outer surface of the filter element, forming the external membrane.

Subsequently DuPont manufactured SiC-SiC composite candle filters using a hybrid architecture (Figure 44). An open mesh Nicalon™ screen served as the candle filter support structure. A Nicalon™ single-ply felt was layered over the mesh, and the unit was subsequently subjected to silicon carbide CVI. A silicon carbide grit was applied to the outer surface of the CVI-SiC felt in order to form an effective particulate barrier filter membrane. Since Nicalon™ is primarily a silicon carbide fiber which contained oxygen, and silicon carbide was deposited along the fiber rigidizing the perform, the material was designated as a SiC-SiC composite filter matrix.



(a)



(b)

Figure 43 — Morphology of the cross-sectioned 3M CVI-SiC composite filter material after 400 hours of exposure at 870°F (1600°F) to 20 ppm NaCl/5-7% steam/air. (a) Alumina fibers within the filtration media; (b) Nextel™ fibers within the structural support triaxial braid. Oxidation of the underlying SiC encapsulating layer, as well as along adjacent fibers led to embrittlement of the matrix during exposure at high temperature to an oxidizing process gas environment.

The DuPont SiC-SiC CFCC composite filter matrix consisted of an ~10-20  $\mu\text{m}$  thick silicon carbide layer that was chemically vapor infiltrated along an ~2-5  $\mu\text{m}$  thick interface coating layer that encapsulated ~15  $\mu\text{m}$  diameter Nicalon™ fibers. Several issues were initially raised as to the oxidative stability of the SiC-SiC matrix, and in particular the stability of the interface coating and Nicalon™ fibers.

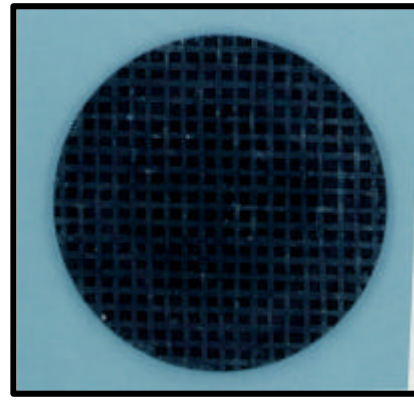
After 400 hours of exposure to an 870°C (1600°F) 5-7% steam/air or 20 ppm NaCl/5-7% steam/air environment, depletion of the interface coating resulted. A mottled crystalline phase formed along the SiC-SiC outer surface which was identified by EDX analysis to contain silicon and oxygen (i.e., 1:1 atomic percent basis). The Si-O phase formed a noncontinuous layer along the surface of the SiC-SiC matrix. The presence of gas phase sodium enhanced surface oxidation of the SiC-SiC matrix, resulting in areas that were enriched with  $\text{SiO}_2$ . Sorption of sodium into the  $\text{SiO}_x$  or  $\text{SiO}_2$  layer that covered the SiC-SiC matrix was not detected by EDX analysis.

In contrast, the fine grained SiC membrane coating of the DuPont SiC-SiC matrix tended to form a sodium-enriched glaze during high temperature alkali/steam/air exposure, which reduced gas flow permeability through the filter disc. The glazed surface would potentially serve as a collection site for adherence of ash fines at process operating temperatures, which may ultimately cause blinding of the filter element surface.

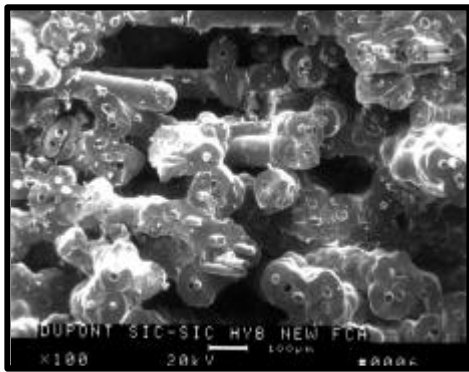
When compared with the strength of the as-manufactured hybrid matrix, the residual strength of the alkali-exposed DuPont SiC-SiC architecture was reduced by ~40% along the mesh or pulse cycled surface of the matrix, while the membrane coated surface experienced an ~58% reduction in strength after 400 hours of high temperature exposure. Based on the load vs deflection curves that were generated during high temperature flexural strength testing, the fracture toughness



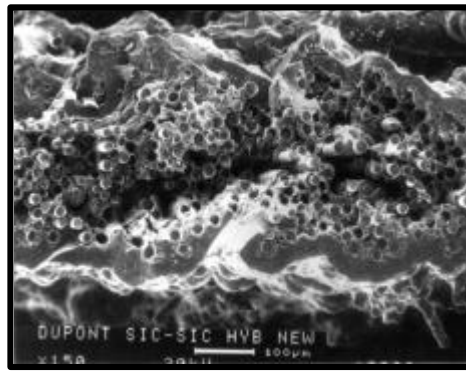
(a)



(b)



(c)



(d)



(e)

Figure 44 — DuPont SiC-SiC CFCC filter architecture. (a) Felt layer surface; (b) Mesh screen support surface; (c) As-manufactured single-ply layer; (d) As-manufactured mesh screen support layer; (e) Presence of an interface layer encapsulating the Nicalon™ fibers in the as-manufactured single-ply felt layer.

of the low fiber volume DuPont SiC-SiC filter matrix decrease, leading to formation of an embrittled matrix.

In order to demonstrate the potential viability and thermal fatigue resistance of the DuPont SiC-SiC CFCC matrix, candle filters were subjected to 3514 accelerated pulse cleaning cycles during 197 hours of operation in 843°C (1550°F) SWPC PFBC simulator test facilities in Pittsburgh, PA. As shown in Figure 45, the interface layer that initially surrounded the Nicalon™ fibers in the single-ply felt layer was removed. Crack formations resulted along the outer periphery of the fibers, and typically had rounded tips, as well as segmented “step-like characteristics.

“Halo-like” areas were readily evident along the periphery of the Nicalon™ fibers in the DuPont SiC-SiC single-ply felt. These areas were generally enriched with oxygen and effectively

demarcated the location to which cracks penetrated. Bonding of the Nicalon™ fiber to the inner surface of the CVI-SiC encapsulating shell often resulted.

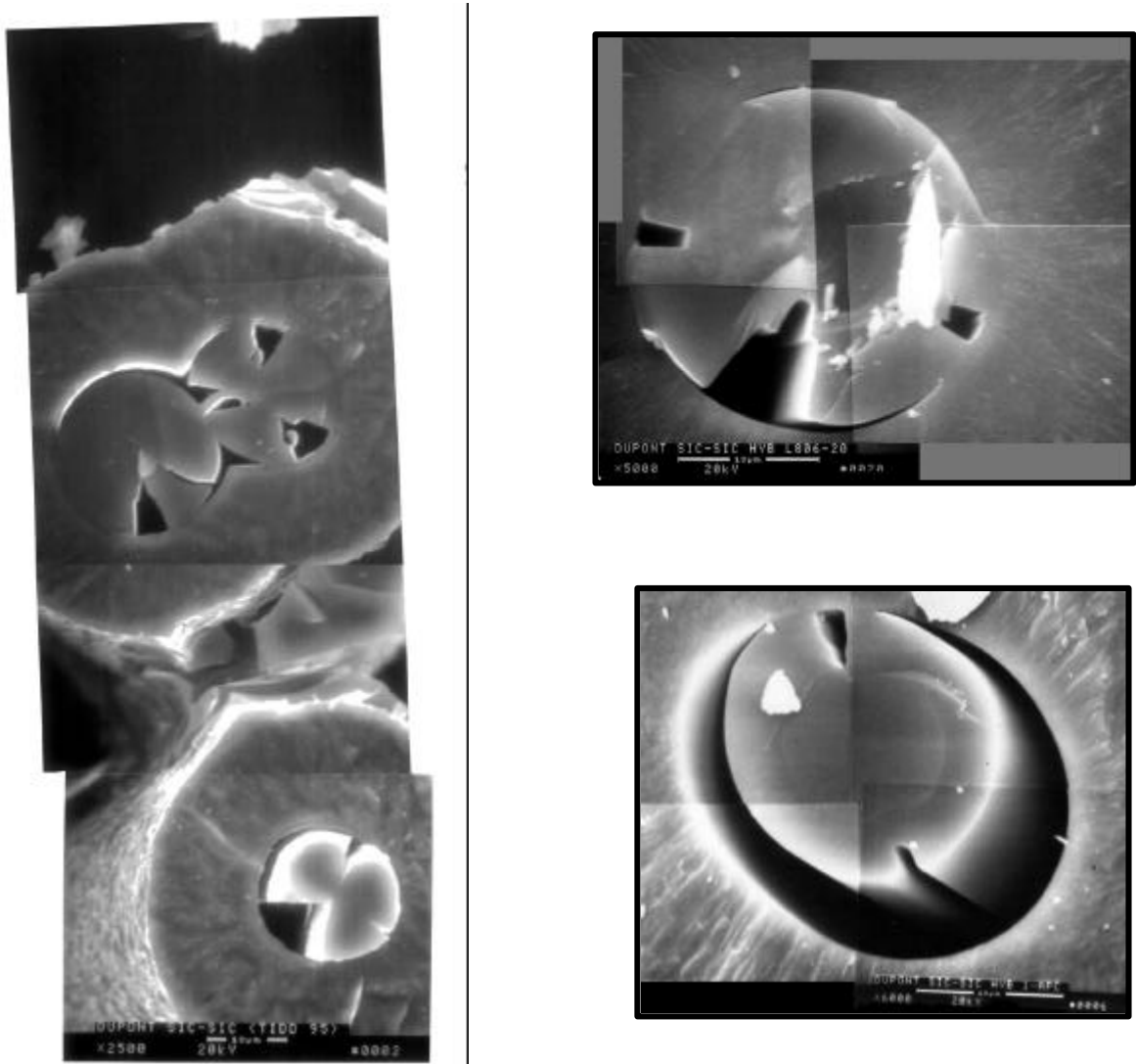


Figure 45 — Morphology of the Dupont SiC-SiC CFCC hybrid filter matrix after accelerated pulse cycle testing in SWPC's PFBC simulator test facility.

Within the mesh screen support layer, thin CVI-SiC bands that followed the contour of the Nicalon™ fibers and perhaps the interface layer were evident. Near the periphery of the fiber bundle or tow (i.e., adjacent to the CVI-SiC encapsulating layer), as well as within the bundle, irregularly shaped Nicalon™ fibers were evident. Melting of the fibers was frequently observed, as well as mottling of the fiber surface. Adjacent to the CVI-SiC encapsulating layer, the melted fibers formed cracks. Void formations that were observed in the fractured mesh screen support layer may have resulted from fiber pullout during sample preparation or alternately reflected removal of the interface phase during exposure to simulated PFBC process operating conditions.

The Nicalon™ fibers in the mesh screen support did not exhibit crack formations along their periphery.

After 197 hours of accelerated pulse cycle testing, oxidation of the outer surface of the CVI-SiC encapsulating layer resulted. Similarly, a reduction in the fracture toughness of the matrix was identified which was attributed to removal of the interface layer in the single-ply felt and mesh screen support layers, and to sintering of the Nicalon™ fibers in the mesh screen support layer.

After ~800 hours of steady-state, thermal transient, and accelerated pulsing of the DuPont SiC-SiC candle filters in the SWPC PFBC simulator test facility which contained ash, as well as gas phase alkali, further changes were evident within the filter material. These included swelling or a volume expansion of the Nicalon™ fibers resulting from oxidation. The fibers completely, or nearly completely filled the void in the CVI-SiC encapsulating shell. Bonding of the fibers to the inner wall of the CVI-SiC shell was also evident within the DuPont single-ply felt layer.

Additional suppliers participated during the 1990's in the development of porous, 2<sup>nd</sup> generation, nonoxide-based CFCC filter elements. These included:

- Textron — Nitride bonded silicon carbide (NBSC)
- Textron — Nitride bonded silicon nitride (NBSN)
- Textron — Reaction bonded silicon nitride (RBSN).

At Textron, 33 μm, carbon monofilaments served as the substrate for chemical vapor deposition (CVD) of silicon carbide. The resulting CVD monofilaments were 100 μm in diameter, and were enriched with outer alternating layers of carbon, silicon, and carbon. Single strands of the CVD monofilament were subsequently filament wound along a mandrel, prior to infiltration with a silicon carbide and silicon powder slurry that contained microballoons. After winding, the infiltrated matrix was subjected to nitridation and high firing. During production of the filter matrix media, microballoons were used to provide porosity within the material, while nitridation of the silicon powder was used to form the bonding phase between the silicon carbide powder and the monofilament surfaces.

### 3. FIELD TESTING

#### 3.1 Overview

In conjunction with the hot gas filter material development efforts, emphasis at the Siemens Westinghouse Power Corporation (SWPC) in the 1990's was focused on the design and operation of Advanced Particulate Filtration (APF) systems, and initiation of field-tested material surveillance programs. At the American Electric Power (AEP) Tidd demonstration plant in Brilliant, OH, the SWPC advanced particulate filtration (APF) system housed 384 commercially available, 1.5 m porous ceramic candle filters, which were subjected to PFBC conditions (Figure 46).<sup>6</sup> Similarly, 128 commercially available, 1.5 m candles were installed and operated in the SWPC APF at the Foster Wheeler PCFBC pilot-scale test facility in Karhula, Finland. The total operating service life of surveillance filters that were installed at these facilities is shown in Table 3. In 1997, the opportunity to continue testing commercially available monolithic elements, and introduce the utilization of alternate monolithic and advanced CFCC candles occurred at Karhula.

Testing was similarly conducted in the SWPC Particle Collection Device (PCD) at the Southern Company Services (SCS) test facility in Wilsonville, AL. Achieving three years of operational filter element life was the primary goal of the SWPC hot gas filter material development and component qualification programs. Efforts to demonstrate operation of the plant and filter life were also focused on the SWPC APF system at the Sierra Pacific Power Company (SPPC), Piñon Pine, Tracey No. 4 Station in Reno, NV, which housed 748 candle filters. Commissioning of the SPPC integrated gasification combined cycle (IGCC) demonstration plant was initiated in 1997.

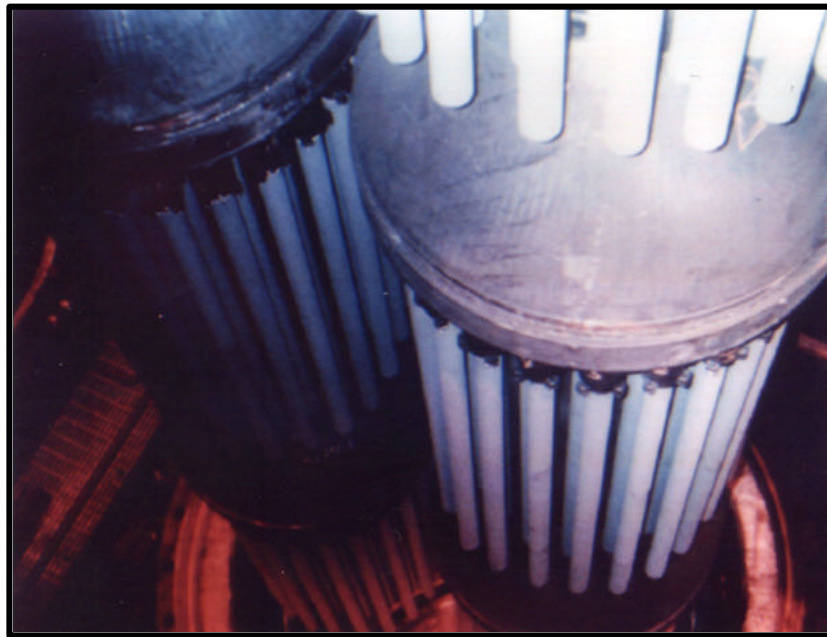


Figure 46 — SWPC APF system at the AEP PFBC Tidd demonstration plant in Brilliant, OH.

<sup>6</sup> Select filter elements which had been operated at the AEP Tidd PFBC test facility were removed, installed and operated in the Foster Wheeler PCFBC test facility in Karhula, Finland. Subsequently, select PFBC/PCFBC field-exposed filter elements were installed in SWPC's PFBC simulator test facility in Pittsburgh, PA, for extended accelerated life testing.

**TABLE 3  
FIELD AND EXTENDED LIFE TESTING**

Filter Supplier & Matrix	Maximum Operating Time, Hrs		Equivalent Exposure Time, Hrs
	PFBC — AEP —	PCFBC — FW Karhula —	Field & Accelerated Testing
Schumacher F40	5855	227 (1)	
Schumacher FT20	1705	2201 (2)	11080; 11080
Pall Vitropore 442T	1705	1341 (1)	
Pall 326		2201 (2)	9662; 11080
Coors P-100A-1 Alumina/Mullite	2815	716 (1) 2201 (2) 3311 (3)	8485; 12211 13356
3M CVI-SiC	1705	627 (4)	
DuPont PRD-66	1705	581 (5)	7517 (6)
3M Oxide CFCC			
McDermott Oxide CFCC		581 (5)	10626
Techniweave Oxide CFCC			
Blasch Mullite Bonded Alumina		581 (5)	10626
Ensto		581 (5)	5611
IF&P REECER			5030 (6)
Other		342 (5)	

(1) 1992-1994 Test Campaign.

(2) 1995-1997 Test Campaign.

(3) 2201 Hrs of operation under PCFBC conditions and 1110 Hrs of operation under PFBC conditions.

(4) 1995-1996 Test Campaign.

(5) 1997 Test Campaign.

(6) New element without field exposure.

### 3.2 Foster Wheeler PCFBC Test Campaigns

Hot gas filtration testing was initiated in the SWPC APF in November 1995 at the Foster Wheeler PCFBC test facility in Karhula, Finland. Three test campaigns were conducted utilizing 1.5 m, high temperature, creep resistant, clay bonded silicon carbide Schumacher Dia Schumalith FT20 and Pall 326 candles in the top and middle filter arrays, respectively, and a mixture of the 1.5 m Coors P-100A-1 alumina/mullite and 1.5 m 3M CVI-SiC composite filter elements in the bottom array (Table 4). In addition, five Coors P-100A-1 alumina/mullite candle filters that had been operated for a period of 1110 hours in the SWPC APF system at the AEP PFBC Tidd demonstration plant in Brilliant, OH, were installed in the bottom array. A total of 1166 hours of hot gas filtration testing was achieved during the 1995-1996 test program in Karhula, Finland.

During Test Segment 1 (TS1-95), the SWPC APF was filled with 112 filter elements, and was operated for a period of 153 hours at temperatures of 826-853°C (1520-1565°F). Illinois No. 6 coal and Linwood limestone were utilized as the feed and sorbent materials. After an initial 22 hours of commissioning, the pressure vessel was slow cooled as a result of plant maintenance, and the three filter arrays were inspected. The 3M CVI-SiC composite candles that were observed to be somewhat loose within the metal filter holders were remounted and tightened to assure adequate sealing.

**TABLE 4**  
**SUMMARY OF PCFBC TESTING IN 1995-1996**

Test Segment	1 (11/1995-12/1995)	2 (2/1996-4/1996)	3 (8/1996-10/1996)
Coal	Illinois No. 6 (Sparta)	Illinois No. 6 (Sparta)	Illinois No. 6 (Sparta)
Sorbent	Linwood Limestone	Linwood Limestone	Linwood Limestone Iowa Industrial Limestone Resized Linwood Limestone
Number of Candles	112	112	128
Schumacher FT20	32-35	35	46
Pall 326	32-35	35	45
Coors Alumina/Mullite	24 (5) - 42 (5) <sup>(a)</sup>	33 (5) <sup>(a)</sup>	32 (4) <sup>(a)</sup>
3M CVI-SiC Composite	24-0	9	5
Operating Hours (Coal)	153 <sup>(b)</sup>	387	626
Operating Temperature, °C (°F)	826-853 (1520-1565)	818-860 (1505-1580)	838-860 (1540-1580)
Operating Pressure, bar	10.7-11.1	10.6-11.3	10.5-10.7
Nominal Face Velocity, cm/s	3.5-4.1	3.1-4.2	3.0-3.4
Inlet Dust Loading, ppmw	12,000-13,500	12,000-15,500	11,000-12,500
d <sub>50</sub> , μm (Malvern)	NA	NA	23 (20-26)

(a) Number of installed PFBC-exposed Coors filter elements (AEP Test Segment 5) shown in parentheses.

(b) Thirty-five hours of initial operation prior to removal of the 3M CVI-SiC composite filters, followed by 118 hours of continuous operation.

NA: Not available.

Testing was reinitiated for a period of 35 hours, prior to a second maintenance outage. Inspection of the filter arrays indicated that failure along the flange of several 3M CVI-SiC composite filters resulted due to the tight clamping and fixturing of the elements within the metal holders. All of the 3M CVI-SiC composite filters that had initially been installed within the SWPC APF were removed in order to eliminate the risk of potential catastrophic failure of the elements during extended PCFBC operation. Testing was reinitiated and continued for an additional 118 hours. After slow cooling of the array in December 1995, post-test inspection of the cluster was conducted which indicated that all filter elements remained intact.

Nine newly manufactured 3M CVI-SiC composite filters were installed in the bottom array, and testing in Test Segment 2 (TS2-96) that was initiated in February 1996 continued for a period of 387 hours prior to shutdown in April 1996. Once again the 112 candle filter cluster assembly was operated at temperatures of 818-860°C (1505-1580°F), removing fines generated during the combustion of Illinois No. 6 coal and Linwood limestone. Post-test inspection of the SWPC APF in April 1996 indicated that failure of five Coors P-100A-1 alumina/mullite candle filters, four 3M CVI-SiC composite filter elements, and one Schumacher Dia Schumalith FT20 filter had occurred during process shutdown primarily as a result of ash bridging between the candles, metal holders, and plenum pipes.

All filter elements were removed from the SWPC APF at the conclusion of TS2-96. The cluster was recandled with previously used and newly manufactured filter elements, and testing was reinitiated in August 1996. As in the first two test segments, the high temperature creep resistant clay

bonded silicon carbide Schumacher Dia Schumalith FT20 filter elements were positioned within the top array, comparable Pall 326 filters filled the middle array, and a mixture of Coors P-100A-1 alumina/mullite and 3M CVI-SiC composite elements filled the bottom array. The 128 candle filter cluster assembly was subjected to 626 hours of PCFBC operation, at temperatures of 838-860°C (1540-1580°F) during Test Segment 3 (TS3-96). In this test campaign both Iowa Industrial limestone and resized Linwood limestone were utilized as sorbents in conjunction with Illinois No. 6 coal. Post-test inspection of the array in October 1996 indicated that limited bridging was evident within the various arrays. All elements remained intact and were subsequently removed from the cluster assembly. Post-test inspection of the candle filters at the conclusion of TS3-96 indicated the fragile nature of the 3M candle filters. Inspection of the clay bonded silicon carbide filter elements indicated that after 1166 hours of PCFBC operation, the 1.5 m candles elongated by 6-9 mm.

The flange of one of the five 3M CVI-SiC composite filters had cracked, presumably as a result of ash fines becoming wedged in between the holder and the outer surface of the flange wall. Neither penetration of fines into the clean gas stream nor catastrophic failure of the element occurred. Similarly ~5-10 mm sections of the outer confinement layer were seen to have been removed along several of the 3M filter elements at the conclusion of TS3-96. This most likely occurred during *in-situ* cleaning of the array during interim inspection and maintenance intervals.

Crack formations were evident near and around the densified plug that formed the closed end cap of three of the forty-five Pall 326 filter elements that were installed and operated in the SWPC APF during TS3-96. Although fines penetration was not observed through the crack formation after 1166 hours of PCFBC operation, continued use of these elements was not recommended.

After each test campaign, surveillance filter elements were removed from the cluster and were subjected to both nondestructive and destructive materials characterization in order to identify the overall integrity of each element, as well as to determine the residual strength of the various filter matrices at process operating temperature, and any microstructural changes that may have occurred as a result of operation in the PCFBC environment. Additional analyses were focused on determining the residual high temperature creep characteristics of the PCFBC-exposed clay bonded silicon carbide filter elements, their potential to undergo oxidation which resulted in the elongation of the Schumacher Dia Schumalith FT20 and Pall 326 candles by 6-9 mm after 1166 hours of PCFBC operation, and the associated impact of ash and ash chemistry on the stability of the various filter matrices.

Pilot-scale testing in the SWPC APF system at the Foster Wheeler test facility in Karhula, Finland, resumed in April 1997 (TS1-97), utilizing previously PCFBC-exposed, commercially available, Coors P-100A-1, Schumacher Dia Schumalith FT20, and Pall 326 filter elements (Table 5). The 128 candle filter cluster was subjected to ~454 hours of operation at temperatures of ~850°C (~1560°F). Eastern Kentucky Beech Fork coal and Gregg Mine Florida limestone were used as feed materials. Testing was terminated in TS1-97 due to failure of three Coors P-100A-1 filter elements that had previously experienced 1110 hours of operation at AEP.

After dismantling and cleaning the entire cluster, 90 candles were installed, and testing resumed in September 1997 (TS2-97). In addition to the Coors P-100A-1, Schumacher Dia Schumalith FT20, and Pall 326 filter elements, seven oxide-based CFCC 3M and McDermott filter elements, as well as seven DuPont PRD-66 filament wound candles, six Blasch mullite bonded alumina filters, four mullite bonded alumina filters, and two Techniweave Nextel™ 720 oxide-based CFCC elements were installed in the bottom filter array. The unit was initially operated for a period of 40 hours at temperatures of 700-720°C (1290-1330°F) prior to detecting dust in the outlet stream.

**TABLE 5**  
**SUMMARY OF PCFBC TESTING IN 1997**

Test Segment	1 (4/1997-6/1997)	2 (9/1997-11/1997)
Coal	Eastern Kentucky	Eastern Kentucky
Sorbent	Florida Limestone	Florida Limestone
Number of Candles	128	90-112
Coors P-100A-1	72	28-33
Schumacher FT20	28	16-28
Pall 326	28	16-22
3M Oxide CFCC	—	7-0
McDermott Oxide CFCC	—	6-7
Techniweave Oxide CFCC	—	2-0
Blasch Mullite Bonded Alumina	—	4-6
DuPont PRD-66	—	7
Ensto Mullite-Bonded Alumina	—	4-6
Other	—	0-3
Operating Hours (Coal)	454	581
Operating Temperature, °C (°F)	820-850 (1510-1560)	700-750 (1290-1380)
Operating Pressure, bar	10-11	9.5-11
Nominal Face Velocity, cm/s	2.4-3.5	2.8-4.0
Inlet Dust Loading, ppmw	6600-10800	5700-9000

Testing was subsequently terminated and the vessel was cooled. Post-test inspection of the filter cluster indicated that the two Techniweave and seven 3M oxide-based CFCC elements had experienced damage during the 40 hours of PCFBC operation. Close inspection of the Techniweave filter elements indicated that sections of the outer membrane through-thickness fibers were removed, and debonding of the outer seam and unwrapping of the 2-D fabric wrap or layered architecture resulted. Pinholes as a result of through-thickness fiber removal permitted ash fines to pass from the o.d. to i.d. surfaces of the PCFBC-exposed filter elements.

Similarly sections from both the outer confinement and filtration mat layers of the 3M oxide-based CFCC elements were removed, again permitting fines to pass from the o.d. to i.d. surfaces of the PCFBC-exposed filter elements. Sections of material beneath the confinement layer were also seen to have been removed along the end caps of the 3M oxide-based CFCC filter elements. Although the Techniweave and 3M elements suffered damage during the 40 hours of PCFBC operation, all elements remained attached to the metal filter holder mounts. All of the damaged Techniweave and 3M PCFBC-exposed filters, and one as-manufactured element of each filter type were returned to SWPC for examination.

Since ash fines had been detected in the outlet gas stream after 40 hours of PCFBC operation, all elements in the bottom array were removed, and cleaned prior to reinstallation. During removal, one of the DuPont PRD-66 filter elements was broken at the base of the flange. This resulted due to the tight fit when ash became wedged in between the flange and filter holder mount. The broken element was replaced with an alternate, newly manufactured DuPont PRD-66 filter. Areas were also evident along the outer surface of the DuPont PRD-66 filter elements that resembled removal of the

outer surface membrane and divot formations that were observed after operation of the oxide-based filament wound filter matrix at the AEP Tidd demonstration plant.

Post-test inspection of the McDermott elements indicated that localized areas of the Saffil and alumina-enriched sol-gel matrix were removed adjacent to and below the outer Nextel™ 610 filament surface. During cleaning of the McDermott elements, the relatively soft matrix led to “pull-out” of material and/or removal of broken Nextel™ 610 filaments. Separation of the internal wrapped filament winding layers within the flange was also evident after completion of PCFBC Test Segment 3. The outer surface fibers along the end cap area of the PCFBC-exposed McDermott filter element were not completely bonded to the outer surface of the filter element. The Blasch or Ensto candles experienced no apparent damage during either PCFBC testing or cleaning of the elements.

Once the bottom filter array and candles were cleaned (i.e., vacuum brushing; water washing), the elements were reinstalled in the array. Coors P-100A-1 alumina/mullite, Schumacher Dia Schumalith FT20, and Pall 326 elements were installed as replacements for the damaged Techniweave and 3M candles. PCFBC testing was then reinitiated and continued for an additional 199 hours of operation at 700-750°C (1290-1380°F).

After 239 hours of service operation in TS2-97, testing was terminated and the unit was slow cooled, prior to inspection of the three filter arrays. During this planned outage, additional candles were installed to fill the bottom array. Testing was reinitiated and continued for an additional 342 hours of operation at temperatures of 700-750°C (1290-1380°F).

After completion of the PCFBC test campaign in 1997, the vessel was slow cooled, opened, and the filters were subsequently inspected. Post-test inspection of the filter arrays clearly indicated that ash bridging had not occurred. The thickness of the dust cake layer along the surface of the top array filter elements was ~2-3 mm, while an ~2-5 mm thick dust cake layer remained along the outer surface of the middle array elements, and an ~2-3 mm dust cake layer remained along the outer surface of the bottom array elements.

With the exception of crack formations around the densified plug inserted into the end cap of a Pall 326 filter element, and scratches along the membrane of the clay bonded silicon carbide filter elements, all elements were intact at the conclusion of PCFBC testing in 1997. Although divot formations were not observed along the outer surface of the DuPont PRD-66 filter elements, cleaning and handling frequently led to the formation of minor abrasions along the outer surface of the DuPont, as well as McDermott elements.

Once again, localized removal of the matrix and fibers along the outer surface of the McDermott candles was identified at the conclusion of PCFBC testing in 1997. Infrequently, fibers along the i.d. wall of the McDermott elements were seen to be torn or were dangling into the i.d. bore of the elements. This most likely resulted from insufficient bonding and adherence of the fibers during pulse cleaning. Thinning along the center of the PCFBC-exposed Blasch end caps resulted in the vicinity of the plug inserts used to cap and seal the filter elements during manufacturing.

Throughout this effort SWPC discussed with each filter element supplier, the need, as well as potential manufacturing approaches required to improve the quality, integrity, and performance of the various elements, in order to achieve extended operating material and component life in advanced coal-fired applications. Many of the manufacturing modifications were implemented by the various filter element suppliers.

#### 4. FILTER FAILURE MECHANISMS

While conducting bench-scale, pilot and demonstration plant testing, failure of filter elements occurred either directly as a response to process operating conditions, or as the result of filter architecture or manufactured construction. Typically for the alumina-based monoliths as Coors P-100A-1 alumina/mullite, thermal fatigue of the matrix resulted in longitudinal crack formations that progressed along the length of the filter body (Figure 47). Extended pulse cycling via the use of compressed air was considered to be primarily responsible for thermal fatigue of the Coors filter matrix, while rapid process or system transients led to thermal shock of the filter matrix. In order to mitigate the issue of thermal fatigue, SWPC adopted the use of a failsafe/thermal regenerator above each filter element in order to “preheat” the incoming pulse cleaning gas and collect particles that penetrated through the porous filter media, prior to delivery of the “clean” process gas to the turbine. In addition to the thermal fatigue and shock issues of the Coors and other supplier-based oxide monolithic materials, the Coors’ filter end cap was radiused in order to eliminate stress risers that ultimately led to crack formations and failure of the filter element (Figure 48).



Figure 47 — Thermal fatigue of the Coors P-100A-1 alumina/mullite filter matrix.



Figure 48 — Coors P-100A-1 alumina/mullite closed end cap. Radiusing of the filter wall in the end cap region eliminated stress risers within the matrix, mitigating failure of the filter body.

During the early development of the Schumacher and Pall clay bonded silicon carbide candle filters, failure primarily resulted from elongation of the filter body at process operating temperatures  $>750^{\circ}\text{C}$  ( $\sim 1380^{\circ}\text{F}$ ). The weight of the filter elements and the plastic nature of the original clay binders at elevated temperatures caused elongation of the nonoxide-based ceramic matrix at the base of the flange, and ultimately fracture at this location with time (Figure 49). In order to eliminate high temperature creep of these matrices, both Schumacher and Pall modified the composition of their clay binder systems.



Figure 49 — Crack formations at the base of the Pall Vitropore filter flange as a result of high temperature creep during operation at AEP.

Schumacher initially manufactured its clay bonded silicon carbide F40 candle filter with a densified silicon carbide flange. Failure was typically seen at the densified-to-porous transition when ash bridging resulted within the filter array (Figure 50). Although initially rigid, both the Schumacher and Pall filter elements experienced plastic deformation, bending, and failure at the base of the flange during an ash bridging event.

Surface oxidation of the silicon carbide grains within the nonoxide-based monolithic filter materials led to a volume expansion with the Schumacher and Pall matrices. As silica formed, crystallization resulted along the surface of the silicon carbide grains, as well as at the base of the ligaments or bond posts. With time, weakening of the matrix at ligament or bond post junction, and removal of the silica encapsulating shell particularly along the i.d. or pulse cycled surface of the filter element occurred. Once the protective oxide layer was removed, the exposed silicon carbide surface reoxidized. With continued spalling and reoxidizing cycles, thinning of the matrix with lowered load bearing capabilities was projected to limit the extended life of the monolithic nonoxide-based porous Schumacher and Pall filter materials.

In contrast to the monolithic filter matrices, appropriate capturing and holding of the “softer” vacuum infiltrated fibrous filter elements within the filter array, as well as significantly lower load bearing capabilities of the filter matrix to withstand pulse cleaning severely limited the viability and life of the IF&P and Fosco candle filters in SWPC’s advanced particulate filtration systems. As shown in Figure 51, hole formations at the base of the flange, longitudinal crack formations along the mold seams, and mid-body fracture were frequently encountered. In order



Figure 50 — Failure of the porous ceramic filter elements as the result of ash bridging within the filter array.



Figure 51 — Failure of the vacuum infiltrated chopped fibrous candle filters.

to utilize the “softer” vacuum infiltrated fibrous filter elements, redesign of the SWPC filter holder, gasket seals, and pulse cleaning and injection ports would be required. In addition, manufacture of the hemi-spherical flange contour would need to be implemented by the filter suppliers, pending redesign of the SWPC existing holder concept.

With respect to the thinner walled, lower load bearing, second-generation CFCC filter elements, variation in the flange geometries required modifications to be made for holding and sealing of the elements within the SWPC filter holders. Crack formations within the flange area (Figure 52) resulting from either improper sealing or capture of ash between the flange and metal holder, led to fracture and/or removal of the CFCC matrix, dislocation of the gasket seals, movement of the element within the holder, and ultimately failure of the filter element.



Figure 52 — Failure of the thinner walled 3M CFCC filter element flange.

Similarly removal of the outer surface membrane of the DuPont PRD-66 filament wound filter matrix resulted in divot formations along the length of the filter body (Figure 53). Divot formations were attributed to gap formations within the filter wall, generated during filament winding of the element. As ash penetrated and packed into the underlying chevron pattern of the DuPont PRD-66 filter element, localized blinding resulted limiting filtration and cleaning of the element.

The contour of the as-manufactured DuPont PRD-66 filter flange was governed by the filament winding process. If improperly captured and held within the filter holder, ash accumulated between the filter and metal mount. The higher thermal expansion of the ash in comparison to the filter flange media frequently led to crack formations and failure of the filter element. When ash accumulated and became lodged between the filter holder and filter, removal of the element without failure was virtually impossible.

Failure of the original Techniweave CFCC filter elements generally resulted along the external longitudinal seam, as well as along the non-integral flange. Inspection of the Techniweave filter elements that had been installed and operated in the SWPC APF at Karhula, Finland indicated

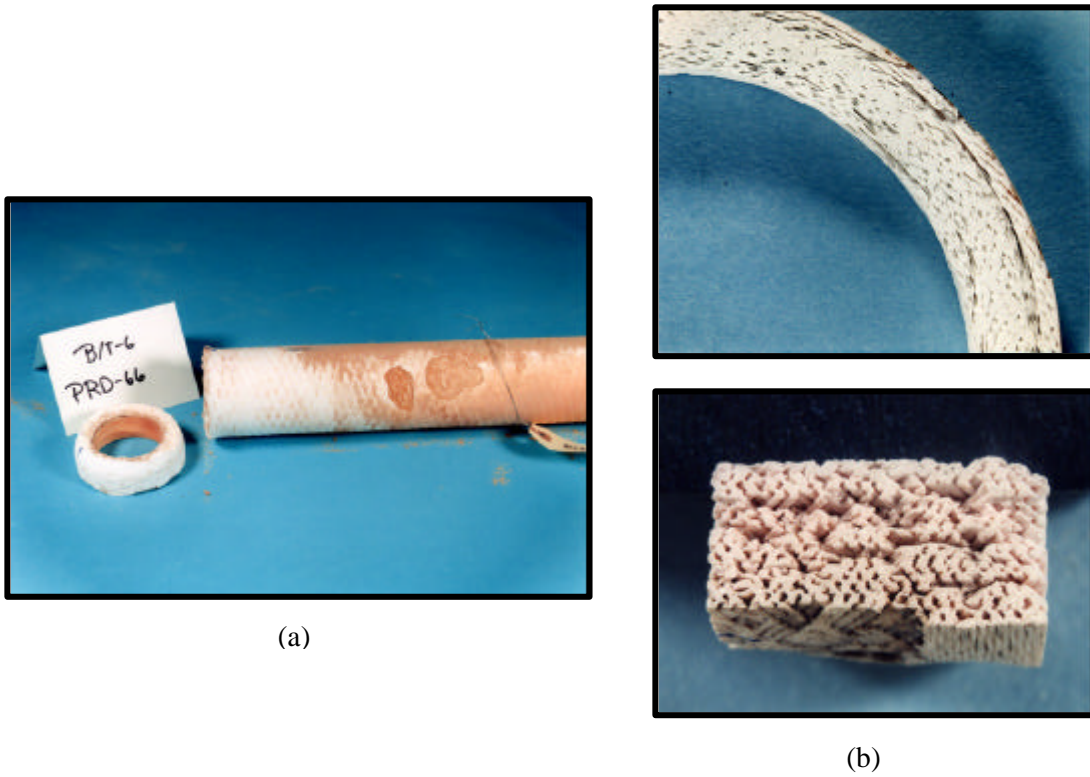


Figure 53 — Failure of the DuPont PRD-66 filter element. (a) Flange failure and divot formation; (b) Gap formations within the cross-sectioned filter wall.

that sections of the outer membrane through-thickness fibers were removed, and debonding of the outer seam and unwrapping of the 2-D fabric wrap or layered architecture resulted (Figure 54). Pinholes as a result of through-thickness fiber removal permitted ash fines to pass from the o.d. to i.d. surfaces of the PCFBC-exposed Techniweave filter elements.

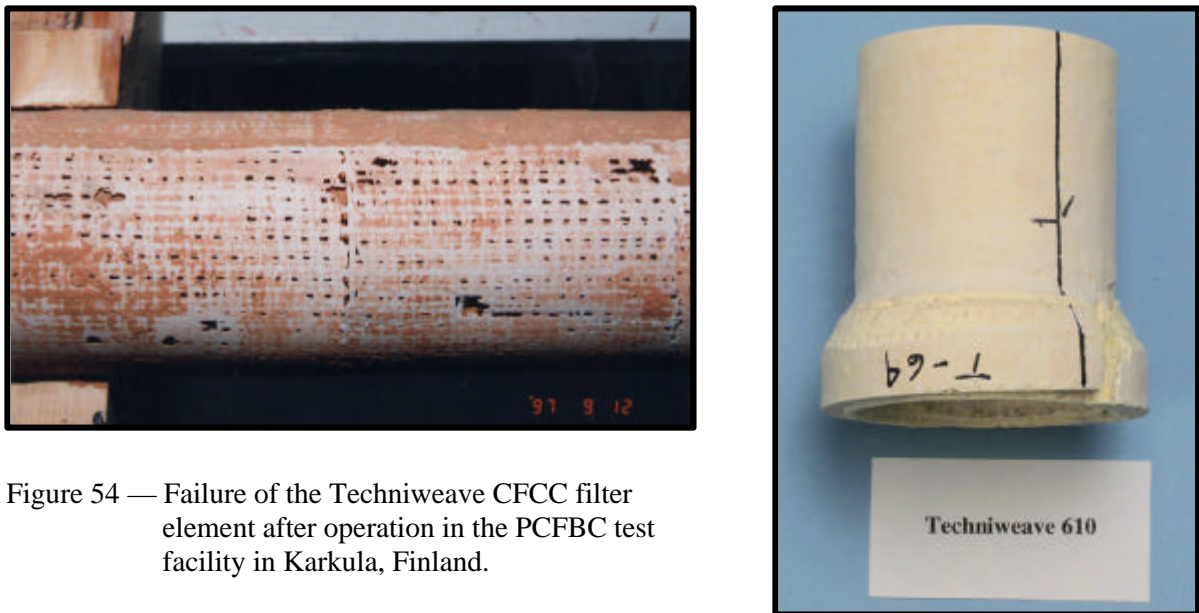


Figure 54 — Failure of the Techniweave CFCC filter element after operation in the PCFBC test facility in Karkula, Finland.

When installed and operated in the PCFBC test facility in Karhula, Finland, removal of sections of the outer confinement layer resulted along the length of the 1.5 m oxide-based 3M CFCC candle filters (Figure 55). With removal of the outer confinement layer, the underlying filtration mat was subsequently removed, exposing the triaxial braid support layer. Ash penetration into the interior of the 3M oxide-based CFCC followed, due to the lack of the filtration media to capture fines. Similarly removal of the filtration mat along the bottom end cap was also observed, permitting fines to readily accumulate within the i.d. bore of the filter element.

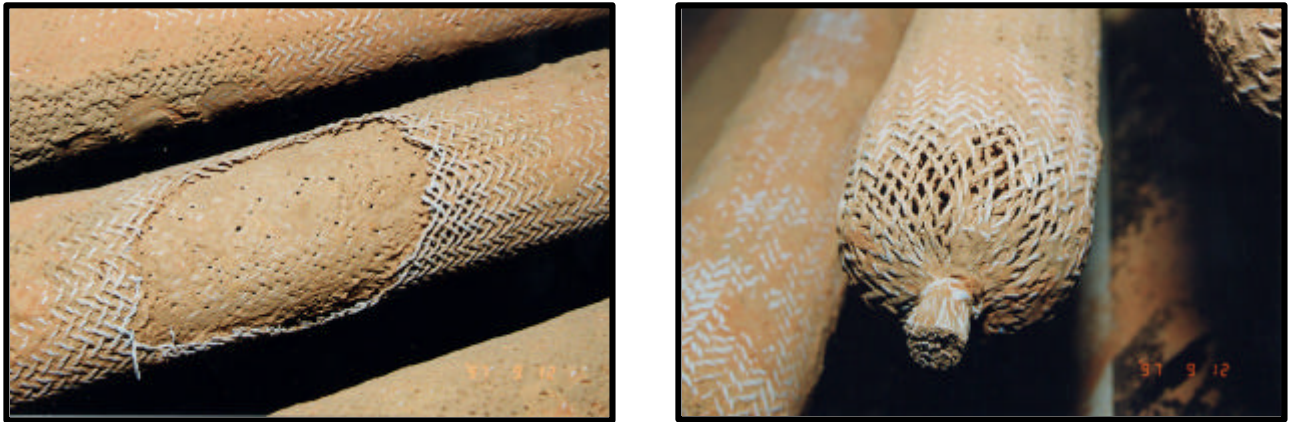


Figure 55 — Failure of the 3M oxide-based CFCC filter elements.

For the McDermott oxide-based CFCC filter element, localized removal of the fibers (Figure 56) along the outer surface of the filter element occurred after use and cleaning of the elements for gas flow permeability measurements, prior to reinstallation within the filter array. Due to architecture of the McDermott CFCC filter matrix, ash penetration into the interior of the filter wall and localized blinding did not occur. In order to adequately capture the flange of the McDermott CFCC filter element, a densified insert was added and bonded to the interior of the



Figure 56 — Removal of fibers along the outer surface of the McDermott CFCC filter element.

flange (Figure 57). In order to close the end cap tip of the McDermott element, a densified plug was inserted. Failure of the flange insert bond can lead to crack formations, separation of the insert section within the flange, improper sealing and dislocation of the gaskets, movement of the element within the holder, and ultimately failure of the filter element. Failure of the bond along the end cap insert leads to debonding and removal, and ultimately a leak path for penetration of ash into the i.d. bore of the filter element and subsequent passage of fines into the plenum and clean gas side of the filter array. In order to mitigate both the flange and end cap failure issues, fabrication of an integral filter element, eliminating the use of seams and bonded inserts is recommended.



Figure 57 — Critical inserts within the McDermott CFCC filter element.

For both the McDermott and Techniweave filter elements which utilized Nextel™ fibers in the construction of the candles, crystallization of the fibers (Figure 58) with extended operating time in the high temperature oxidizing PFBC/PCFBC environment containing steam and/or gas phase alkali was projected to lead to embrittlement of the matrix, reducing the original fracture toughness of the CFCC architecture.

High temperature oxidation and spalling of the thin CVI-SiC layer deposited along the outer surface of the 3M nonoxide-based CFCC filter elements typically reduced the strength of the outer confinement and filtration mat layers during operation in PFBC/PCFBC test facilities. Once oxidized to silica and/or removed from the outer surface of the Nextel™ or alumina fibers, failure of the outer confinement layer resulted (Figure 59). Subsequent removal of the underlying filtration mat layer followed, and penetration of fines into and through the open structure of the underlying triaxial support braid occurred. In addition to the mechanical failure experienced by the 3M CFCC filters, operation in the combustion gas environment similarly led to oxidation along the internal surface of the CVI-SiC layer. This inherently led to bonding of the silica-enriched CVI-SiC layer to the underlying Nextel™ fiber, which resulted in the reduction of fracture toughness of the CFCC matrix, and ultimately embrittlement of the filter element.

In contrast to the 3M nonoxide CFCC filter architecture, DuPont fabricated their CFCC filter element utilizing Nicalon™ fibers. As shown in Figure 60, failure of the filter element resulted along the longitudinal seam. During operation in the high temperature combustion gas environment,

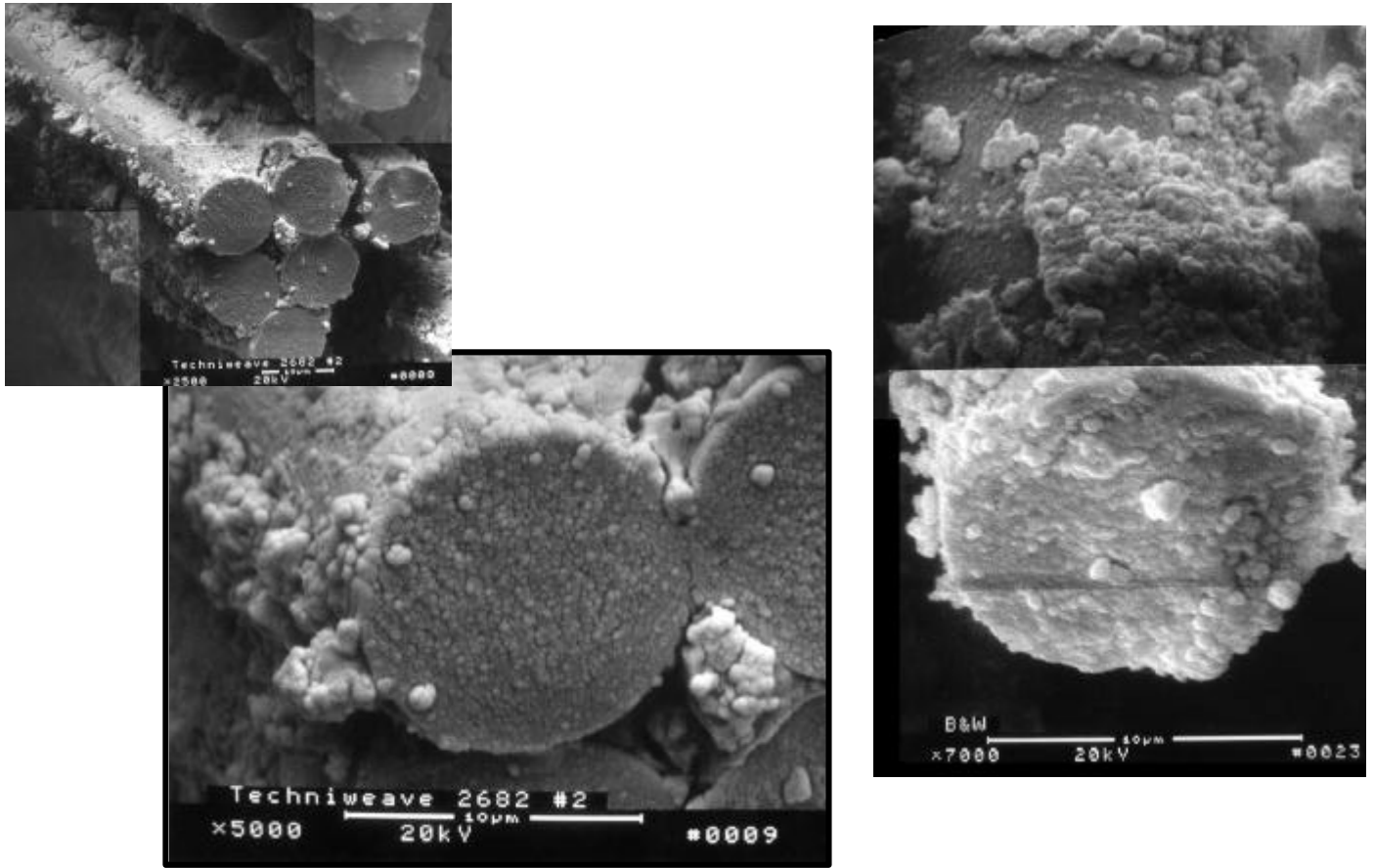
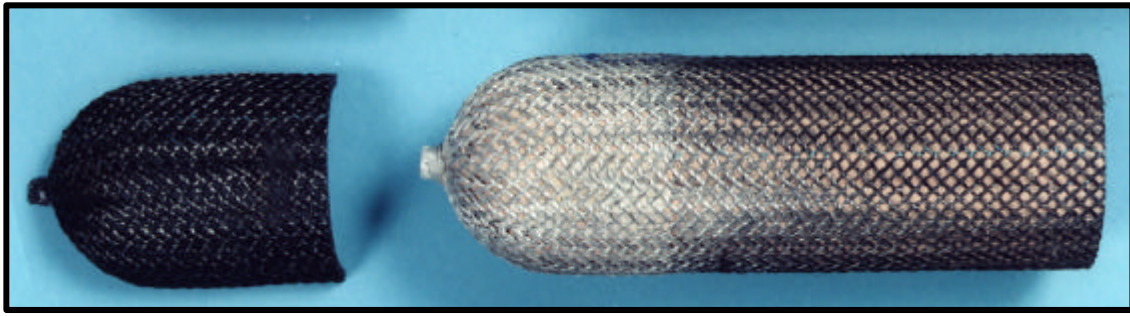


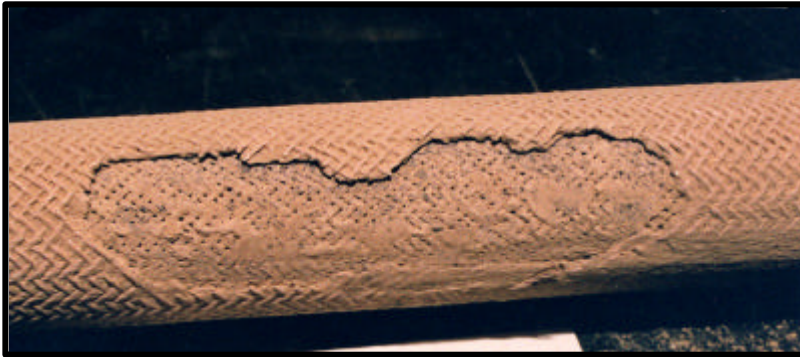
Figure 58 — Crystallization of the Nextel™ fibers within the oxide-based CFCC filter matrices.

the interface layer between the CVI-SiC layer and the underlying Nicalon™ fibers was removed. Volume expansion resulting from oxidation of the Nicalon™ fibers also occurred, causing swelling of the fibers to fill the internal cavity of the deposited CVI-SiC layer. During startup/shutdown of the filter system, crack formations resulted within the oxidized Nicalon™ fiber. The number of startup/shutdown cycles was reflected by the number of step-changes identified along the cross-sectioned surface of the Nicalon™ fibers. Similar to the 3M CVI-SiC CFCC matrix, oxidation of the CVI-SiC encapsulating shell occurred along both outer and inner surfaces. When the silica-enriched inner surface contacted the contained oxidized Nicalon™ fiber, bonding resulted, leading to embrittlement and loss of fracture toughness of the CFCC filter matrix.

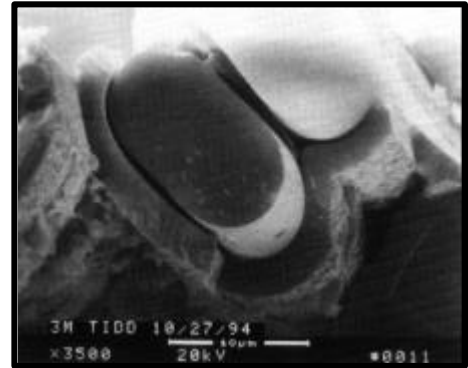
When failure of candles resulted within the filter arrays, ash was carried into the plenum and into the “clean” gas side of the filter vessel. During pulse cleaning, ash fines were carried into the i.d bore of intact filter elements. As ash fines accumulated within the end caps of intact elements, crack formations resulted within the filter walls due to the higher thermal expansion of the packed ash fines relative to the porous ceramic filter body. With time and repeated thermal cycling, failure of the monolithic and CFCC filter elements occurred. In order to mitigate reentrainment and collection of ash fines, SWPC installed fail-safe/regenerator units above the flange of each filter element. Proper seating of the fail-safe/regenerator and gasket seals during filter installation was essential to assure extended operating service life of the various filter elements.



(a)



(b)



(c)

Figure 59 — Failure of the 3M nonoxide-based CFCC filter element. (a) Oxidation of the outer confinement and filtration mat layers; (b) Removal of the outer confinement and filtration mat layers; (c) Removal of the as-manufactured interface layer between the encapsulating CVI-SiC outer shell and underlying Nextel™ fibers. Oxidation along the inner surface of the CVI-SiC shell enhanced bonding with the underlying fibers, and ultimately embrittlement of the CFCC filter matrix.

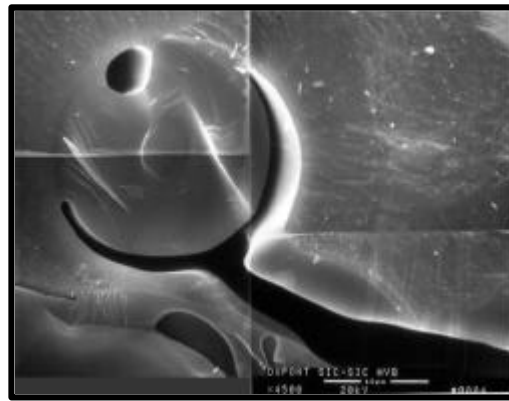
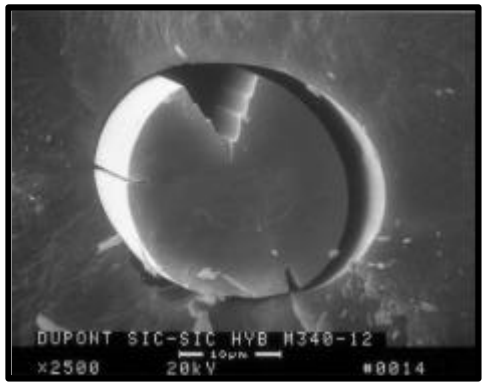
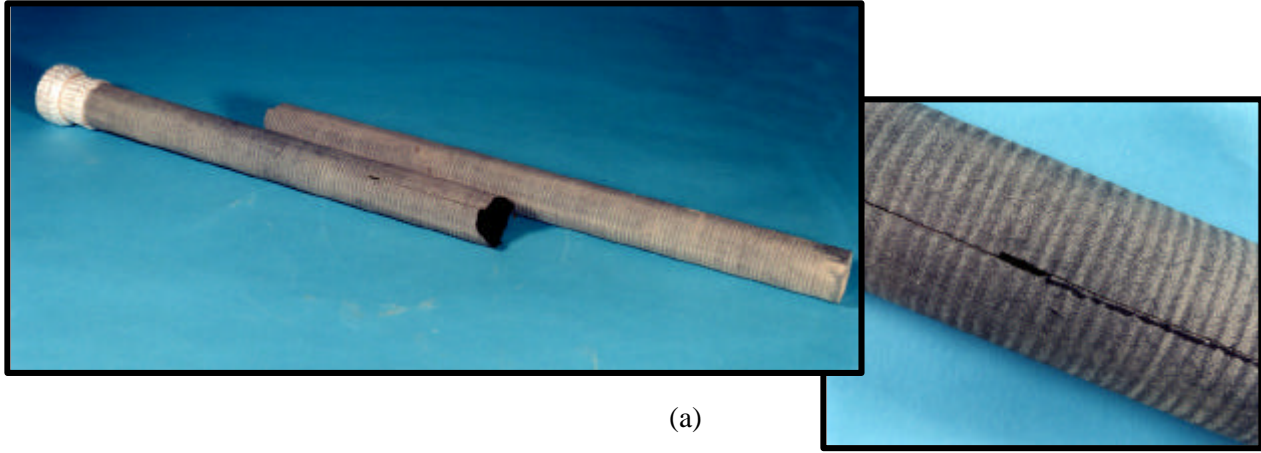


Figure 60 — Failure of the DuPont SiC-SiC CFCC filter matrix. (a) Longitudinal seam failure; (b) Removal of the interface layer and oxidation of the Nicalon™ fiber; (c) Oxidation of the internal surface of the CVI-SiC encapsulating layer and bonding with the oxidized Nicalon™ fiber.

## 5. ACCELERATED LIFE TESTING PROGRAMS

### 5.1 Assessment of Advanced Second Generation Candle Filters — Phase I

Under the Filter Component Assessment program, Siemens Westinghouse Power Corporation (SWPC) initially evaluated the long-term thermal, chemical, and mechanical stability of the advanced second-generation candle filter materials, through high temperature, bench-scale, simulated, pressurized fluidized-bed combustion (PFBC) corrosion testing beginning in 1994 (Table 6). In this phase of the program, porous 3M CVI-SiC and DuPont PRD-66 mini-candles, and porous DuPont CFCC SiC-SiC and IF&P Fibrosic™ coupons were exposed for a maximum of 400 hours to an 870°C (~1600°F) 5-7% steam/air and 5-7% steam/air/20 ppm NaCl flow-through environment [16]. This effort was followed by an evaluation of the mechanical and filtration performance capabilities of the advanced second-generation filter elements in SWPC's bench-scale PFBC test facility in Pittsburgh, PA [13,16]. Arrays of 1.4-1.5 m 3M CVI-SiC, DuPont PRD-66, DuPont SiC-SiC, and IF&P Fibrosic™ candles were subjected to steady state process operating conditions, increased severity thermal transients, and accelerated pulse cycling test campaigns which represented ~1760 hours of equivalent filter operating life.

**TABLE 6**  
**ADVANCED SECOND GENERATION CANDLE FILTER**  
**MATERIAL STABILITY AND PERFORMANCE EVALUATION**

1994	1996-1997	1997	1997	1997	2001	2003
High Temperature Corrosion	AEP PFBC Testing at Brilliant, OH	Qualification Testing at SWPC STC	Foster Wheeler PCFBC Testing at Karhula, Finland	Phase I Accelerated Life Testing at SWPC STC (~1 yr)*	Phase II Accelerated Life Testing at SWPC STC (~2.5 yr)*	Phase III Accelerated Life Testing At SWPC STC
Simulated PFBC Performance Evaluation						

\* Equivalent Operating Life.

SWPC subsequently participated in material surveillance programs that marked entry of the 3M CVI-SiC and DuPont PRD-66 candle filters in SWPC's Advanced Particulate Filtration (APF) system on a slipstream at the American Electric Power (AEP) Tidd demonstration plant in Brilliant, OH [1]. SWPC then conducted an extended, accelerated life, qualification program, evaluating the performance of the

- 3M, McDermott, and Techniweave oxide-based CFCC filter elements
- Process modified DuPont PRD-66 elements
- Blasch, Scapa Cerafil™, and Specific Surface monolithic candles

for use in our APF system at the Foster Wheeler pressurized circulating fluidized-bed combustion (PCFBC), pilot-scale, test facility in Karhula, Finland [13,16].

Based on qualification testing conducted by SWPC in 1997, and implementation of production modifications by the various candle filter suppliers,

- Eight 1.5 m DuPont filament wound PRD-66
- Eight 1.5 m McDermott oxide-based CFCC
- Eight 1.5 m 3M oxide-based CFCC
- Two 1.5 m Techniweave oxide-based CFCC
- Eight 1.5 m oxide-based monolithic Blasch candle filters

were manufactured and delivered for installation in the bottom filter array of the 128 SWPC candle APF system in Karhula, Finland. The remainder of the filter system contained Schumacher Dia Schumalith clay bonded silicon carbide FT20, Pall clay bonded silicon carbide 326, and Coors P-100A-1 alumina/mullite filter elements.

After ~40 hours of operation at temperatures of 700-720°C (1290-1330°F), dust was detected in the outlet gas stream of the APF indicating failure of either the filter elements, gaskets, and/or metal holder assembly. Post-test disassembly of the filter array identified that failure of two Techniweave and seven 3M oxide-based CFCC elements had occurred. During removal of the entire bottom array that housed the failed filter elements, one DuPont PRD-66 candle was additionally broken. After manual cleaning of the filter array, Coors P-100A-1 alumina/mullite, Schumacher Dia Schumalith FT20, Pall 326, and DuPont PRD-66 elements were installed as replacements for the failed candle filters. PCFBC testing was then reinitiated and continued for an additional 541 hours of operation at 700-750°C (1290-1380°F). Post-test inspection of the APF indicated that all candle filters were intact.

In March 1998, SWPC initiated an extended accelerated filter life test program in which PCFBC and/or PFBC-aged candle filters were subjected to simulated high temperature, high pressure combustion gas operating conditions in order to demonstrate the feasibility of matrix-conditioned elements to achieve extended service operation (Table 7) [13,14]. As part of the Phase I accelerated life test program, the PCFBC and/or PFBC-tested Schumacher FT20, Pall 326, and Coors P-100A-1 alumina/mullite candle filters used in this effort previously experienced 1035-3311 hours of service life, while the McDermott CFCC, DuPont PRD-66 and Blasch mullite bonded alumina candle filters experienced 581 hours of service operation.

Sixteen candles were installed in the filter array which then underwent 40.5 hours of steady state PFBC operation at 843°C (1550°F) and 68 psig. Subsequently the filter array was subjected to 20089 accelerated pulse cleaning cycles, representing 10045 hours or >1 year of equivalent field service life. Twelve filter elements which included monolithic oxides and nonoxides, and oxide-based filament wound and CFCC matrices successfully demonstrated their ability to achieve >1 year of equivalent PCFBC/PFBC operating life. Failure of three candles however resulted during conduct of the accelerated pulse cycle test program. These included:

- Thermal fatigue failure of a 3761 equivalent operating hour Coors P-100A-1 alumina/mullite candle.
- Failure at the base of the flange of a 3108 equivalent operating hour DuPont PRD-66 filament wound candle.
- Delamination and failure at the base of the flange of a 2373 equivalent operating hour 3M CVI-SiC candle filter.

**TABLE 7**  
**SUMMARY OF THE EXTENDED FILTER LIFE TEST PROGRAM — PHASE I**

Array Location/ Supplier	Steady State 3/23/98- 3/26/98	Accelerated Pulse Cycling				
		3/26/98-4/3/98 (2836 Pulses)	5/21/98- 5/28/98 (284 Pulses)	6/2/98- 6/10/98 (1935 Pulses)	6/16/98- 7/24/98 (4974 Pulses)	8/4/98- 8/21/98 (3494 Pulses)
<b>Total Cumulative Number of Pulses</b>		<b>2836 *</b>	<b>3120</b>	<b>5055</b>	<b>10029</b>	<b>13523</b>
1	—	—	—	—	—	—
2 Coors	FC-044 (M12) 2166 Hrs	FC-044 (M12) 2166 Hrs	FC-044 (M12) 2166 Hrs	FC-044 (M12) 2166 Hrs	FC-044 (M12) 2166 Hrs	FC-044 (M12) 2166 Hrs
3 Coors	FC-065 (M10) 2166 Hrs	FC-065 (M10) 2166 Hrs	FC-065 (M10) 2166 Hrs	FC-065 (M10) 2166 Hrs	FC-065 (M10) 2166 Hrs	FC-065 (M10) 2166 Hrs
4 Coors	AB33 (T14) 3311 Hrs	AB33 (T14) 3311 Hrs	AB33 (T14) 3311 Hrs	AB33 (T14) 3311 Hrs	AB33 (T14) 3311 Hrs	AB33 (T14) 3311 Hrs
5 Coors	FC-001 (M14) 2201 Hrs	FC-001 (M14) 2201 Hrs	FC-001 (M14) 2201 Hrs <sup>4</sup>	P-100A-1 (New)	P-100A-1 (New)	P-100A-1 (New)
6 Coors/ Ensto	FC-023 (T15) 2201 Hrs	FC-023 (T15) 2201 Hrs <sup>1</sup>	FC-058 (M26) 2166 Hrs	FC-058 (M26) 2166 Hrs	FC-058 (M26) <sup>6</sup> 2166 Hrs	E-141-97 (B25) 581 Hrs
7 Pall 326/ 3M CVI-SiC	R1-656 (M2) 1035 Hrs	R1-656 (M2) 1035 Hrs <sup>2</sup>	R5-631 (M22) 1035 Hrs	R5-631 (M22) 1035 Hrs	R5-631 (M22) <sup>6</sup> 1035 Hrs	3M-51171 (B12) 626 Hrs <sup>7</sup>
8 Schumacher FT20/ IF&P REECER	S350F/16 (T2) 1035 Hrs	S350F/16 (T2) 1035 Hrs	S350F/16 (T2) 1035 Hrs	S350F/16 (T2) 1035 Hrs	S350F/16 (T2) <sup>6</sup> 1035 Hrs	IF&P 0 Hrs
9 Schumacher FT20	S350F/32 (T3) 1035 Hrs	S350F/32 (T3) 1035 Hrs	S350F/32 (T3) 1035 Hrs	S350F/32 (T3) 1035 Hrs	S350F/32 (T3) 1035 Hrs	S350F/32 (T3) 1035 Hrs
10 Pall 326	R1-658 (M3) 1035 Hrs	R1-658 (M3) 1035 Hrs	R1-658 (M3) 1035 Hrs	R1-658 (M3) 1035 Hrs	R1-658 (M3) 1035 Hrs	R1-658 (M3) 1035 Hrs
11 Schumacher FT20	S350F/60 (T5) 1035 Hrs	S350F/60 (T5) 1035 Hrs	S350F/60 (T5) 1035 Hrs	S350F/60 (T5) 1035 Hrs	S350F/60 (T5) 1035 Hrs	S350F/60 (T5) 1035 Hrs
12 Pall 326	R1-659 (M17) 1035 Hrs	R1-659 (M17) 1035 Hrs	R1-659 (M17) 1035 Hrs	R1-659 (M17) 1035 Hrs	R1-659 (M17) 1035 Hrs	R1-659 (M17) 1035 Hrs
13	—	—	—	—	—	—
14 DuPont PRD- 66	D581 (B42) 581 Hrs	D581 (B42) 581 Hrs	D581 (B42) 581 Hrs	D581 (B42) 581 Hrs <sup>5</sup>	D571C (New)	D571C (New)
15 McDermott	B&W 7-5-29 (B32) 581 Hrs	B&W 7-5-29 (B32) 581 Hrs	B&W 7-5-29 (B32) 581 Hrs	B&W 7-5-29 (B32) 581 Hrs	B&W 7-5-29 (B32) 581 Hrs	B&W 7-5-29 (B32) 581 Hrs
16 Pall 326	R1-667 (M4) 1035 Hrs	R1-667 (M4) 1035 Hrs <sup>3</sup>	R5-667 (M23) 1035 Hrs	R5-667 (M23) 1035 Hrs	R5-667 (M23) 1035 Hrs	R5-667 (M23) 1035 Hrs
17 Schumacher FT20	S350F/43 (T4) 1035 Hrs	S350F/43 (T4) 1035 Hrs	S350F/43 (T4) 1035 Hrs	S350F/43 (T4) 1035 Hrs	S350F/43 (T4) 1035 Hrs	S350F/43 (T4) 1035 Hrs
18 Blasch	BP4-270P7/97 (B41) 581 Hrs	BP4-270P7/97 (B41) 581 Hrs	BP4-270P7/97 (B41) 581 Hrs	BP4-270P7/97 (B41) 581 Hrs	BP4-270P7/97 (B41) 581 Hrs	BP4-270P7/97 (B41) 581 Hrs
19	—	—	—	—	—	—
Elements removed for characterization; Elements removed as a result of <i>in-situ</i> or failure during maintenance.						
Replacement elements.						

**TABLE 7 (Cont'd.)  
SUMMARY OF THE EXTENDED FILTER LIFE TEST PROGRAM — PHASE I**

	<b>Accelerated Pulse Cycling</b>	<b>Thermal Transients</b>	<b>Comments</b>
<b>Array Location/ Supplier</b>	<b>8/27/98-10/5/98</b>	<b>11/11/98-12/10/98</b>	
<b>Total Cumulative Number of Pulses</b>	<b>20089</b>	<b>30 Thermal Transients</b>	
1	—	—	
2 Coors	FC-044 (M12) 2166 Hrs <sup>8</sup>	FC-059 (M13) 2166 Hrs	FC-059 (M13) Intact — Continued Life Testing Planned
3 Coors	FC-065 (M10) 2166 Hrs	FC-065 (M10) 2166 Hrs	FC-065 (M10) Intact — Continued Life Testing Planned
4 Coors	AB33 (T14) 3311 Hrs	HOLD	—
5 Coors	P-100A-1 (New)	P-100A-1 (New)	P-100A-1 Intact — Continued Life Testing Planned
6 Ensto	E-141-97 (B25) 581 Hrs	E-141-97 (B25) 581 Hrs	E-141-97 (B25) Intact — Continued Life Testing Planned
7	—	—	—
8 IF&P REECER	IF&P 0 Hrs	IF&P 0 Hrs	IF&P REECER Intact — Continued Life Testing Planned
9 Schumacher FT20	S350F/32 (T3) 1035 Hrs	S350F/32 (T3) 1035 Hrs	S350F/32 (T3) Intact — Continued Life Testing Planned
10 Pall 326	R1-658 (M3) 1035 Hrs	R1-658 (M3) 1035 Hrs	R1-658 (M3) Intact — Continued Life Testing Planned
11 Schumacher FT20	S350F/60 (T5) 1035 Hrs <sup>8</sup>	S350F/80 (T6) 1035 Hrs	S350F/80 (T6) Intact — Continued Life Testing Planned
12 Pall 326	R1-659 (M17) 1035 Hrs <sup>8</sup>	R3-656 (M21) 1035 Hrs	R3-656 (M21) Intact — Continued Life Testing Planned
13 Coors	—	P-100A-1 New <sup>10</sup>	Circumferential failure at ~24 inches from the bottom closed end cap. Failure occurred between thermal transient #19 and #20.
14 DuPont PRD-66	D571C (New)	D571C (New) <sup>9</sup>	D571C Intact — Continued Life Testing Planned
15 McDermott	B&W 7-5-29 (B32) 581 Hrs	B&W 7-5-29 (B32) 581 Hrs <sup>9</sup>	Depressions, debonding, and separation of areas visible along the flange i.d.; Removal of chopped fiber material in localized areas along o.d. surface exposing subsurface filament fiber bundles.
16 Pall 326	R5-667 (M23) 1035 Hrs	R5-667 (M23) 1035 Hrs <sup>9</sup>	R5-667 (M23) Intact — Continued Life Testing Planned
17 Schumacher FT20	S350F/43 (T4) 1035 Hrs	S350F/43 (T4) 1035 Hrs <sup>9</sup>	S350F/43 (T4) Intact — Continued Life Testing Planned
18 Blasch	BP4-270P7/97 (B41) 581 Hrs	BP4-270P7/97 (B41) 581 Hrs <sup>9</sup>	Longitudinal crack formation extending ~ 2 inches from the bottom end cap to ~20 inches along the length of the candle filter.
19	—	—	—
	Elements removed for characterization; Elements removed as a result of <i>in-situ</i> or failure during maintenance.		
	Replacement elements.		

**TABLE 7 (Cont'd.)**  
**SUMMARY OF THE EXTENDED FILTER LIFE TEST PROGRAM — PHASE I**

\* Modification to the filter vessel shroud.

1. Originally intact, but broken during handling and removal from the filter array.
2. Failed after 2836 pulse cycles. Candle located adjacent to the shroud. Location was in direct line with the inlet combustion gas.
3. Thermally worn outer membrane section location was in direct line with the inlet combustion gas.
4. Failed after 3120 pulse cycles. Initially 5 pulse cycles were delivered on restart to acquire high speed thermocouple data, followed by 5-1/2 hours of steady state testing, with pulse cleaning prior to shutdown. Subsequently 278 additional pulse cycles were delivered to the array prior to identifying a slight decrease in the pressure drop across the array. Effective cumulative operating life of 3761 hours (2201 PCFBC hours; 1560 accelerated pulse cycling hours).
5. Failure of the PRD-66 filter element at the base of the flange after 581 hours of PCFBC operation and subsequently 5055 accelerated pulse cleaning cycles. Effective cumulative operating life of 3108 hours (581 PCFBC hours; 2527 accelerated pulse cycling hours).
6. Elements removed for material characterization.
7. Failure of 3M CVI-SiC composite element: 626 hrs PCFBC operation; 3494 accelerated pulse cleaning cycles.
8. Elements removed for material characterization at the completion of 20089 accelerated pulse cleaning cycles.
9. Elements instrumented with an outside/inside thermocouple (2 total; at the base of the flange).
10. New Coors P-100A-1 alumina/mullite element (out-of-spec) instrumented with 5 thermocouples; Three (3) along outside (top; middle; bottom) and two (2) thermocouples along i.d. bore (top/bottom) at nearly equivalent positions as along the outside wall.

Due to the absence of the filter shroud during the initial stages of testing, direct gas impingement resulted which removed the outer surface membrane of the 2453 equivalent operating hour Pall 326 filter element. Thermal fatigue failure of a second 2453 equivalent hour Pall 326 filter occurred at a similar location.

In order to simulate a sequence of projected commercial turbine trip events during the course of plant life, the filter array was then subjected to 30 thermal transients in which an initial temperature drop of 180°F/min was experienced, with cooling continuing until temperatures of ~350°C (~660°F) were achieved during an 11-13 minute period. Subsequently the array was reheated to 843°C (1550°F) within a 25-30 minute period. After completion of testing in December 1998, thirteen of the fifteen elements remained intact, surviving both the accelerated pulse cycle and thermal transient test campaigns. A newly manufactured Coors P-100A-1 alumina/mullite filter element, which had been fabricated with the originally designed square vs radiused end cap, failed. Crack formations were seen along the surface of the PCFBC-aged/accelerated pulse cycled Blasch candle. Strength testing was conducted on select filter elements in order to determine the impact of long-term thermal fatigue and/or thermal transient exposure on the stability of the various porous ceramic filter matrices. Typically the residual strength of the monolithic oxide- and nonoxide-based filter matrices was retained (i.e., stabilized) after 12111 equivalent hours of simulated PFBC service operation.

## **5.2 Extended Accelerated Life Testing — Phase II**

Continued extended life testing of aged filter elements was subsequently undertaken by SWPC to demonstrate feasibility of porous ceramic filter elements to achieve an equivalent of 2-3 years of commercial service life. The objectives of the Phase II accelerated filter life testing were to identify the potential viability and performance of aged candle filters during an additional ~20000

equivalent hours (~2.5 yrs) of simulated PFBC service operation. Candle filters that were used in this effort included both oxide and nonoxide-based monolithic elements, as well as advanced continuous fiber ceramic composite (CFCC) and filament wound elements. The candles had experienced

- Prior operation in either the Foster Wheeler PCFBC test facility in Karhula, Finland, with subsequent accelerated PFBC life testing in the SWPC PFBC simulator test facility in Pittsburgh, PA, or
- Had been operated at the Southern Company Services (SCS) Power System Development Facility (PSDF) in Wilsonville, AL.

### 5.2.1 Accelerated Pulse Cycle Exposure

Testing was initiated on August 17, 2001, exposing an array of previously accelerated life-tested ceramic candles, as well as field-tested, and newly manufactured filter elements to 800°C (1470°F), simulated PFBC conditions (Table 8). In order to simulate extended life, the filter array was pulse cycled every ~2.23 minutes.<sup>7</sup> At the conclusion of each workday, an isokinetic dust loading sample was taken in an attempt to demonstrate the condition of various filter elements and/or gasket seals. The absence of dust in the outlet gas stream implied that the filter array was intact. Conversely, the presence of dust in the outlet gas stream would imply failure (i.e., fracture; crack(s); leak(s); etc.) of an element, gasket seal, and/or metal structure within the filter system.

Testing continued through the morning of October 1, 2001, when 20260 pulse cleaning cycles had been delivered to the filter array (Test Campaign No. 1). Testing was terminated and the filter vessel slow cooled in order to minimize thermal shock of the ceramic elements. Once cooled, the filter array was opened and inspected. All elements were seen to be intact. The following elements were removed from the filter array for room temperature gas flow resistance measurements and destructive characterization:

- Pall 326 R1-658 (M3)
- Schumacher FT20 S350F/43 (T4).

Testing in Test Campaign No. 2 resumed on October 10, 2001, and continued through November 19, 2001. At the conclusion of Test Campaign No. 2, the filter array had been subjected to an additional 20715 pulse cleaning cycles, simulating 10357.5 hrs of operational life. For both Test Campaign No. 1 and Test Campaign No. 2, the filter array had experienced a total of 40975 pulse cleaning cycles or 20487.5 equivalent hours of simulated operating life. All filter elements were seen to have remained intact within the filter array during conduct of accelerated life testing. At the conclusion of the second accelerated pulse cycling campaign, the following filter elements were removed from the filter array for room temperature gas flow resistance measurements and destructive characterization:

- Ensto 141-97 (B25)
- Schumacher FT20 S350F/32 (T3)
- PRD-66 D571C New
- Pall 326 R5-667 (M23).

---

<sup>7</sup> Prior testing at SWPC STC demonstrated that the matrix and surface temperature of the 10 mm thick monolithic filter elements returned to the initial 800°C (1470°F) process operating temperature at ~2.23 minutes after delivery of the pulse cleaning cycle [13].

**TABLE 8  
EXTENDED FILTER LIFE TESTING — PHASE II**

Filter Identification	Prior Exposure Time, Hrs	Accelerated Pulse Cycling		Cumulative Equivalent Operating Time, Hrs
		Test Campaign 1 20260 Cycles; 10,130 Hrs	Test Campaign 2 40975 Cycles; 20,487.5 Hrs (Total)	
Pall 326 R1-658 (M3)	1035 PCFBC 10044.5 * 30 TT **	10130	—	21209.5 30 TT
Schumacher FT20 S350F/43 (T4)	1035 PCFBC 10044.5 * 30 TT	10130	—	21209.5 30 TT
McDermott — SCS #1259	179 SCS	→	20487.5	20666.5
Ensto 141-97 (B25)	581 PCFBC 5030 * 30 TT	→	20487.5	26098.5 30 TT
Schumacher FT20 S350F/32 (T3)	1035 PCFBC 10044.5 * 30 TT	→	20487.5	31567.0 30 TT
PRD-66 D571C New	7517 * 30 TT	→	20487.5	28004.5 30 TT
Pall 326 R5-667 (M23)	1035 PCFBC 8626.5 * 30 TT	→	20487.5	30149.0 30 TT
Techniweave New #2682 #2	—	→	20487.5 30 TT	20487.5 30 TT
Coors P-100A-1 FC065 (M10)	2166 PCFBC 10044.5 * 30 TT	→	20487.5 30 TT	32698 60 TT
McDermott — SCS #1258	179 SCS	→	20487.5 30 TT	20666.5 30 TT
McDermott (R. Wagner/SCS) #787	1360 SCS	→	20487.5 30 TT	21847.5 30 TT
IF&P Recrystallized SiC New	5030 * 30 TT	→	20487.5 30 TT	25517.5 60 TT
Schumacher FT20 — SCS #1173	1241 SCS	→	20487.5 30 TT	21728.5 30 TT
Pall 326 — SCS #307	2830 SCS	→	20487.5 30 TT	23317.5 30 TT
PRD-66 — SCS #582	SCS	→	20487.5 30 TT	SCS/20487.5 30 TT

\* Equivalent exposure hours achieved in Accelerated Filter Life Testing — Phase I.

\*\* TT: Thermal transients.

## 5.2.2 Thermal Transient Testing

The remaining filter elements were subjected to thermal transient testing. As in prior efforts, an element was instrumented with ten high-speed thermocouples to measure both the outer and inner candle filter wall surface temperatures during exposure to the 30 thermal transient cycles. The element selected for instrumentation in this test campaign was the IF&P recrystallized SiC candle filter.

Thermal transient testing was initiated on December 7, 2001, and completed on December 13, 2001. The candle filter array experienced 30 thermal transients in which the air flow into the 843°C (1500°F) filter vessel was adjusted to achieve an initial temperature drop of 180°F/min with cooling continuing until temperatures of ~350°C (660°F) were achieved during an 11-13 minute period. Each transient event was followed by rapid reheating of the filter array to 843°C (1500°F). Ash was fed after completion of each thermal transient event in order to assure that the filter array had remained intact. Upon completion of the 30 thermal transient cycles, the filter system was disassembled. All of the elements were seen to be intact after having been subjected to 40975 accelerated pulse cleaning cycles (i.e., 20487.5 equivalent exposure hours), and 30 thermal transient cycles. Each filter element was inspected and subjected to residual strength characterization and microstructural analyses.

### **5.2.3 Material Characterization**

Table 9 identifies the residual compressive and tensile strength of the various accelerated life-tested filter matrices when 10 mm (0.39 in) c-ring sections were removed from each element and tested at room temperature (25°C (77°F)), and at simulated process operating conditions (800°C (~1470°F)). Table 10 identifies the ultimate load applied during c-ring compressive and tensile testing of the accelerated life-tested filter materials. Table 11 provides similar information resulting from diametral testing of 10 mm (0.39 in) o-ring sections removed from each accelerated life-tested filter element.

Figures 61 and 62 graphically illustrate the room and high temperature residual compressive and tensile strengths of the advanced monolithic and second generation ceramic candle filters from early stages of life (i.e., as-manufactured matrix; PFBC/PCFBC field-tested materials) through both accelerated life testing programs conducted at SWPC STC. The compressive strength (i.e., outer or o.d. surface) of the various filter elements was generally retained with extended simulated process operating time, while the tensile strength (i.e., i.d. or pulse cycled surface) of the candles tended to slightly decrease with time possibly as the result of extended pulse cycling, aging and/or phase changes within the filter element.

**TABLE 9  
RESIDUAL FILTER ELEMENT ROOM AND HIGH TEMPERATURE STRENGTH<sup>8</sup>**

Element	Exposure Time, Hrs	Compressive Strength, psi		Tensile Strength, psi	
		25°C	800°C	25°C	800°C
Techniweave New 2682 #1	0	1985±441 (9) *	1775±587 (9)	1030±695 (9)	1055±300 (9)
Schumacher 1105 (SCS)	1241	1597±79 (9)	1940±393 (9)	1724±184 (9)	2609±367 (9)
Pall 4-980 (SCS)	2640	3124±161 (9)	3645±355 (9)	3348±388 (9)	3764±398 (9)
McDermott 784 (SCS)	802	491±280 (9)	495±166 (9)	248±67 (9)	220±71 (9)
DuPont 639 (SCS)	SCS Background	1185±116 (9)	1269±188 (9)	1183±202 (9)	1543±546 (9)
Pall 326 R1-658 (M3)	21209.5 (30 TT)**	2101±117 (9)	2841±362 (9)	1871±272 (9)	3193±430 (9)
Schumacher FT20 S350F/43 (T4)	21209.5 (30 TT)	2389±135 (9)	3352±620 (9)	2141±275 (9)	3586±637 (9)
McDermott — SCS #1259	20666.5	546±96 (9)	613±282 (9)	715±97 (9)	748±188 (9)
Ensto 141-97 (B25)	26098.5 (30 TT)	1042±389 (9)	1003±153 (9)	1675±214 (9)	1485±270 (9)
Schumacher FT20 S350F/32 (T3)	31567.0 (30 TT)	2272±123 (9)	3569±148 (9)	2266±154 (9)	3429±462 (9)
PRD-66 D571C New	28004.5 (30 TT)	1242±149 (9)	1593±180 (9)	963±292 (9)	1010±657 (9)
Pall 326 R5-667 (M23)	30149.0 (30 TT)	1875±223 (9)	2643±302 (9)	2226±230 (9)	2798±261 (9)
Techniweave New #2682 #2	20487.5 (30 TT)	1735±297 (9)	1789±575 (9)	739±411 (9)	1060±303 (9)
Coors P-100A-1 FC065 (M10)	32698.0 (60 TT)	2084±239 (9)	2312±184 (9)	2487±191 (9)	2699±372 (9)
McDermott — SCS #1258	20666.5 (30 TT)	474±142 (9)	458±136 (9)	482±180 (9)	677±194 (9)
McDermott (R. Wagner/SCS #787)	21847.5 (30 TT)	390±204 (8)	465±254 (9)	402±281 (9)	497±298 (9)
IF&P Recrystallized SiC New	25517.5 (60 TT)	4418±404 (9)	3702±240 (9)	4906±606 (9)	4356±483 (9)
Schumacher FT20 — SCS #1173	21728.5 (30 TT)	1581±250 (9)	2191±653 (9)	1667±253 (9)	2790±234 (9)
Pall 326 — SCS #307	23317.5 (30 TT)	2685±194 (9)	3021±394 (9)	2918±237 (9)	2869±481 (9)
PRD-66 — SCS #582	SCS/20487.5 (30 TT)	1024±135 (9)	1424±267 (9)	930±296 (9)	1304±516 (9)

\* Number in parentheses indicates the number of samples tested.

\*\* TT: Number of thermal transient events conducted.

<sup>8</sup> Appendix A summarizes c-ring compressive and tensile strength data generated for the various porous ceramic filter materials after PCFBC field exposure or accelerated life testing at SWPC STC.

**TABLE 10**  
**RESIDUAL FILTER ELEMENT ROOM AND HIGH TEMPERATURE**  
**LOAD BEARING CAPABILITIES**

Element	Exposure Time, Hrs	Ultimate Compressive Load, lbs		Ultimate Tensile Load, lbs	
		25°C	800°C	25°C	800°C
Techniweave New 2682 #1	0	1.94±0.38 (9) *	1.73±0.54 (9)	0.87±0.57 (9)	0.91±0.22 (9)
Schumacher 1105 (SCS)	1241	27.40±1.57 (9)	33.84±6.90 (9)	19.22±1.63 (9)	29.12±3.76 (9)
Pall 4-980 (SCS)	2640	51.63±5.05 (9)	60.04±7.80 (9)	37.04±4.20 (9)	41.47±5.39 (9)
McDermott 784 (SCS)	802	1.56±0.93 (9)	1.49±0.52 (9)	0.67±0.18 (9)	0.58±0.18 (9)
DuPont 639 (SCS)	SCS Background	8.44±0.87 (9)	9.10±1.32 (9)	6.50±0.98 (9)	8.40±2.95 (9)
Pall 326 R1-658 (M3)	21209.5 (30 TT) **	35.68±3.33 (9)	48.07±6.79 (9)	20.73±3.05 (9)	34.94±4.45 (9)
Schumacher FT20 S350F/43 (T4)	21209.5 (30 TT)	37.01±3.09 (9)	51.23±10.25 (9)	22.37±3.35 (9)	37.34±6.86 (9)
McDermott — SCS #1259	20666.5	1.57±0.23 (9)	1.67±0.72 (9)	1.66±0.15 (9)	1.76±0.40 (9)
Ensto 141-97 (B25)	26098.5 (30 TT)	26.00±9.60 (9)	25.02±4.24 (9)	25.39±3.20 (9)	22.34±3.97 (8)
Schumacher FT20 S350F/32 (T3)	31567.0 (30 TT)	34.86±3.22 (9)	54.51±3.43 (9)	23.47±2.06 (9)	35.74±5.24 (9)
PRD-66 D571C New	28004.5 (30 TT)	8.56±1.01 (9)	11.01±1.27 (9)	5.13±1.57 (9)	5.41±3.57 (9)
Pall 326 R5-667 (M23)	30149.0 (30 TT)	31.66±3.67 (9)	44.74±6.96 (9)	25.24±3.13 (9)	31.47±3.14 (9)
Techniweave New #2682 #2	20487.5 (30 TT)	1.78±0.31 (9)	1.97±0.58 (9)	0.69±0.39 (9)	1.03±0.28 (9)
Coors P-100A-1 FC065 (M10)	32698.0 (60 TT)	32.74±4.75 (9)	35.00±3.80 (9)	25.96±3.01 (9)	27.88±3.42 (9)
McDermott — SCS #1258	20666.5 (30 TT)	1.60±0.40 (9)	1.58±0.36 (9)	1.26±0.63 (9)	1.89±0.48 (9)
McDermott (R. Wagner/SCS) #787	21847.5 (30 TT)	1.18±0.58 (8)	1.26±0.52 (9)	1.03±0.74 (9)	1.51±0.81 (9)
IF&P Recrystallized SiC New	25517.5 (60 TT)	39.22±8.43 (9)	31.24±6.39 (9)	31.04±3.62 (9)	26.71±1.77 (9)
Schumacher FT20 — SCS #1173	21728.5 (30 TT)	29.60±2.28 (9)	38.76±11.44 (9)	19.13±2.75 (9)	32.41±2.48 (9)
Pall 326 — SCS #307	23317.5 (30 TT)	45.94±4.59 (9)	51.32±7.46 (9)	32.80±3.04 (9)	32.66±5.51 (9)
PRD-66 — SCS #582	SCS/20487.5 (30 TT)	7.07±0.97 (9)	9.73±1.71 (9)	4.87±1.55 (9)	6.93±2.70 (9)

\* Number in parentheses indicates the number of samples tested.

\*\* TT: Thermal transients.

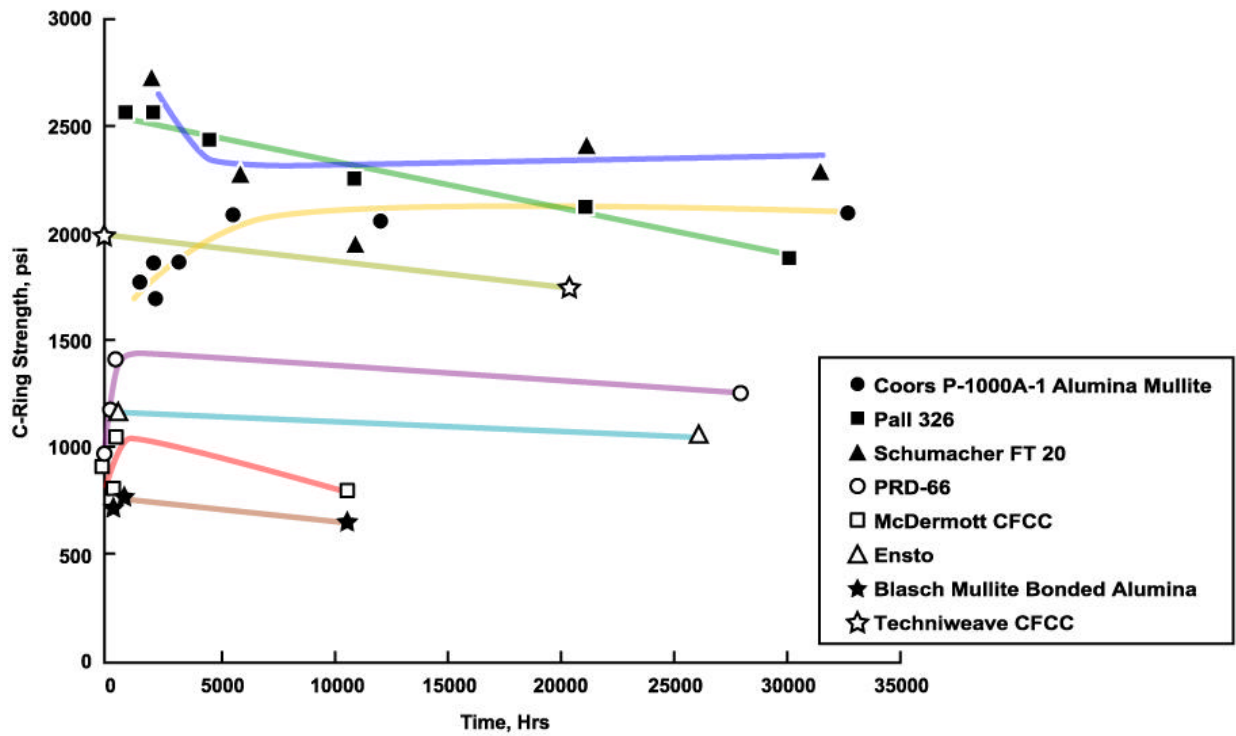
**TABLE 11**  
**RESIDUAL FILTER ELEMENT ROOM AND HIGH TEMPERATURE**  
**MATERIAL DIAMETRAL STRENGTH AND LOAD BEARING CAPABILITIES**

Element	Exposure Time, Hrs	Ultimate Strength, psi		Ultimate Load, lbs	
		25°C	800°C	25°C	800°C
Techniweave New 2682 #1	0	2301±657 (4) *	1679±141 (4)	6.08±1.02 (4)	4.95±0.29 (4)
Schumacher 1105 (SCS)	1241	1767±60 (4)	2492±149 (4)	75.68±3.46 (4)	109.00±4.82 (4)
Pall 4-980 (SCS)	2640	3384±216 (4)	3334±309 (4)	146.70±11.11 (4)	146.23±18.68 (4)
McDermott 784 (SCS)	802	762±68 (4)	549±108 (4)	7.25±0.69 (4)	5.58±0.84 (4)
DuPont 639 (SCS)	SCS Background	1662±116 (4)	1867±106 (4)	33.10±1.78 (4)	37.30±1.23 (4)
Pall 326 R1-658 (M3)	21209.5 (30 TT)**	2375±163 (4)	2865±86 (4)	97.53±8.14 (4)	127.50±8.03 (4)
Schumacher FT20 S350F/43 (T4)	21209.5 (30 TT)	2531±41 (4)	3578±178 (4)	94.63±3.24 (4)	139.03±6.07 (4)
McDermott — SCS #1259	20666.6	786±41 (4)	773±26 (4)	7.03±0.22 (4)	6.50±0.16 (4)
Ensto 141-97 (B25)	26098.5 (30 TT)	1613±156 (4)	1529±60 (4)	99.58±7.47 (4)	90.08±3.51 (4)
Schumacher FT20 S350F/32 (T3)	31567.0 (30 TT)	2440±95 (4)	3483±272 (4)	90.43±4.52 (4)	139.30±11.95 (4)
PRD-66 D571C New	28004.5 (30 TT)	1214±144 (4)	1458±188 (4)	23.03±2.65 (4)	28.98±3.73 (4)
Pall 326 R5-667 (M23)	30149.0 (30 TT)	2158±68.87 (4)	2873±238 (4)	97.03±3.57 (4)	123.93±12.06 (4)
Techniweave New #2682 #2	20487.5 (30 TT)	1893±206 (4)	1647±363 (4)	6.25±0.37 (4)	5.38±1.06 (4)
Coors P-100A-1 FC065 (M10)	32698.0 (60 TT)	1998±162 (4)	1901±104 (4)	78.80±4.48 (4)	75.53±4.56 (4)
McDermott — SCS #1258	20666.5 (30 TT)	730±46 (4)	616±40 (4)	7.03±0.45 (4)	6.83±0.46 (4)
McDermott (R. Wagner/SCS) #78	21847.5 (30 TT)	716±139 (4)	730±192 (4)	6.45±1.11 (4)	6.60±1.58 (4)
IF&P Recrystallized SiC New	25517.5 (60 TT)	4673±230 (4)	3751±320 (4)	106.65±11.47 (4)	93.33±9.37 (4)
Schumacher FT20 — SCS #1173	21728.5 (30 TT)	1760±20 (4)	2634±157 (4)	78.18±2.64 (4)	117.00±7.32 (4)
Pall 326 — SCS #307	23317.5 (30 TT)	2706±218 (4)	3151±69 (4)	119.48±4.11 (4)	143.65±4.77 (4)
PRD-66 — SCS #582	SCS/20487.5 (30 TT)	1376±135 (4)	2054±51 (4)	26.13±2.45 (4)	39.30±1.50 (4)

\* Number in parentheses indicates the number of samples tested.

\*\* TT: Thermal transients.

### Room Temperature Compressive Strength



### High Temperature Compressive Strength

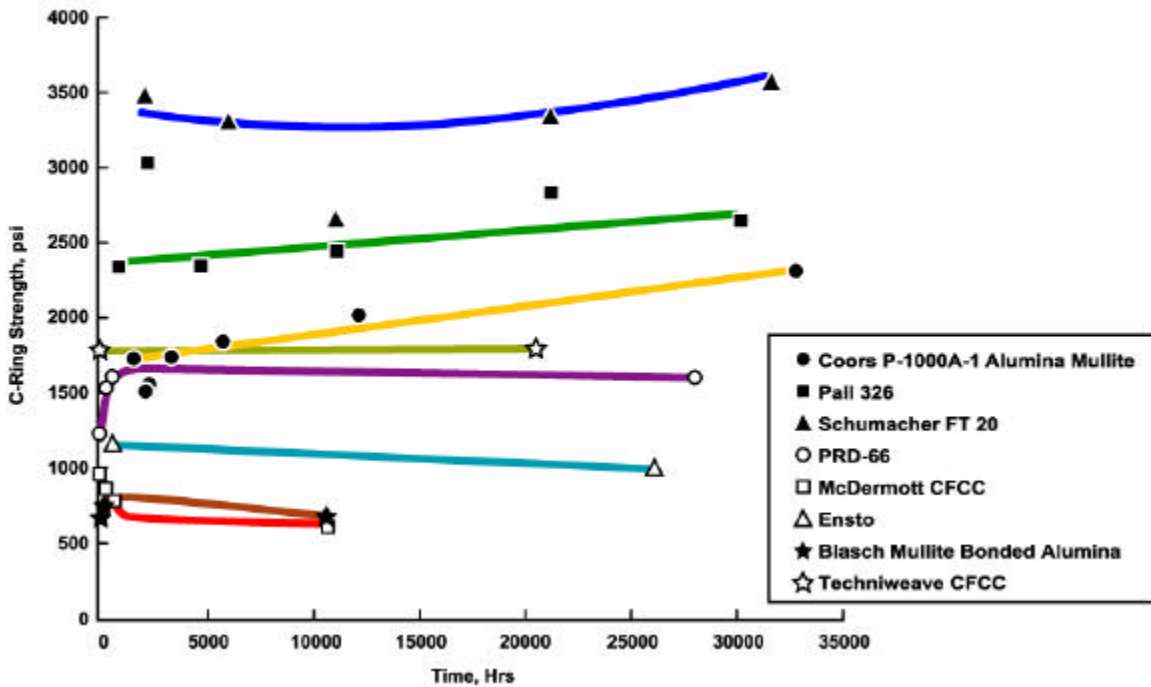


Figure 61 — Residual room and process temperature compressive strength of the various ceramic candle filter materials as a function of field and extended simulated PFBC accelerated life testing.

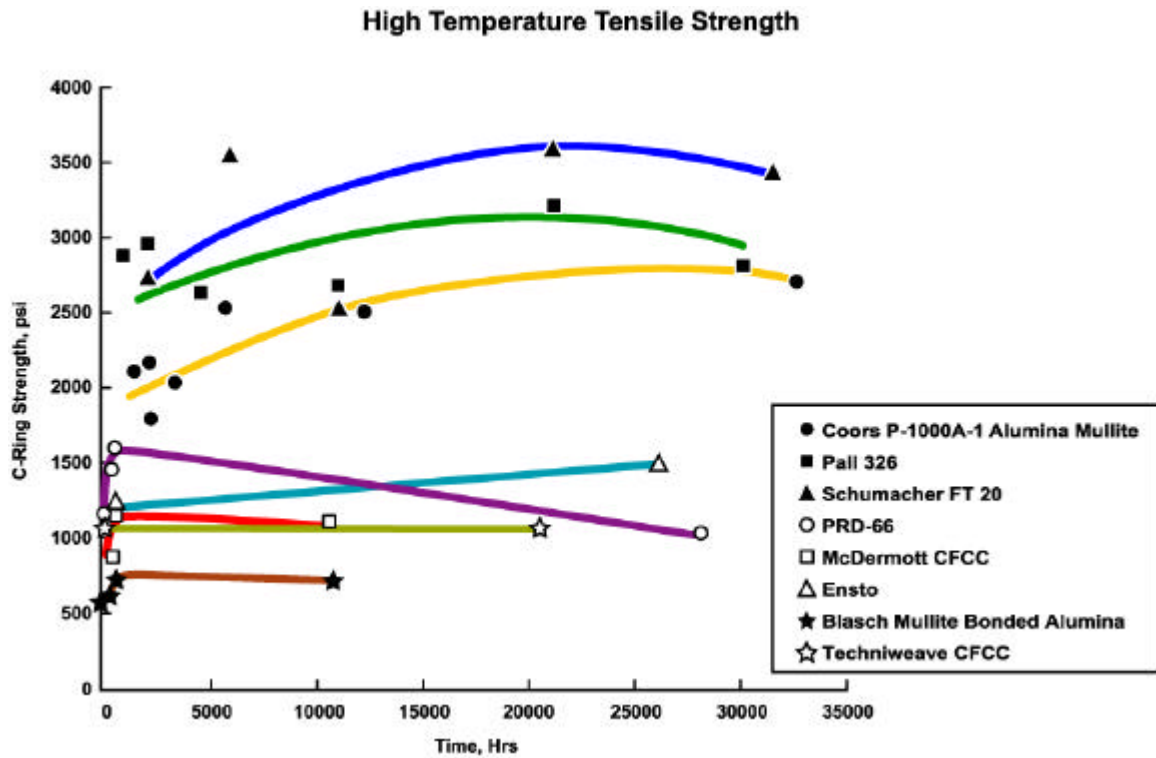
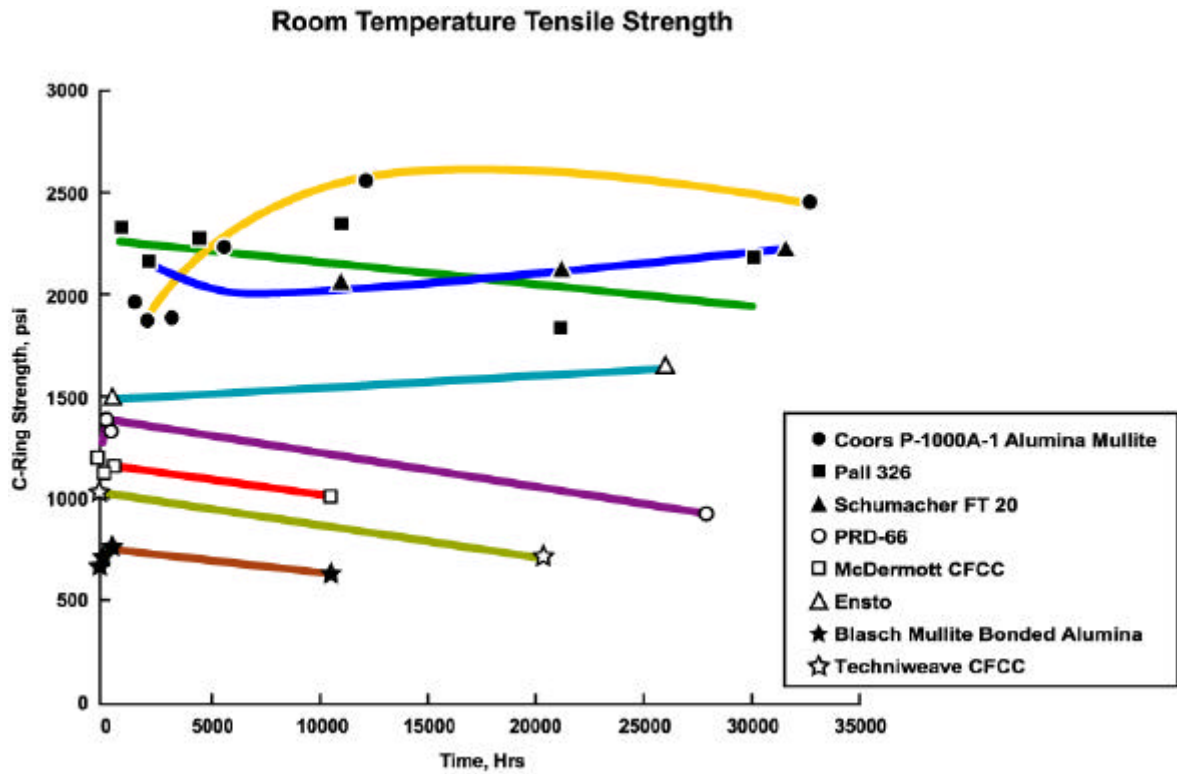


Figure 62 — Residual room and process temperature tensile strength of the various ceramic candle filter materials as a function of field and extended simulated PFBC accelerated life testing.

### 5.3 Accelerated Life Testing and High Temperature Corrosion Studies — Phase III

In conjunction with SWPC's Metal Filters for PFBC Applications Program [20], a final series of accelerated PFBC filter life tests was conducted using 1.5 and 2.0 m ceramic, as well as metal candle filters (Figure 63). As shown in Table 12, 1.5 m DuPont PRD-66 filament wound elements, 1.5 m Techniweave CFCC candles, 1.5 m Blasch mullite bonded alumina candles, and 1.5 and 2.0 m Filtros recrystallized silicon carbide filter elements were installed within the filter array. Testing was conducted for

- 81 hours at 840°C (1550°F) steady state filtration operating conditions
- 10111 accelerated pulse cleaning cycles, representing 5055 hours of operating life
- 17 thermal transients (Figure 64)

in order to demonstrate not only particulate filtration collection capability of the 1.5 and 2.0 m filter elements, but also the stability of the metal and 2.0 m ceramic elements to withstand extended life under accelerated pulse cycling and extreme thermal transient conditions. At the conclusion of testing, all ceramic filter elements were intact (Figure 65). The Blasch element was, however, broken on disassembly and removal from the filter array.



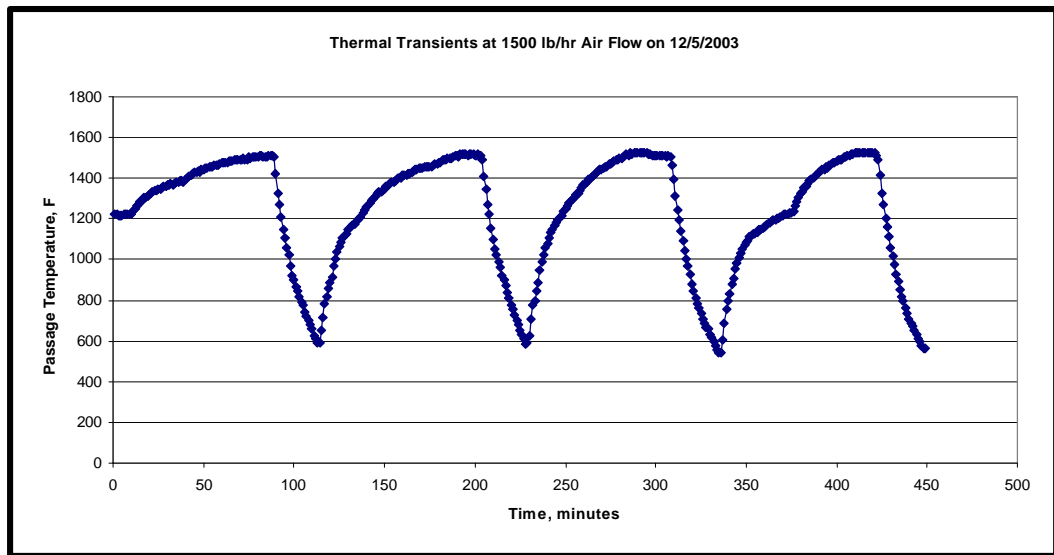
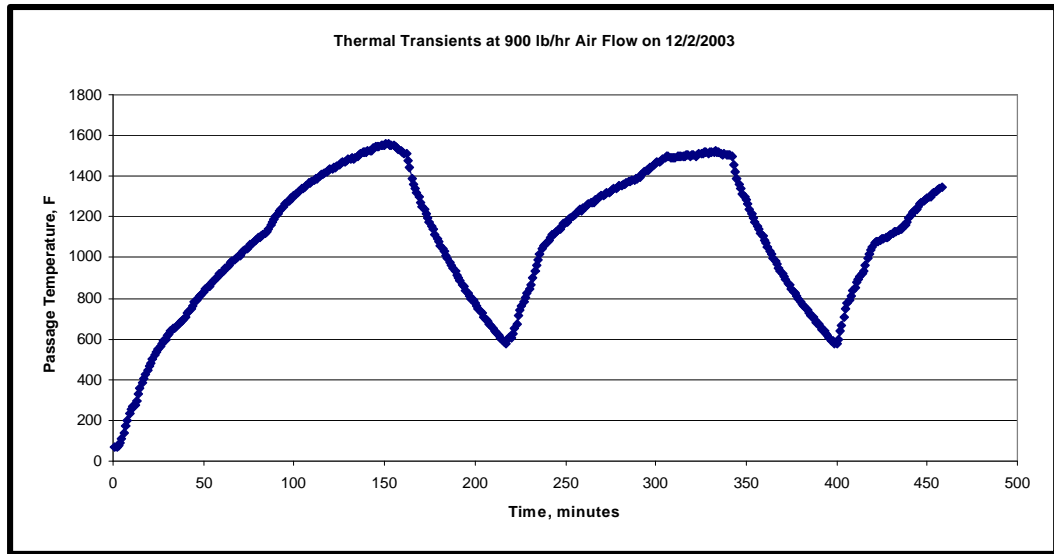
Figure 63 — Ceramic and metal candle filter array.

**TABLE 12  
CANDLE FILTER ARRAY — STEADY STATE, ACCELERATED PULSE CYCLING AND  
THERMAL TRANSIENT TESTING — PHASE III<sup>(a)</sup>**

<b>Array Position</b>	<b>Filter Element</b>	<b>Length, m</b>	<b>Steady State Testing</b>	<b>Accelerated Pulse Cycle Testing</b>	<b>Thermal Transient Testing</b>
1	DuPont PRD-66 <i>C736</i>	1.5	Intact; Planned Removed after Steady State Testing	—	—
2	Techniweave CFCC <i>IP3488-AITF2-03</i>	1.5	Intact; Planned Removed after Steady State Testing	—	—
3	Blasch <i>#3</i>	1.5	Intact; Planned Removed after Steady State Testing	—	—
4	Filtros SiC <i>#2</i>	1.5	Intact; Planned Removed after Steady State Testing	—	—
5	Bekaert/Mott Fecralloy <i>SW030122 006</i>	1.5	Intact; Retained for Continued Testing	Wrinkling of the Filtration Media; Gap Formed along the Longitudinal Seam Observed after Completion of Accelerated Pulse Cycle Testing; Element Retained within the Array for Thermal Transient Testing	Intact; Canted/Bowed; Wrinkling of the Filtration Media; Gap along the Longitudinal Seam Observed; Cross-Sectioned for Microstructural Analysis
6	Microfiltrex Fecralloy <i>ICC108618</i>	1.5	Intact; Retained for Continued Testing	Wrinkling of the Filtration Media at the Metal Joiner Ring Observed after Completion of Accelerated Pulse Cycle Testing; Retained within the Array for Thermal Transient Testing	Intact; Canted/Bowed; Wrinkling of the Filtration Media at the Metal Joiner Ring; Cross-Sectioned for Microstructural Analysis
7	DuPont PRD-66 <i>C-638</i>	1.5	Intact; Retained for Continued Testing	Intact; Retained for Thermal Transient Testing	Intact
8	Techniweave CFCC <i>IP3488 AITF 1-03</i>	1.5	Intact; Retained for Continued Testing	Intact; Retained for Thermal Transient Testing	Intact
9	Blasch <i>#9</i>	1.5	Intact; Retained for Continued Testing	Intact; Retained for Thermal Transient Testing	Broken on Removal from the Filter Array
10	Filtros SiC <i>#1</i>	1.5	Intact; Retained for Continued Testing	Intact; Retained for Thermal Transient Testing	Intact
11	Pall FeAl <i>#11</i>	1.5	Intact; Retained for Continued Testing	Intact; Retained for Thermal Transient Testing	Intact; Cross-Sectioned for Microstructural Analysis
12	USF 316L* <i>D215 #6</i>	1.5	Intact; Retained for Continued Testing	Intact; Retained for Thermal Transient Testing	Intact; Cross-Sectioned for Microstructural Analysis
13	Filtros SiC <i>#2</i>	2.0	Intact; Retained for Continued Testing	Intact; Retained for Thermal Transient Testing	Intact
14	Bekaert/Mott Fecralloy <i>SW03 122 001</i>	2.0	Element Removed after Steady State Testing; Hole through the Filtration Media; Wrinkling of the Filtration Media; Gaps/Openings along the Longitudinal Seam Weld	—	—
15	—	—	—	—	—
16	—	—	—	—	—
17	—	—	—	—	—
18	DuPont PRD-66 <i>C-738</i>	1.5	Intact; Retained for Continued Testing	Intact; Retained for Thermal Transient Testing	Intact
19	Pall FeAl <i>#16</i>	2.0	Intact; Retained for Continued Testing	Intact; Retained for Thermal Transient Testing	Intact

\* Commercial Grade Media.

- (a) Steady State Testing: 81 hr 6 min; 14 pulse cleaning cycles delivered to the filter array.  
Accelerated Pulse Cycle Testing: 419 hr 46 min; 10110 pulse cleaning cycles delivered to the filter array.  
Thermal Transient Testing: 87 hr 45 min; 17 thermal transients conducted.



Number of Transients Conducted	Temperature Decrease during Transient Event			Temperature Increase during System Reheat		
	840°C (1550°F) to 600°C (1112°F), min	DT (°F)/ Initial 1 min	DT (°F)/ Initial 5 min	600°C (1112°F) to 840°C (1550°F), min	DT (°F)/ Initial 1 min	DT (°F)/ Initial 5 min
2	~65	-50	-172	~130	+45	+180
5	~35-40	-68	-280	~125	+49	+164
10	~24	-86	-338	~88	+82	+259

Figure 64 — Temperature profile during thermal transient testing.



Figure 65 — Filter elements at the conclusion of steady state, accelerated pulse cycling and thermal transient testing. From left to right: 2.0 m Pall FeAl; 1.5 m U.S. Filter/Fluid Dynamics 316L; 1.5 m Pall FeAl; 1.5 m Bekaert/Mott Fecralloy; 1.5 m Microfiltrex Fecralloy metal media filter elements; 1.5 m Filtros recrystallized SiC; 1.5 m Techniweave CFCC; two 1.5 m DuPont PRD-66; and 2.0 m Filtros recrystallized SiC ceramic filter elements.

In a parallel effort at SWPC STC, 1.5 m McDermott CFCC, DuPont PRD-66 filament wound, Techniweave CFCC, Blasch mullite bonded alumina, Filtros recrystallized silicon carbide, and Bekaert/Mott Fecralloy elements were exposed for periods of 282 hrs to an 840°C (1550°F) simulated PFBC process gas environment containing 20 ppm SO<sub>2</sub>/SO<sub>3</sub> and 1 ppm NaCl (Table 13). Inspection of the filter array after system cool-down indicated that the Blasch element had circumferentially fractured with longitudinal cracks radiating from the fracture surface along the mold seams (Figure 66). While all the remaining ceramic elements were intact, the Bekaert/Mott Fecralloy filtration media was wrinkled and distorted along the area adjacent to the metal joiner ring. Both the Blasch and Bekaert/Mott elements were removed from the filter array, and a 1.5 m Schumacher clay bonded silicon carbide FT20 and 1.5 m Pall iron aluminide candle were installed in the filter plenum. Testing was reinitiated, and continued for an additional 204 hours. Post-test inspection of the filter array indicated that all of the ceramic filters were intact, while failure of the Pall iron aluminide resulted along/within the filtration media near the welded joiner ring (Figure 67).

**TABLE 13  
CANDLE FILTER ARRAY — HIGH TEMPERATURE CORROSION TESTING —  
PHASE III**

Position	Test Segment No. 1 282 Hrs; 579 Pulse Cycles		Test Segment No. 2 204 Hrs; 424 Pulse Cycles	
	Element	Comment	Element	Comment
1	McDermott CFCC ? <i>#1262 SCS</i>	Element Intact; Continued Testing	McDermott CFCC <i>#1262 SCS</i>	Element Intact; 486 Hrs of Exposure
2	DuPont PRD-66 ? <i>C741 New</i>	Element Intact; Continued Testing	DuPont PRD-66 <i>C741 New</i>	Element Intact; 486 Hrs of Exposure
3	Techniweave CFCC ? <i>IP3488 AITF 4-03</i>	Element Intact; Continued Testing	Techniweave CFCC <i>IP3488 AITF 4-03</i>	Element Intact; 486 Hrs of Exposure
4	Blasch Mullite Bonded Alumina <i>#4</i>	Circumferential Fracture with Longitudinal Crack Formations along Mold Seams	Schumacher Clay Bonded SiC FT20	Element Intact; 204 Hrs of Exposure
5	Filtros Recrystallized SiC ? <i>#3</i>	Element Intact; Continued Testing	Pall FeAl	Failure Resulted along/within the Filtration Media near the Welded Joiner Rings
6	Bekaert/Mott Fecralloy <i>SW03 122 005</i>	Wrinkling and Distortion of the Filtration Media along the Area Adjacent to the Metal Joiner Ring	Filtros Recrystallized SiC <i>#3</i>	Element Intact; 486 Hrs of Exposure

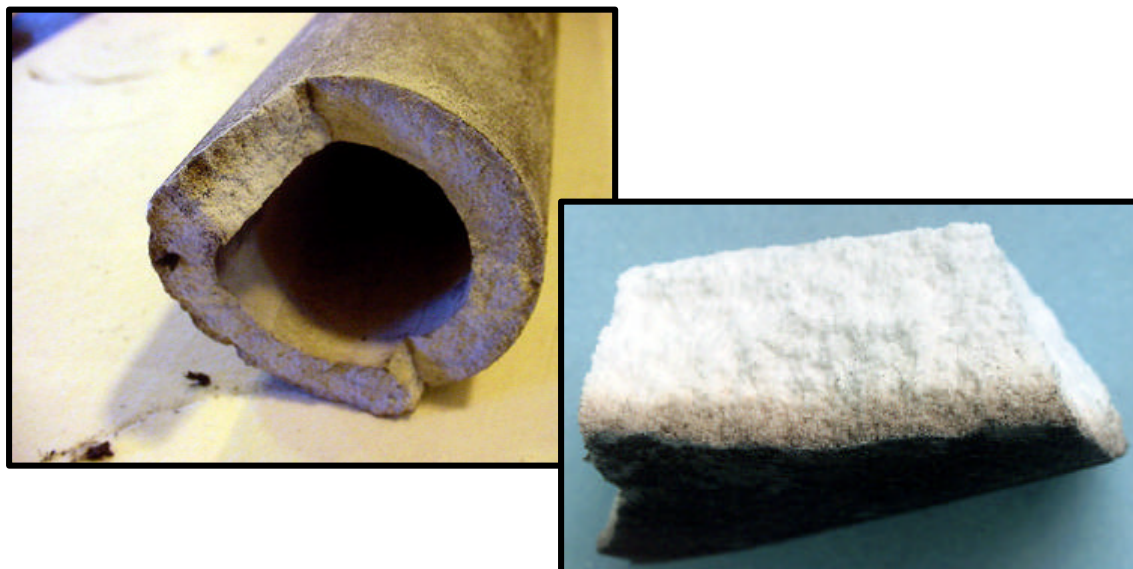


Figure 66 — Failure of the Blasch mullite bonded alumina candle filter after 282 hours of operation in the 840°C (1550°F), simulated PFBC process gas environment containing gas phase sulfur and alkali (Test Segment No. 1).



Figure 67 — Candle filters at the conclusion of Test Segment No. 2 — 486 hours of exposure at 840°C (1550°F) in the simulated PFBC process gas environment containing gas phase sulfur and alkali. Elements from left to right include: Filtros recrystallized SiC; Pall iron aluminide; Schumacher clay bonded SiC FT20; Techniweave CFCC; DuPont PRD-66; and McDermott CFCC.

Post-test room temperature gas flow resistance measurements and microstructural analyses were conducted on each simulated PFBC-exposed porous filter matrix. As shown in Figure 68, the gas flow resistance of the cleaned, post-accelerated life-tested McDermott, Schumacher and Filtros filter elements increased slightly in comparison to their as-manufactured resistances. In contrast, the post-test gas flow resistance of the cleaned Techniweave filter element was substantially higher than its as-manufactured resistance indicating that ash fines were retained within the outer surface or within the wall of the filter element.

Microstructural analysis indicated that the open porosity through the cross-sectioned filter wall of the various filter matrices had been retained after 204-486 hours of operation in the gas phase alkali and sulfur-laden, simulated PFBC process gas environment. Sodium was typically identified along and within the o.d. surface and outer membrane of each filter. Sorption of sodium within the interior of the filter wall was generally limited or not detectable.

As shown in Figure 69, after 204 hours of exposure, sodium, sulfur and chlorine resulted within the aluminosilicate binder phase that encapsulated the Schumacher FT20 silicon carbide structural support grains that were primarily located within the porous matrix near the o.d. surface of the filter wall. In contrast to the Schumacher FT20 filter matrix, sorption of sulfur, alkali, and chlorine was limited within the Filtros recrystallized silicon carbide filter matrix after 486 hours of simulated PFBC operation. Surface oxidation of the silicon carbide grains extensively resulted within the cross-sectioned wall near the o.d. surface of the filter element (Figure 70). A discontinuous silica-enriched layer formed along the surface of the structural support grains that were present within the center or along the i.d. (pulse cycled) surface of the filter element. Within these areas, ~2 μm silica-enriched features were observed to have formed along the mottled surface of the underlying silicon carbide grains.

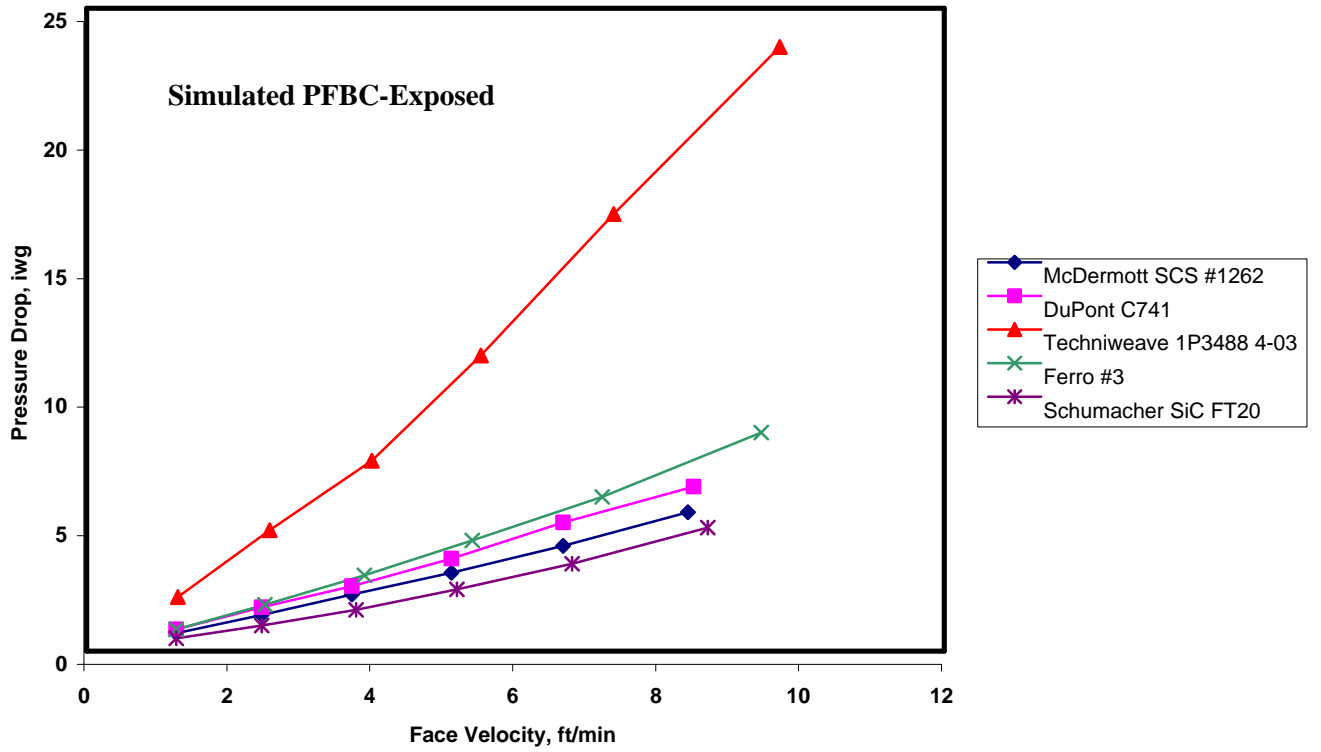
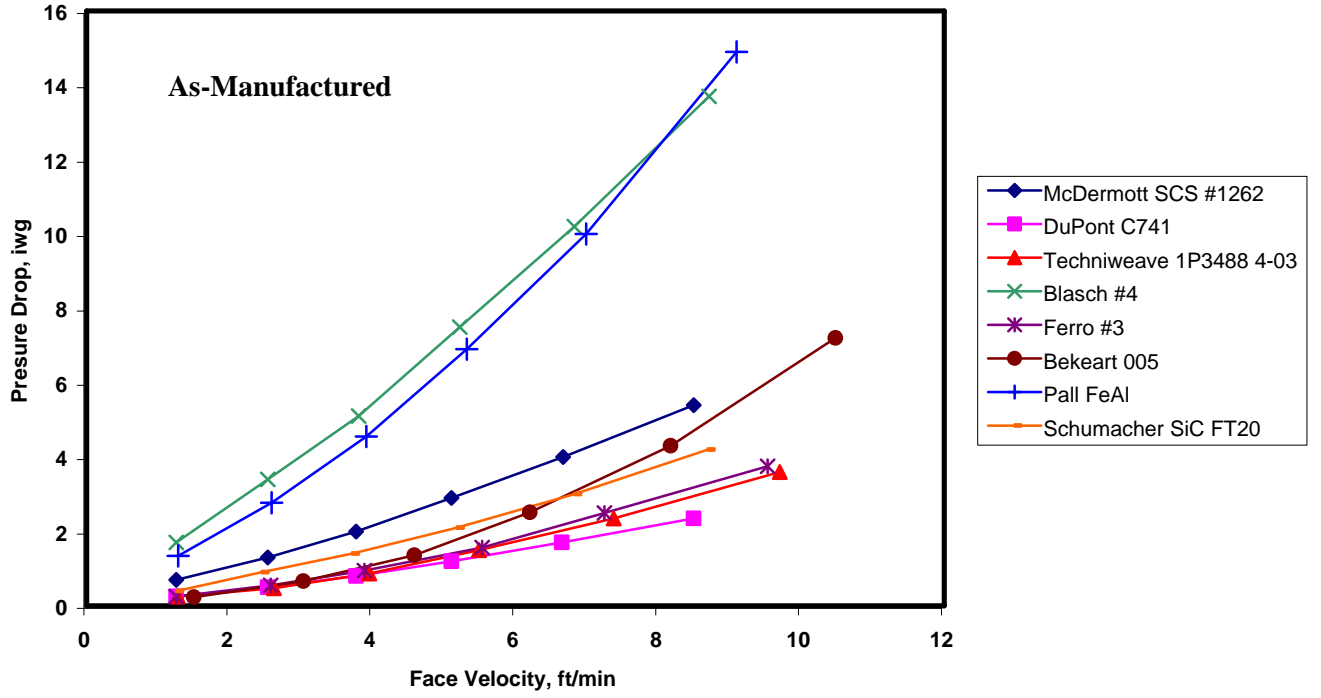


Figure 68 — Room temperature gas flow resistance through the porous filter elements.

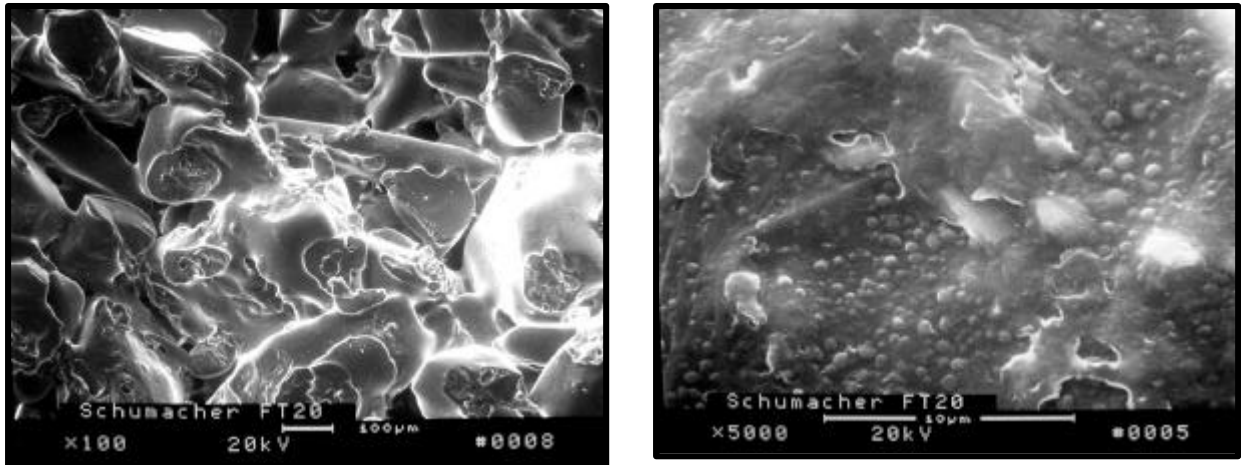


Figure 69 — Schumacher clay bonded silicon carbide FT20 filter matrix after 204 hours of operation in the gas phase alkali and sulfur-laden, 840°C (1550°F), simulated PFBC process gas environment. Sorption of sodium, sulfur and chlorine into the oxide that encapsulated the silicon carbide structural support grains established a phase gradient within the filter matrix along the o.d surface of the filter element.

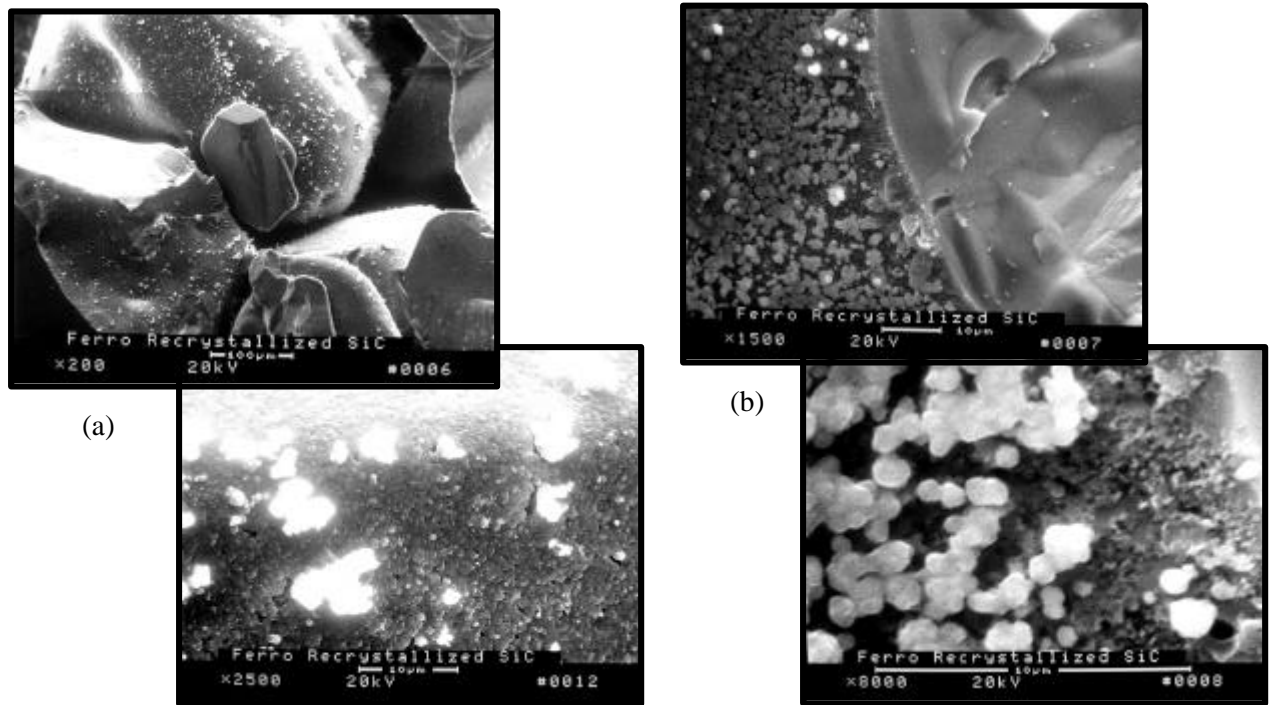


Figure 70 — Morphology of the Filtros recrystallized silicon carbide filter matrix after 486 hours of operation in the gas phase alkali and sulfur-laden, 840°C (1550°F), simulated PFBC process gas environment. (a) Near the outer surface of the cross-sectioned filter surface; (b) Along the mid-section and i.d. or pulse cycled surface of the filter element.

Gas phase sodium readily adsorbed along the surface of the mullite-enriched binder phase that was present along the outer surface of the alumina grains within the 282 hour, alkali and sulfur-laden, simulated PFBC-exposed Blasch filter matrix (Figure 71). Limited sodium was identified to have penetrated into the cross-sectioned filter ligament, as well as within the matrix along the i.d. or pulse cycled surface of the Blasch filter wall. Similarly extensive sorption of alkali resulted within the outer membrane of the DuPont PRD-66 filter matrix after 486 hours of exposure to the alkali and sulfur-laden simulated PFBC process gas environment, while limited sorption resulted within the underlying structural support filaments (Figure 72).

An alkali sulfate phase was identified within the o.d. surface of the McDermott filter element after 486 hours of operation in the simulated PFBC process gas environment (Figure 73). Limited concentrations of sodium were detected within the interior of the McDermott filter architecture. Although crystallization was observed throughout the Nextel™ fibers, the fracture toughness of the porous CFCC filter matrix was retained.

In contrast to the McDermott filter matrix, loss of fracture toughness and embrittlement of the Techniweave CFCC filter matrix resulted after 486 hours of operation in the gas phase alkali and sulfur-containing, simulated PFBC process gas environment. Low concentrations of sodium were detected along the cross-sectioned o.d. surface of the Techniweave filter matrix (Figure 74). Sodium was not detected within the interior of the filter wall.

Unlike the porous ceramic filter matrices, and ~50-100 μm thick oxide layer formed along the outer surface of the Pall iron aluminide filter matrix after 204 hours of operation in the gas phase alkali and sulfur-containing, simulated PFBC process gas environment (Figure 75). Iron sulfate-enriched crystalline features resulted along the surface of the Pall FeAl pore cavities.

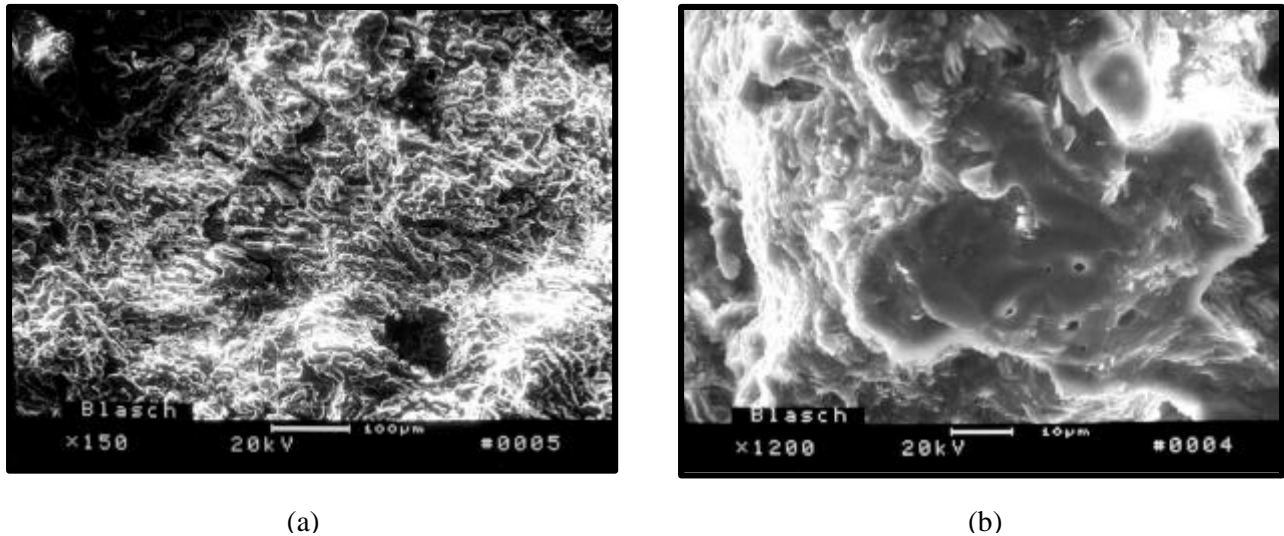


Figure 71 — Morphology of the Blasch filter matrix after 282 hours of exposure to the gas phase alkali and sulfur-laden, 840°C (1550°F), simulated PFBC process gas environment. (a) Striated platelet matrix formations within the mid-section of the filter wall; (b) Non-crystalline morphology within the interior of the fresh fractured ligament.

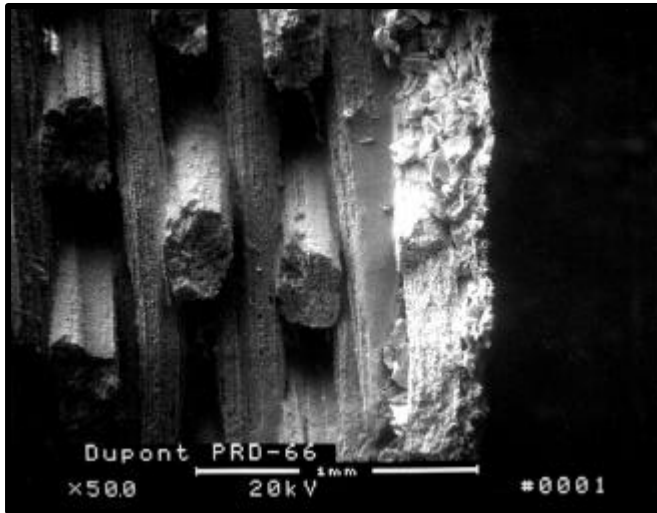


Figure 72 — Microstructure of the DuPont PRD-66 filter matrix after 486 hours of exposure to the gas phase alkali and sulfur-laden, 840°C (1550°F), simulated PFBC process gas environment. In comparison to an as-manufactured DuPont PRD-66 filter matrix, negligible microstructural changes were detected.

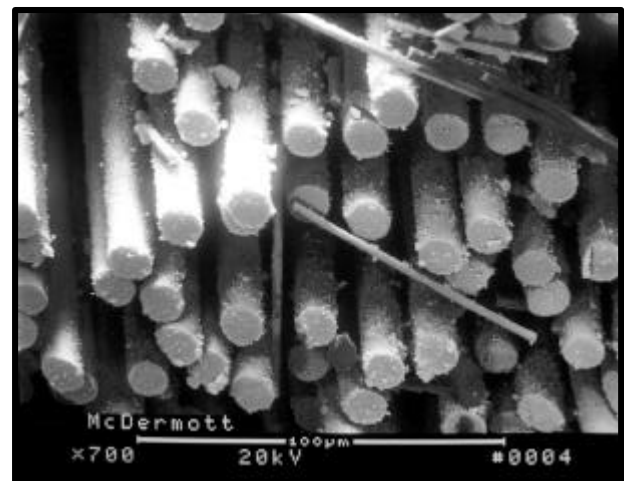
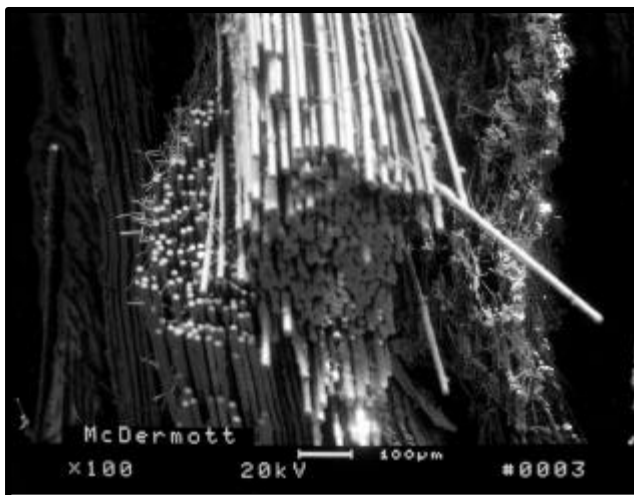


Figure 73 — Microstructure of the McDermott CFCC filter matrix after 486 hours of operation in the gas phase alkali and sulfur-laden, 840°C (1550°F), simulated PFBC process gas environment.

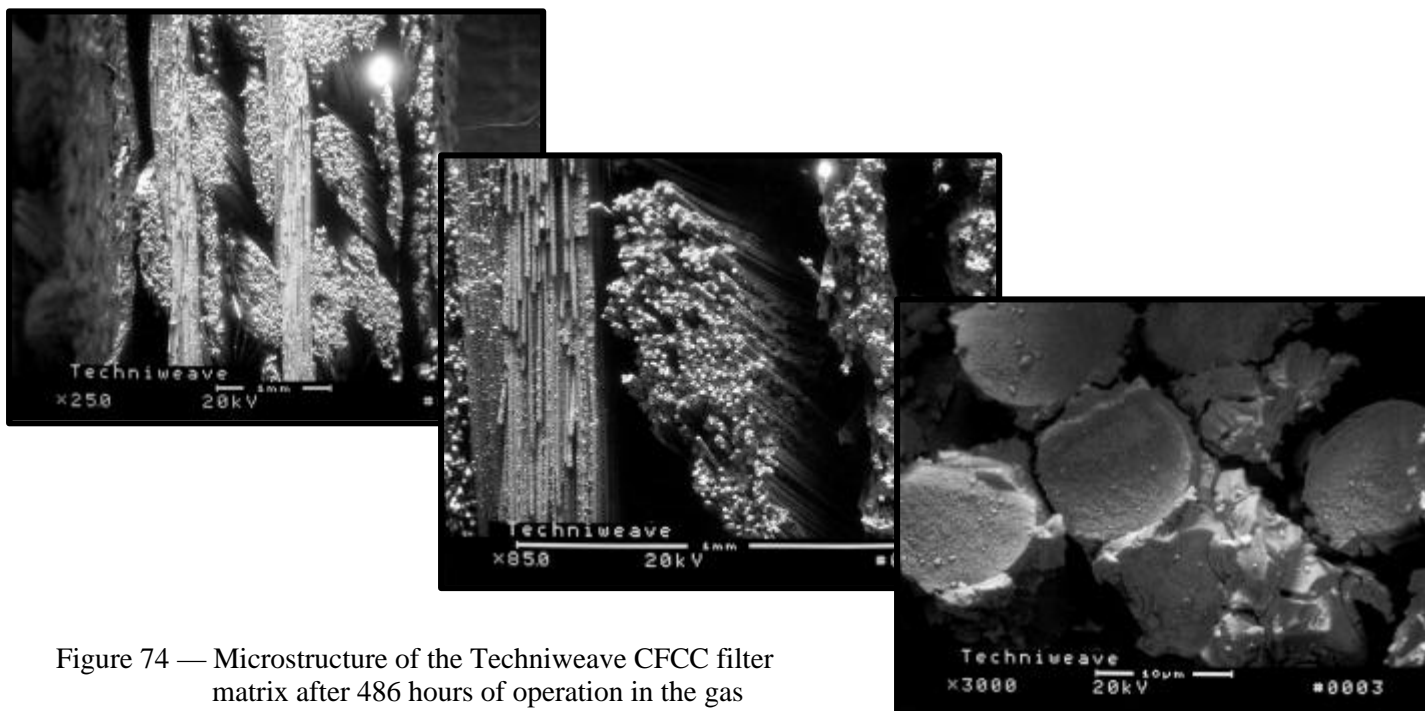


Figure 74 — Microstructure of the Techniweave CFCC filter matrix after 486 hours of operation in the gas phase alkali and sulfur-laden, 840°C (1550°F), simulated PFBC process gas environment.

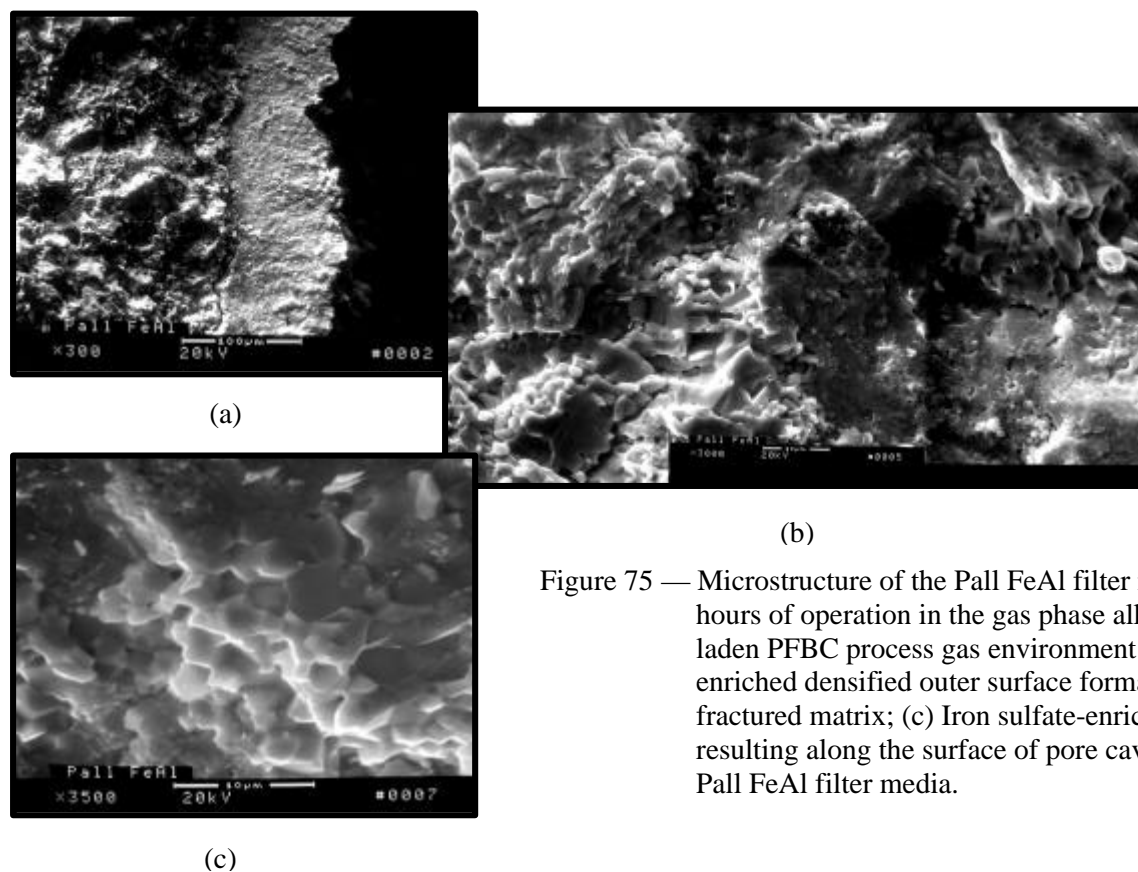


Figure 75 — Microstructure of the Pall FeAl filter matrix after 204 hours of operation in the gas phase alkali and sulfur-laden PFBC process gas environment. (a) Iron oxide-enriched densified outer surface formation; (b) Fresh fractured matrix; (c) Iron sulfate-enriched features resulting along the surface of pore cavities within the Pall FeAl filter media.

## 6. SUMMARY AND CONCLUSIONS

As shown in Figure 76, development of the hot gas filter technology began in the 1970's when porous metal filter media as Hastelloy X were used to construct filter elements. Accelerated oxidation or corrosion, and loss of tensile strength and load bearing capability of the porous metal filter media resulted when these elements were tested. As proposed pressurized fluidized-bed combustion (PFBC) system operating temperatures were increased to 870°C (1600°F), efforts were refocused through the early 1990's on the development of filter systems which utilized monolithic ceramic clay bonded silicon carbide candle filters (Figure 77). For operation in combustion gas environments, oxide-based, porous ceramic filter matrices were developed in order to achieve the chemical stability requirements for materials during long-term operation (Figure 78).

Both oxide, as well as nonoxide porous ceramic filters were installed and operated in Siemens Westinghouse's Advanced Particulate Filtration systems at the American Electric Power PFBC Tidd Demonstration Plant in Brilliant, OH, and at the Foster Wheeler pressurized circulating fluidized-bed combustion (PCFBC) test facility in Karhula, Finland. Siemens Westinghouse conducted extensive filter material surveillance programs for candles that were operated in each test facility. Failure of the oxide-based candles was attributed to thermal fatigue of alumina/mullite matrix resulting during long-term pulse cycling of the elements, as well as to thermal shock of the matrix during plant thermal transient events (Table 14). For the nonoxide-based clay bonded silicon carbide elements, elongation and failure of the candles resulted which lead to improvements and

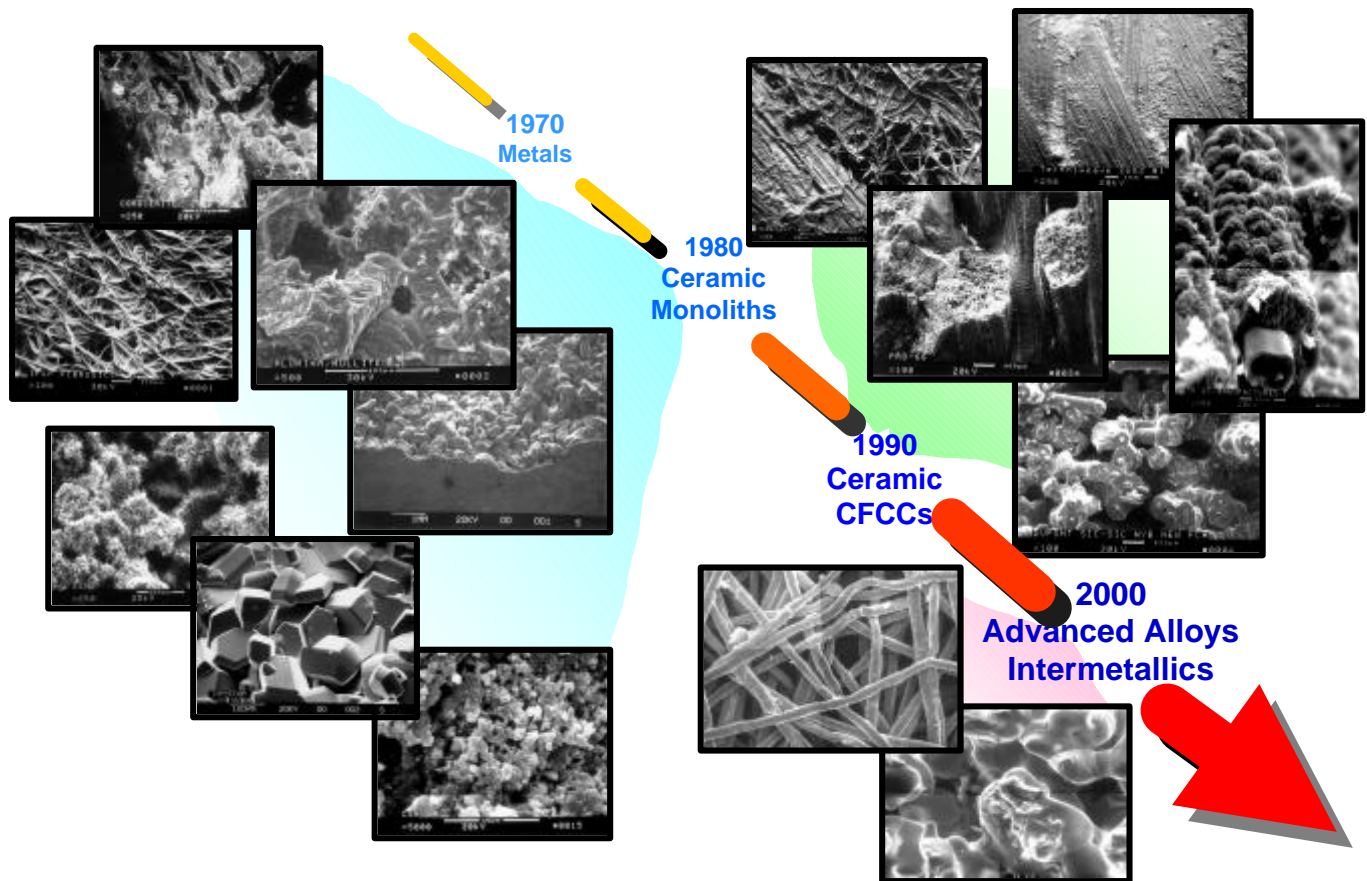


Figure 76 — Porous hot gas filter material technology development.

stabilization of the clay binder, while oxidation of the silicon carbide grains and volume expansion of the component were addressed through the inclusion of oxidation resistant grain and/or binder additives.

To provide a more “ruggedized” filter system, emphasis in the mid-1990’s was focused on the development and manufacture of advanced oxide- and nonoxide-based, porous second-generation, continuous fiber ceramic composite and filament wound filter elements which were projected to have significantly improved fracture toughness characteristics over that of the first-generation monolithic ceramic filter materials (Figures 79 and 80). When tested in Siemens Westinghouse filter systems, oxidation of the nonoxide-based elements led to brittle failure of the candles. Debonding of external particulate filtration membranes, and failure along seams and non-integral flanges and end caps of the advanced second-generation oxide-based candle filters also occurred.

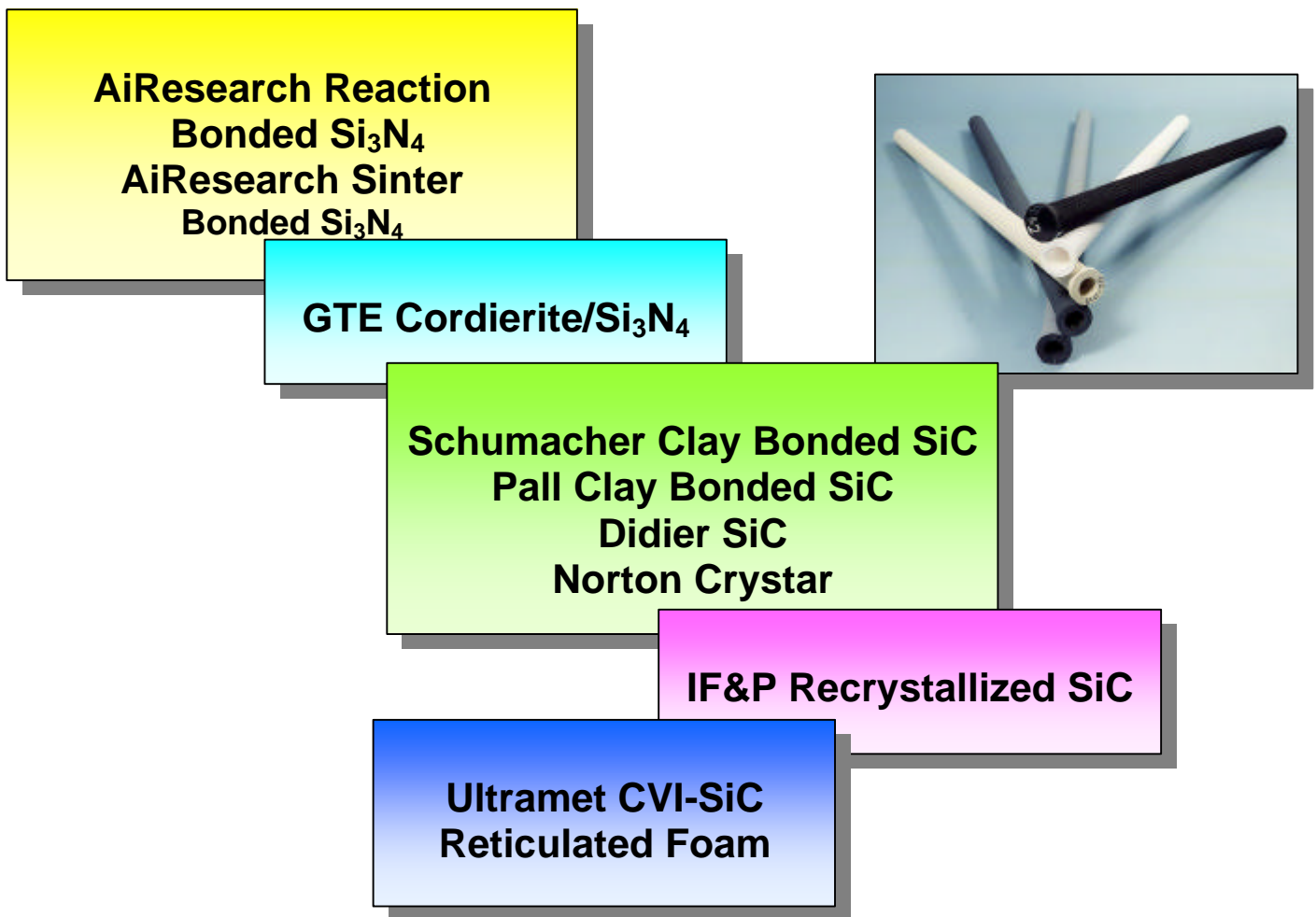


Figure 77 — Porous monolithic nonoxide-based ceramics used for hot gas filter technology development.

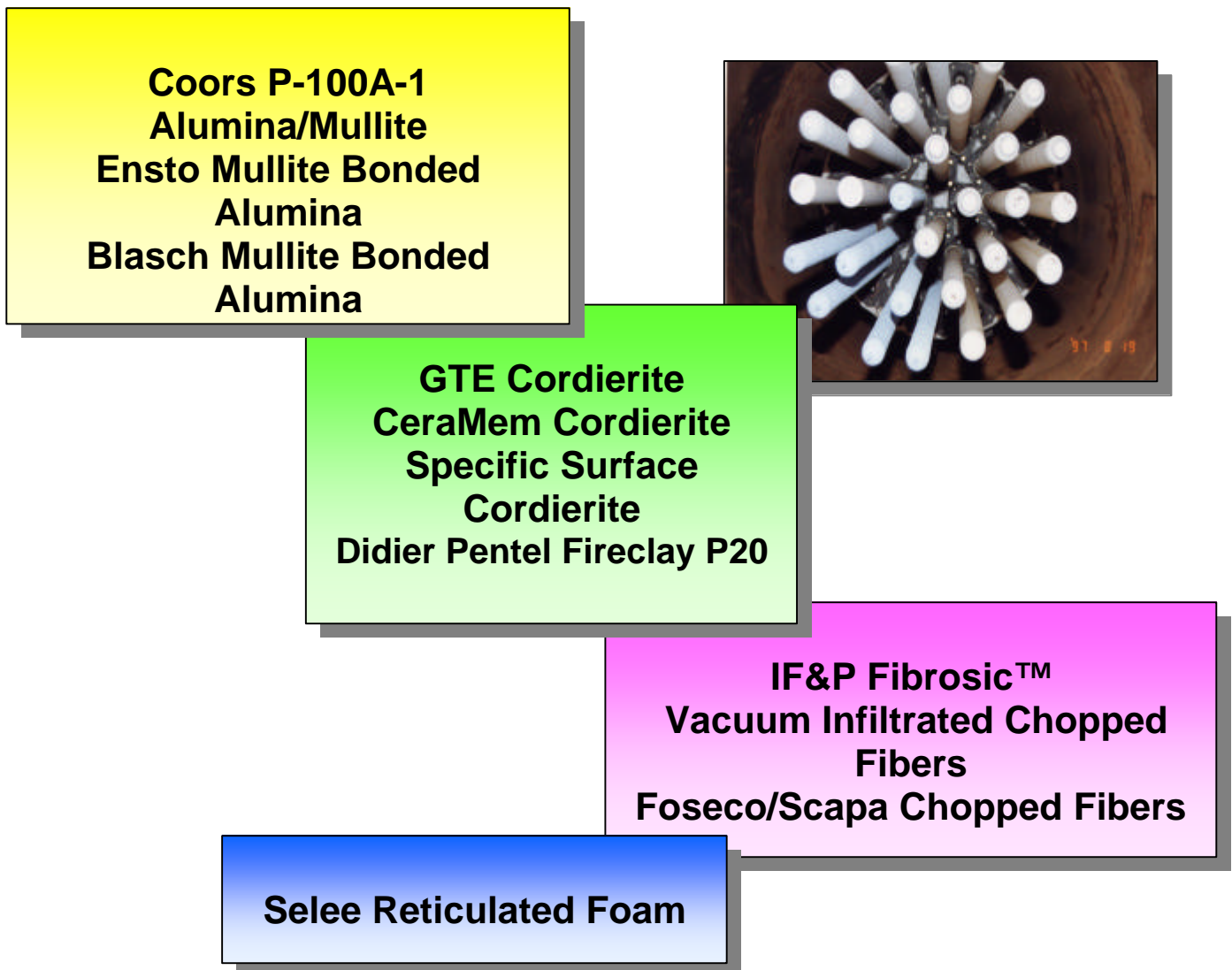


Figure 78 — Porous monolithic oxide-based ceramics used for hot gas filter technology development.

Throughout this effort SWPC discussed with each filter element supplier, the need, as well as potential manufacturing approaches required to improve the quality, integrity, and performance of the various elements, in order to achieve extended operating material and component life in advanced coal-fired applications. Many of the manufacturing modifications were implemented by the various filter element suppliers.

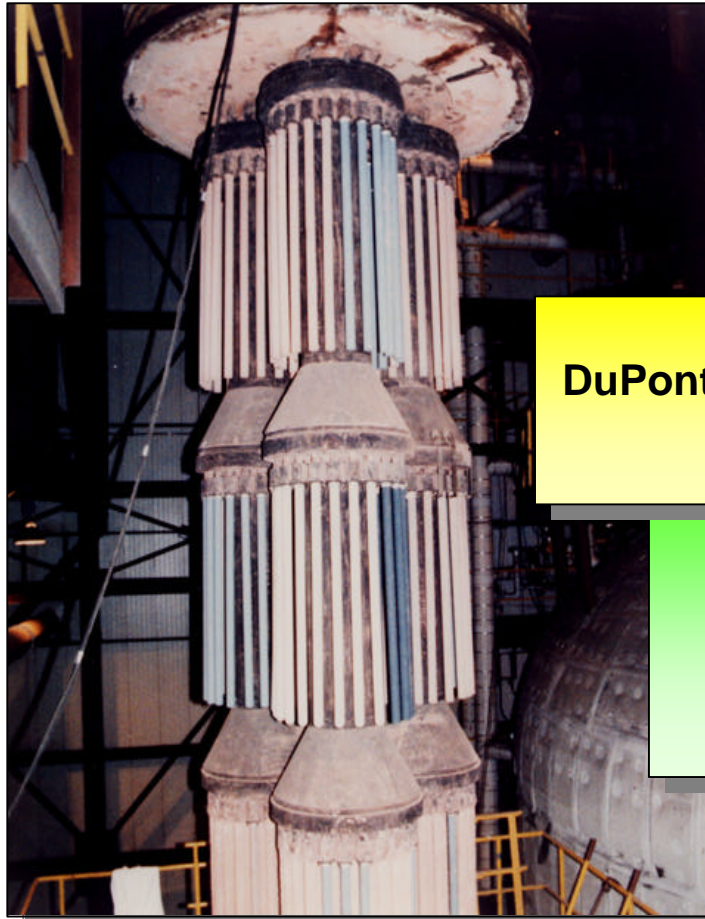
At the peak of the hot gas filter development program, nearly twenty suppliers were involved in the development, manufacture and supply of 1-1.5 m porous ceramic candle filter elements. Due to the lack of market opportunity, a maximum of six filter suppliers are currently available. However, during the years between 1980 and 2000, significant improvements were made not only to the materials themselves, but also to component design, architecture and manufacturing of the filter elements. These improvements resulted in production of elements that met quality assurance and control criteria, as well as filter geometry and process operating design specifications, and were readied for extended long-term use in advanced PFBC/PCFBC applications. In the Filter Component Assessment program, Siemens Westinghouse demonstrated the viability of the select

**TABLE 14  
POROUS CERAMIC FILTER FAILURE MECHANISMS**

Monolithic Ceramics		2 <sup>nd</sup> -Generation Materials	
Rigid Ceramics	Chopped Fibrous Matrices	Oxide-Based Matrices	Nonoxide-Based Matrices
<ul style="list-style-type: none"> <li>• Thermal Fatigue/Shock Identified for the Oxide-Based Monoliths</li> <li>• High Temperature Oxidation/Volume Expansions Identified for the Nonoxide Monoliths</li> <li>• High Temperature Creep for Original Clay Bonded SiC Matrices</li> <li>• Loss of Nonoxide-Based Material Gas Flow Permeability and Filtration Due to the Formation of Amorphous Glassy Phase in the Presence of Gas Phase Alkali</li> </ul>	<ul style="list-style-type: none"> <li>• Low Strength/Low Load Bearing Characteristics</li> <li>• Modifications Required for Adequate Sealing and Mounting of Flange into Filter Holder Array</li> </ul>	<ul style="list-style-type: none"> <li>• Retention of Outer Membrane Architecture</li> <li>• Low Strength/Low Load Bearing Characteristics</li> <li>• Modifications Required for Adequate Sealing and Mounting of Flange into Filter Holder Array</li> <li>• Fiber Embrittlement</li> </ul>	<ul style="list-style-type: none"> <li>• High Temperature Oxidation</li> <li>• Fiber Embrittlement</li> <li>• Reduction in Fracture Toughness Characteristics Related to Brittle Fracture</li> <li>• Outer Confinement Layer Architecture Debond/Delamination</li> <li>• Seam Debonding</li> <li>• Low Load Bearing Characteristics</li> <li>• Modifications Required for Adequate Sealing and Mounting of Flange into Filter Holder Array</li> <li>• Loss of Nonoxide-Based Material Gas Flow Permeability and Filtration Due to the Formation of Amorphous Glassy Phase in the Presence of Gas Phase Alkali</li> </ul>

porous ceramic materials and components to achieve  $\geq 3$  years of equivalent filter operating life under accelerated simulated PFBC operating conditions. Siemens Westinghouse similarly demonstrated the capability of suppliers to manufacture 2.0 m porous ceramic filter elements, and the capability of the elements to be successfully tested in our bench-scale PFBC filter vessel. As a result of conduct of the Filter Component Assessment program and participation in numerous field surveillance programs, the McDermott oxide-based CFCC filter elements are recommended as the hot gas filter material technology for extended  $\sim 800\text{-}900^\circ\text{C}$  ( $\sim 1470\text{-}1650^\circ\text{F}$ ) PFBC/PCFBC field service use. In addition, the Schumacher/Pall clay bonded silicon carbide filter elements are recommended for PFBC/PCFBC field service operations not exceeding  $\sim 750\text{-}800^\circ\text{C}$  ( $\sim 1380\text{-}1470^\circ\text{F}$ ).

Towards the end of the 1990's, advanced corrosion resistant porous metal and intermetallic filter media were considered as a potential low risk alternative for use in PFBC hot gas filtration



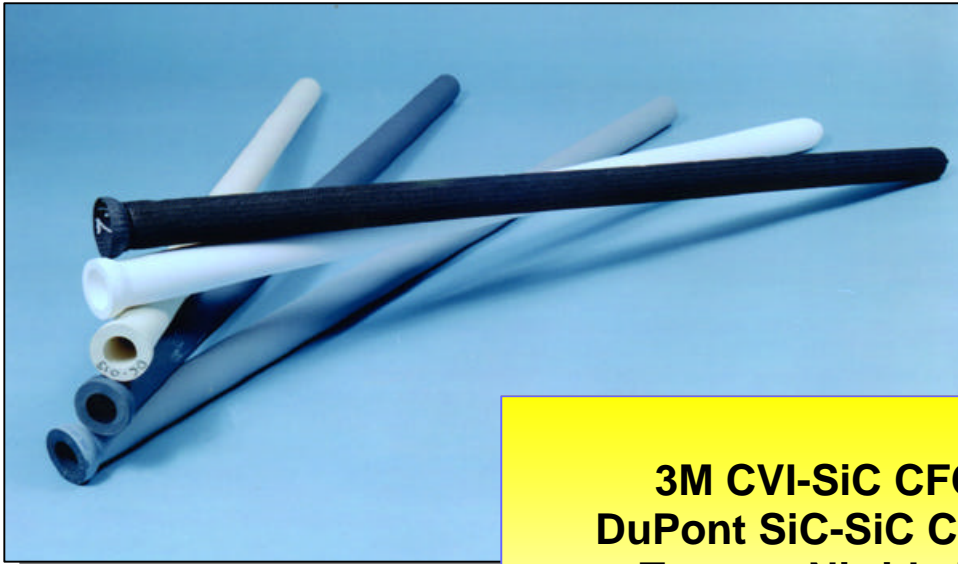
**DuPont PRD-66 Filament  
Wound**

**3M Nextel CFCC  
McDermott Nextel CFCC  
Techniweave Nextel CFCC  
Americom CFCC**

Figure 79 — Porous second-generation oxide-based ceramics used for hot gas filter technology development.

systems, particularly when installed in second-generation PCFBC systems operating at temperatures of 650-750°C (1200-1400°F). Porous advanced metal and intermetallic filters were expected to be non-brittle (i.e., ductile), and exhibit improved thermal stress damage tolerance in comparison to ceramic filter elements. Advantages over ceramic candles also included eliminating the need for thermal regenerators, the ability to directly weld metal filters to support structures to form hermetic seals, eliminating the use of ceramic fiber dust seals, and the ability to form metals in a wide variety of shapes. These advantages would permit more robust designs to be considered, improve packaging, lower system costs, and increase process operating reliability.

In September 1998, Siemens Westinghouse initiated effort on the Metal Filters for Pressurized Fluid Bed Combustion Applications program to develop and evaluate the use of porous, high temperature, sinter bonded fiber and powder metal media candle filters in PFBC and PCFBC systems. Advanced alloys selected for evaluation in this program included Haynes 230, Haynes 214, Haynes 188, Haynes 556, iron aluminide (FeAl), and Fecralloy (FeCrAl(Y)) porous metal media manufactured by U.S Filter/Fluid Dynamics (USF), Pall Advanced Separation Systems, Mott Corporation, Fairey Microfiltrex, and Technetics. Elements constructed from 310S, Inconel 600, and



**3M CVI-SiC CFCC (Nextel)  
DuPont SiC-SiC CFCC (Nicalon)  
Textron Nitride Bonded SiC  
Textron Nitride Bonded Si<sub>3</sub>N<sub>4</sub>  
Textron Reaction Bonded Si<sub>3</sub>N<sub>4</sub>**

Figure 80 — Porous second-generation nonoxide-based ceramics used for hot gas filter technology development.

Hastelloy X were included as commercially available materials for comparison with the performance and stability of the advanced alloys and intermetallic media in this program.

Testing of composite candle filters constructed from joined metal media filter sections was conducted in Siemens Westinghouse's bench-scale PFBC particulate filtration system in Pittsburgh, PA. Composite candle filter elements were installed and operated in a 650°C (1200°F), 760°C (1400°F), and 840°C (1550°F), pressurized (1.103 kPa (147 psi)), simulated PFBC process gas environment containing 6% O<sub>2</sub>, 7% CO<sub>2</sub>, 73% N<sub>2</sub>, 14% H<sub>2</sub>O, and 20 ppm (max) SO<sub>2</sub>, for periods of ~250, 500, and 1000 hours. Post-test characterization of each commercially available, advanced alloy metal media, and intermetallic filter media included determination of the residual process temperature strength, and an assessment of the microstructural and/or phase stability of the porous filter matrix. Testing was similarly conducted at 840°C (1550°F) in the absence of gas phase sulfur, and with the addition of 1 ppm gas phase alkali in the sulfur-laden simulated PFBC process gas environment.

Based on testing conducted in the Metal Filters for PFBC Applications program, porous sinter bonded FeAl and Fecralloy media were identified as candidate materials for construction of metal filter elements for installation and potential extended operation in high temperature, gas phase alkali-free, PFBC/PCFBC applications. In the presence of 1 ppmv gas phase alkali, accelerated oxidation, pore closure, crack formations through the surface oxide, and/or removal of filter media sections limit the use of all porous sinter bonded metal media filter elements during operation in an 840°C (1550°F) PFBC/PCFBC process gas environment.

As a result of hot gas filter materials development conducted by Siemens Westinghouse, Figure 81 illustrates the recommended PFBC/PCFBC and IGCC operating temperatures for ceramic, advanced alloy and intermetallic filter elements. The stability of the oxide-based monolithic ceramic matrices remains the critical factor for selection of filter media when elements are installed and operated at temperatures  $\geq 800^{\circ}\text{C}$  ( $\geq 1470^{\circ}\text{F}$ ). Oxidation of the nonoxide ceramics, as well as advanced alloys results in the presence of steam in PFBC/PCFBC applications when process operating temperatures exceed  $700\text{--}800^{\circ}\text{C}$  ( $1290\text{--}1470^{\circ}\text{F}$ ). Accelerated oxidation of the advanced alloys and intermetallics occurs when gas phase alkali is present in the combustion gas. Pore closure leads to a reduction in gas flow through the matrix, restricting the use of these materials with extended operating time. Embrittlement of the ductile metal also results.

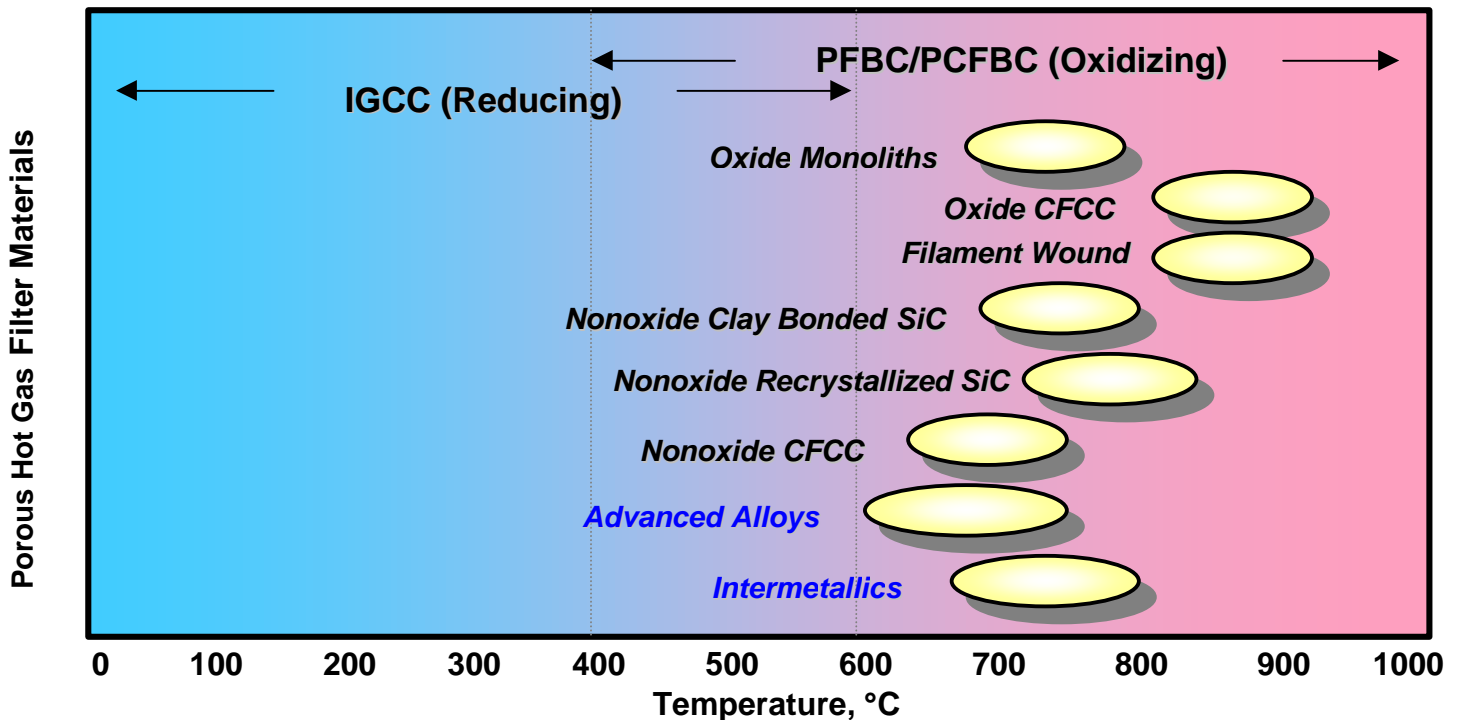


Figure 81 — Recommended maximum operating temperatures for hot gas filter material stability.

In the presence of gas phase alkali at temperatures  $>700\text{--}800^{\circ}\text{C}$  ( $>1290\text{--}1470^{\circ}\text{F}$ ), glass and eutectic phases result within the nonoxide ceramic-based monoliths. For the nonoxide monoliths, pore closure can occur, particularly within the fine grains contained in the filtration membrane layer. Spalling of the surface oxide formed along the outer surface of the silicon carbide grains can occur within continued plant startup and shutdown cycles, permitting exposure of fresh surfaces for continued oxidation, thinning of the structural support grains, and overall reduction in the strength of the filter matrix. For nonoxide CFCC matrices, accelerated oxidation, formation of the glass and eutectic phases, overall pore closure and embrittlement of the matrix occurs. In order to mitigate these responses, use of the nonoxide ceramic-based monoliths and CFCC filter materials is recommended for temperatures  $<700\text{--}750^{\circ}\text{C}$  ( $<1290\text{--}1380^{\circ}\text{F}$ ), under conditions that limit the presence of gas phase alkali in the process gas environment. For IGCC applications which operate at temperatures  $<700^{\circ}\text{C}$  ( $<1290^{\circ}\text{F}$ ), the oxide-based CFCC, nonoxide monolithic ceramics, advanced alloys and intermetallics are considered as viable materials for extended operation.

For all high temperature applications, removal of ash from the filter array is a critical issue to prevent bridging events that catastrophically limit the effective use of the hot gas filtration system. Alternate filter system designs as the inverted candle filter configuration provide additional robustness to the extended life of the hot gas filter elements.

Over the past 30 years, significant advancements have been made in the development and understanding of the response of porous high temperature materials for use in future advanced coal-fired systems. These achievements are directly transferable to technologies related to the development of ceramic turbine blades and vanes, catalytic combustors, as well as generation of advanced gas separation membranes for use in FutureGen applications.

## 7. REFERENCES

1. M. J. Mudd, J. D. Hoffman, and W. P. Reinhart, "Tidd Hot Gas Clean Up Program," Final Report, American Electric Power Service Corporation, DOE Contract No. DE-FC21-89MC26042, July 1995.
2. M. A. Alvin, "Assessment of PCFBC-Exposed Advanced Candle Filters," Topical Report, DOE/FETC Contract No. DE-AC21-94MC31147, July 21, 1997.
3. M. A. Alvin, J. E. Lane, and T. E. Lippert, "Thermal/Chemical Degradation of Ceramic Cross-Flow Filter Materials," Phase I Topical Report, DOE/METC Contract No. DE-AC-88MC25034, November 30, 1989.
4. M. A. Alvin, T. E. Lippert, J. E. Lane, and D. M. Bachovchin, "Thermal/Chemical Stability of Ceramic Cross Flow Filter Materials," AR&TD Direct Utilization and Instrumentation and Diagnostics Contractors' Review Meeting, Pittsburgh, PA, September 16-18, 1990.
5. M. A. Alvin, T. E. Lippert, D. M. Bachovchin, J. E. Lane, and R. E. Tressler, "Thermal/Chemical Stability of Ceramic Cross Flow Filter Materials," Eleventh Annual Gasification and Gas Stream Cleanup Systems Contractors' Review Meeting, Morgantown, WV, August 13-15, 1991.
6. M. A. Alvin, D. M. Bachovchin, T. E. Lippert, R. E. Tressler, and K. R. McNerney, "Thermal/Chemical Stability of Ceramic Cross Flow Filter Materials," Twelfth Annual Gasification and Gas Streams Cleanup Systems Contractors Review Meeting, Morgantown, WV, September 15-17, 1992.
7. M. A. Alvin, T. E. Lippert, E. S. Diaz, and E. E. Smeltzer, "Thermal and Chemical Stability of Ceramic Candle Filter," Advanced Coal-Fired Power Systems 1995 Review Meeting, Morgantown, WV, June 27-29, 1995.
8. M. A. Alvin, "Porous Ceramic Hot Gas Filters — Materials and Applications," Second International Conference on Heat Resistant Materials, Gatlinburg, TN, September 11-14, 1995.
9. M. A. Alvin, "Thermal/Chemical Degradation of Cross Flow Filter Materials," Final Report, DOE Contract No. DE-AC21-88-M25034, October 20, 1997.
10. M. A. Alvin, T. E. Lippert, E. S. Diaz, and E. E. Smeltzer, "Filter Component Assessment," Advanced Coal-Fired Power Systems 1995 Review Meeting, Morgantown, WV, June 27-29, 1995.
11. M. A. Alvin, T. E. Lippert, E. S. Diaz, and E. E. Smeltzer, "Filter Component Assessment," Advanced Coal-Fired Power Systems 1996 Review Meeting, Morgantown, West Virginia, July 16-18, 1996.
12. M. A. Alvin, T. E. Lippert, E. S. Diaz, E. E. Smeltzer, and G. J. Bruck, "Filter Component Assessment," Advanced Coal Based Power and Environmental Systems 1997 Contractor's Review Meeting, Pittsburgh, PA, DOE/FETC Contract No. DE-AC21-94MC31147, July 22-24, 1997.
13. M. A. Alvin, "Assessment of PCFBC-Exposed and Accelerated Life-Tested Candle Filters," Topical Report, Siemens Westinghouse Power Corporation, DOE/NETL Contract No. DE-AC21-94MC31147, September 30, 1999.
14. M. A. Alvin, Hot Gas Filter Development and Performance. High Temperature Gas Cleaning (Editors: Dittler, Hemmer, and Kasper) Volume II, 1999, pp. 455-467.
15. M. A. Alvin, "Assessment of Ceramic and Metal Media Filters in Advanced Power Systems," ASME International Gas Turbine & Aeroengine Congress & Exhibition Meeting New Orleans, June 4, 2001.
16. M. A. Alvin, "Advanced Second Generation Hot Gas Candle Filters," Topical Report, Siemens Westinghouse, DOE/NETL Contract No. DE-AC21-94MC31147, January 31, 2002.
17. M. A. Alvin, "Assessment of Ceramic Filters for Advanced Coal-Based Power Generation Applications," Nineteenth Annual International Pittsburgh Coal Conference, September 25, 2002.

18. M. A. Alvin, "Accelerated Life Testing of Ceramic Candle Filters," Topical Report, Siemens Westinghouse, DOE/NETL Contract No. DE-AC21-94MC31147, February 28, 2003.
19. M. A. Alvin, "Assessment of Metal Filters for Advanced Coal-Based Power Generation Applications," Fifth International Symposium on Gas Cleaning at High Temperature, Morgantown, WV, September 19, 2002.
20. M. A. Alvin, "Metal Filters for Pressurized Fluid Bed Combustion (PFBC) Applications," Final Report, Siemens Westinghouse Power Generation, DOE/NETL Contract No. DE-AC26-98FT40002, January 2, 2004.
21. M. A. Alvin and T. E. Lippert, "Mechanical Analysis of a Cross Flow Filter," Final Report, Westinghouse Science and Technology Center, DOE/METC Contract No. DE-AC21-86MC23252, January 23, 1995.
22. R. A. Newby, M. A. Alvin, G. J. Bruck, T. E. Lippert, E. E. Smeltzer, and M. E. Stampahar, "Optimization of Advanced Filter Systems," Final Report, Siemens Westinghouse, DOE/NETL Contract No. DE-AC26-97FT33007, June 2002.

## 8. ACKNOWLEDGMENTS

I wish to acknowledge Mr. Richard Dunst, Mr. Theodore McMahon, Mr. Richard Dennis, and Dr. Norman Holcombe at DOE/NETL for their guidance and technical support during conduct of the hot gas filter material development programs. In addition I wish to acknowledge the personnel from the various organizations who participated in the development and performance evaluation of the hot gas filter elements:

**Siemens Westinghouse Power Corporation:** Tom Lippert, Jerry Bruck, Gene Smeltzer, Dennis Bachovchin, George Schneider, John Meyer, Art Fellers, Harry Morehead

**American Electric Power:** Mike Mudd, John Hoffman, Arnie Goodnight

**Foster Wheeler Karhula:** Juhani Isaksson, Reijo Kuivalainen, Timo Eriksson, Pekka Lehtonen, Folke Engstrom

**Sierra Pacific Power Company:** Sherry Dawes, Brent Higginbotham

**Southern Company Services and Southern Research Institute:** Howard Hendrix, Guan Xiaofeng, Bob Dahlin, Carl Landham, Jack Spain, Todd Snyder, Duane Pontius, Randall Rush

**Oak Ridge National Laboratory:** Dave Stinton, Rod Judkins, Peter Tortorelli, Edgar Lara-Curzio, Nancy Cole

**Argonne National Lab:** J. P. Singh, Ken Natesan, William Ellingson

**Coors Ceramics:** Kevin McNerney, Robert Lucernini, Connie Cameron, Ed Mahardy, John Cook, Rick Kleiner

**Ensto:** Börje Hildén, Terjo Ek

**Blasch Precision Ceramics:** Dave Larsen, Jeff Bolebruch

**Industrial Filter and Pump:** Jim Zievers, Paul Eggerstedt

**Schumacher:** Michael Durst, Max Muller, Eberhard Freude, Astrid Walsch, Karsten Schulz, Phil Seymour

**Pall Advanced Separation Systems:** John Sawyer, Nelson Sobel, Steve Geibel, Mark Johnson

**Refractron:** Bob Stanton, Chad Sheckler

**3M:** Ed Fischer, Tim Gennrich, William Nitardy, Bill Weaver, Joseph Eaton, Doug Pysner, Mike Lynn

**DuPont:** Liz Connolly, Jeff Chambers, George Forsythe, Warren Hewett, Paul Gray, James Weddell, Al Fresco, John Garnier

**McDermott:** Rich Wagner

**Albany Techniweave:** Jean LaCostaouec, Jay Lane

**Textron:** Steve DiPietro, Bruce Thompson

**Ultramet:** Ed Stankiewicz

**Filtros/Ferro:** Phil Way, Allan Schilling

**CeraMem:** Rich Abrams, Bruce Bishop, Robert Goldsmith

**Specific Surface:** Andrew Jeffery, Mark Parish

**Scapa:** Joseph Weitham, Gary Elliott, Paul Wroblewski

**LoTec Inc.:** Santosh Limaye, Chris Barra

**Sumitomo:** Paul Oyama, Ken-Ichi Nishio, Kingo Akahori

**Kyocera:** Bob Whitlock, Tatsumi Maeda, Yoshinori Matsumura

**Ceramic Composites:** John Hanigofsky

**Kaiser:** H. O. Davis

**Third Millenium Technologies:** Sam Weaver

**Selee:** Guilio Rossi

***AiResearch:*** Jim VanAckeren, Doug Twait

***GTE:*** Joe Cleveland, Bob Long

***VPI:*** Jesse Brown, Nancy Brown

***Naval Warfare Research:*** Inna Tamaly

***U.S.Filter/Fluid Dynamics:*** Bob Smith, Nat Quick, Alex Sobelevsky, Matt June, Andy Gorin, Rick Range

***Microfiltrex:*** Tony McDowell, Ian Boxall, Alan Crane

***Technetics:*** Doug Chappel

***Mott:*** Sunil Jha

***Bekaert Fibre Technologies/Mott:*** Gary Rawlings, Mike Wilson, Ken Rubow

***Ames:*** Iver Anderson

***Idaho National Lab:*** Richard Wright

**APPENDIX A**  
**FILTER MATERIAL STRENGTH**

C-ring compressive and tensile strength data generated at SWPC STC for the various porous ceramic filter materials after PCFBC field exposure or accelerated life testing are presented in Table A-1.

<b>TABLE A-1 — RESIDUAL ROOM AND HIGH TEMPERATURE STRENGTH AFTER PFBC/PCFBC AND ACCELERATED LIFE TESTING</b>					
Filter Matrix Identification Number	Total PCFBC and/or Equivalent Operating Time, Hrs (Number Thermal Transients)	Compressive Strength, psi		Tensile Strength, psi	
		25°C	~800°C	25°C	~800°C
<b>Coors P-100A-1</b>					
FC040 (M6)	1661	1756±77	1722±127	1983±164	2123±185
FC018 (M16)	2201	1692±93	1530±172	1891±178	1790±279
FC059 (M13)	2166 (30 TT)	1824±211	1511±366	2160±79	2154±189
AB13 (M15)	3311 (PFBC/PCFBC)	1857±113	1749±251	1902±194	2045±104
FC058 (M26)	5762.5	2073±180	1844±320	2258±135	2530±294
FC044 (M12)	12210.5	2057±157	2010±323	2589±708	2527±552
FC065 (M10)	32698.0 (60 TT)	2084±239	2312±184	2487±191	2699±372
<b>Pall 326</b>					
R3 656 (M21)	1035 (30 TT)	2542±306	2346±445	2333±307	2878±214
R2 669 (M18)	2201	2543±144	3039±113	2178±180	2963±149
R5 631 (M22)	4631.5	2421±109	2358±292	2289±333	2631±335
R1 659 (M17)	11079.5	2255±156	2443±198	2366±348	2674±430
R1 658 (M3)	21209.5 (30 TT)	2101±117	2841±362	1871±272	3193±430
R5 667 (M23)	30149.0 (30 TT)	1875±223	2643±302	2226±230	2798±261
<b>4-980</b>					
	2640	3124±161	3645±355	3348±388	3764±398
<b>307</b>					
	23317.5 (30 TT)	2685±194	3021±394	2918±237	2869±481
<b>Schumacher FT20</b>					
S350F/7 (T18)	2201	2681±114	3452±230	2168±98	2724±224
S350F/16 (T2)	6049.5	2269±125	3308±222	2324±86	3555±346
S350F/60 (T5)	11079.5	1935±192	2651±272	2071±84	2528±157
S350F/43 (T4)	21209.5 (30 TT)	2389±135	3352±620	2141±275	3586±637
S350F/32 (T3)	31567.0 (30 TT)	2272±123	3569±148	2266±154	3429±462
<b>1105</b>					
	1241	1595±79	1940±393	1724±184	2609±367
<b>1173</b>					
	21728.5 (30 TT)	1581±250	2191±653	1667±253	2790±234
<b>DuPont PRD-66</b>					
D583	—	976±107	1223±103	1041±170	1159±202
D580 (B51)	342	1170±76	1533±125	1405±146	1464±293
D587 (B50)	581	1400±91	1599±137	1346±263	1581±190
D571C New	28004.5 (30 TT)	1242±149	1593±180	963±292	1010±657
<b>639</b>					
	SCS — Background	1185±116	1269±188	1183±202	1543±546
<b>582</b>					
	SCS/20487.5 (30 TT)	1024±135	1424±267	930±296	1304±516

**TABLE A-1 (Cont'd.) — RESIDUAL ROOM AND HIGH TEMPERATURE STRENGTH  
AFTER PFBC/PCFBC AND ACCELERATED LIFE TESTING**

Filter Matrix Identification Number	Total PCFBC and/or Equivalent Operating Time, Hrs (Number Thermal Transients)	Compressive Strength, psi		Tensile Strength, psi	
		25°C	~800°C	25°C	~800°C
<b>McDermott CFCC</b>					
7-6-3	—	898±166	956±346	1207±202	1008±228
B&W 7-5-15 (B14)	342	798±176	858±256	1139±207	878±143
B&W 7-5-30 (B33)	581	1032±198	765±202	1165±195	1155±237
B&W 7-5-29 (B32)	10625.5 (30 TT)	787±198	633±231	1038±201	1094±228
784	802	491±280	495±166	248±67	220±71
1259	20666.5	546±96	613±282	715±97	748±188
1258	20666.5 (30 TT)	474±142	458±136	482±180	677±194
787	21847.5 (30 TT)	390±204	465±254	402±281	497±298
<b>Ensto</b>					
129-97	581	1155±108	1156±167	1512±123	1219±42
141-97 (B25)	26098.5 (30 TT)	1042±389	1003±153	1675±214	1485±270
<b>Blasch</b>					
BP4-270C-7/97	—	734±91	710±144	685±131	544±121
BP-4-270J 7/97 (B39)	342	709±167	689±166	728±86	610±113
BP-4 270N7/97 (B40)	581	752±70	789±76	762±45	726±121
BP4-270P7/97 (B41)	10625.5 (30 TT)	644±98	652±112	652±130	707±180
<b>Techniweave</b>					
2682 #1	—	1985±441	1775±587	1030±695	1055±300
2682 #2	20487.5 (30 TT)	1735±297	1789±575	739±411	1060±303
<b>IF&amp;P Recrystallized SiC</b>					
New	25517.5 (60 TT)	4418±404	3702±240	4906±606	4356±483